NAVAL POSTGRADUATE SCHOOL
Monterey, California

THESIS

A COMPOSITE STUDY OF THE MADDEN-JULIAN OSCILLATION AND NORTEASTERLY COLD-SURGES DURING THE NORTHERN WINTER MONSOON

by

John W. Simms IV

March 2000

Thesis Advisor: Chih-Pei Chang
Co-Advisor: Patrick A. Harr

Approved for public release; distribution is unlimited.

REPORT DOCUMENTATION PAGE

Form Approved OMB No. 0704-0188

1. AGENCY USE ONLY *(Leave blank)*	2. REPORT DATE	3. REPORT TYPE AND DATES COVERED
	March 2000	Master's Thesis

4. TITLE AND SUBTITLE
A Composite Study of the Madden-Julian Oscillation (MJO) and Northeasterly Cold-surges During the Northern Winter Monsoon

5. FUNDING NUMBERS

6. AUTHOR(S)
Simms, John W., IV

7. PERFORMING ORGANIZATION NAME(S) AND ADDRESS(ES)
Naval Postgraduate School
Monterey, CA 93943-5000

8. PERFORMING ORGANIZATION REPORT NUMBER

9. SPONSORING / MONITORING AGENCY NAME(S) AND ADDRESS(ES)

10. SPONSORING / MONITORING AGENCY REPORT NUMBER

11. SUPPLEMENTARY NOTES
The views expressed in this thesis are those of the author and do not reflect the official policy or position of the Department of Defense or the U.S. Government.

12a. DISTRIBUTION / AVAILABILITY STATEMENT
Approved for public release; distribution unlimited.

12b. DISTRIBUTION CODE

13. ABSTRACT *(maximum 200 words)*

During the northern winter monsoon, the Madden-Julian Oscillation (MJO) and northeasterly cold-surges are active over the eastern Indian Ocean and western Pacific. The MJO consists of an active (wet) phase and inactive (dry) phase and varies over global spatial and intraseasonal time scales. Interactions between the MJO and northeasterly cold-surges, which vary over regional space and synoptic time scales, are examined. The interactions are examined between 1979-1998 using winds at 1000 hPa and a representation of convection during the northern winter monsoon. To identify interactions, the active and inactive phases of the MJO are divided into early or late phases (based on MJO duration). Examination of composite maps based on cold-surges defined to occur during each phase of the MJO revealed that the phase of the MJO acts to either enhance or weaken a cold-surge that may have been forced by the mid-latitudes. When MJO convection is located over the South China Sea, the surge intensifies. The favorable convection pattern dominates the unfavorable pressure-wind pattern of the MJO. When the MJO dry-phase is over the South China Sea, mid-latitude forcing appears to interact favorably with the pressure-wind pattern of the MJO to dominate the unfavorable MJO convection pattern.

14. SUBJECT TERMS	15. NUMBER OF PAGES
Northern winter monsoon, Madden-Julian Oscillation (MJO), northeasterly cold-surges	103
	16. PRICE CODE

17. SECURITY CLASSIFICATION OF REPORT	18. SECURITY CLASSIFICATION OF THIS PAGE	19. SECURITY CLASSIFI- CATION OF ABSTRACT	20. LIMITATION OF ABSTRACT
Unclassified	Unclassified	Unclassified	UL

NSN 7540-01-280-5500

Standard Form 298 (Rev. 2-89)
Prescribed by ANSI Std. 239-18

Approved for public release; distribution is unlimited

A COMPOSITE STUDY OF THE MADDEN-JULIAN OSCILLATION (MJO) AND NORTHEASTERLY COLD-SURGES DURING THE NORTHERN WINTER MONSOON

John W. Simms IV
Lieutenant, United States Navy
B. S., University of South Carolina, 1994

Submitted in partial fulfillment of the
requirements for the degree of

MASTER OF SCIENCE IN METEOROLOGY

From the

NAVAL POSTGRADUATE SCHOOL
March 2000

Author: _____
John W. Simms IV

Approved by: _____
Chih-Pei Chang, Thesis Advisor

_____
Patrick A. Harr, Co-Advisor

_____
Carlyle Wash, Chairman
Department of Meteorology

ABSTRACT

During the northern winter monsoon, the Madden-Julian Oscillation (MJO) and northeasterly cold-surges are active over the eastern Indian Ocean and western Pacific. The MJO consists of an active (wet) phase and inactive (dry) phase and varies over global spatial and intraseasonal time scales. Interactions between the MJO and northeasterly cold-surges, which vary over regional space and synoptic time scales, are examined. The interactions are examined between 1979-1998 using winds at 1000 hPa and a representation of convection during the northern winter monsoon. To identify interactions, the active and inactive phases of the MJO are divided into early or late phases (based on MJO duration). Examination of composite maps based on cold-surges defined to occur during each phase of the MJO revealed that the phase of the MJO acts to either enhance or weaken a cold-surge that may have been forced by the mid-latitudes. When MJO convection is located over the South China Sea, the surge intensifies. The favorable convection pattern dominates the unfavorable pressure-wind pattern of the MJO. When the MJO dry-phase is over the South China Sea, mid-latitude forcing appears to interact favorably with the pressure-wind pattern of the MJO to dominate the unfavorable MJO convection pattern.

TABLE OF CONTENTS

ACKNOWLEDGEMENT

I would like to personally thank Professor C. P. Chang and Professor Pat Harr for their guidance and enthusiasm throughout this entire project. I want to extend my thanks further to Professor Harr for all the long days of editing and putting this project together because without your help this would not have been possible. I would also like to thank the staff personnel, especially Mike Cook and Hway-Jen Chen for their responsive support of providing data in a usable format and in writing code for my programs. This research was supported in part by the Office of Naval Research, Marine Meteorology Program.

I especially want to thank my wife, Yvonne, for providing me the patience and love needed to accomplish this project. I couldn't have done it without you. I also want to thank my daughters, Jessica and Rachel, for putting up with the endless days and nights where I was at school instead of being home. Hopefully, they realize all the hard work and perserverance will pay dividends in the end and that I will always love them. And lastly, I want to thank my parents for giving me the love and support I've needed through the years to make my life successful and prosperous.

I. INTRODUCTION

Some of the most important features of the tropics are the large areas of convection contained in the Inter-tropical Convergence Zone (ITCZ) and the South Pacific Convergence Zone (SPCZ). These tropical regions play a significant role in the earth's climate and are areas in which a significant number of tropical cyclones form. On an inter-annual basis, convective areas in the ITCZ and SPCZ are enhanced as a result of the convection moving from south/southeast Asia during the northern summer monsoon to the maritime continent (Indonesia and Malaysia) and the northern Australia equatorial region during the northern winter monsoon. On intraseasonal time scales, The Madden-Julian Oscillation (Madden and Julian, 1971) influences convection over ITCZ and SPCZ, and over synoptic time scales northeasterly cold surges also significantly affects convection in the ITCZ and SPCZ. This paper contains a composite study of the relationship between the Madden-Julian Oscillation (MJO) and northeasterly cold surges during the northern winter monsoon (Australian summer monsoon), which occurs from December to March.

The MJO is a global-scale disturbance (longitudinally) and the dominant mode of intraseasonal variability in the tropical troposphere (Leibmann et al., 1994). The MJO signal has a rather broad period window ranging from 20 to 60 days with the most frequent occurrence around 45 days, and is present over 75% of the time (Madden and Julian, 1972). The MJO signal at the equator is in the eastward-moving zonal wavenumbers 1-3 and has a strong annual cycle, which peaks between 5 and 15 degrees latitude of the summer hemisphere (Leibmann et al., 1994).

Several studies (Rui and Wang, 1990; Wang and Rui, 1990; Weickmann and Khalsa, 1990) have identified the preferred tracks of convection throughout the MJO life cycle. They showed that during the onset of the MJO convection remains stationary over the eastern Indian Ocean. This large, broad region of convection begins to propagate eastward and weakens as it moves over the maritime continent. Once the convective region has moved over the warm water of the western Pacific, convection is significantly enhanced. The convection continues to move eastward across the warmer waters of the western Pacific. As the convective region slows down and approaches the dateline, it weakens and continues to move into the eastern Pacific. It should be noted that during the northern winter the primary signal slows down and a convective band propagates to the southeast into the SPCZ (Taylor, 1998).

The two main signature features that aid in the identification of the MJO are "super-cloud clusters" (SCC) and westerly-wind bursts (WWB). The SCC is a large, well-organized area of convection with a zonal dimension of over a 1000 km. A MJO is composed of several eastward moving SCC's. Each SCC is composed of several smaller cloud clusters (CC) that propagate to the west with a lifetime of 1 to 2 days (Madden and Julian, 1994). The typical period of duration for a SCC is between two and ten days and the propagation speed is approximately 5 to 15 ms^{-1}. This propagation exists due to the formation of cloud clusters on the eastern border and dissipating cloud clusters on the western border (Ferreirra et al., 1996). The heating pattern of the SCC associated with the MJO imposes a pattern of Rossby gyres (Matsuno, 1966; Gill, 1980) and near equatorial wind bursts to the west of the heat source and a Kelvin wave signature to the east of the heat source. As the MJO propagates eastward, this circulation pattern moves

along with the MJO from the eastern Indian Ocean to the western Pacific. When the weakening convection approaches the dateline and moves over the Western Hemisphere, the Kelvin wave breaks free.

The entire tropical region of the eastern Indian Ocean and western Pacific is dominated by northeasterly trade winds from 20N to the equator as part of the northern winter monsoon. Over the extreme western Pacific and South China Sea, the northeasterly flow undergoes periods of intensification that persists over synoptic time scales. This intensification of the northeasterly flow is known as a "cold surge". Cold surges originate in the mid-latitudes as a result of migratory anticyclones, which form over Siberia and Mongolia and will be termed the Siberian-Mongolian high. When the Siberian-Mongolian high builds to at least 1045 hPa, the high-pressure system collapses and a cold surge is initiated. As the cold surge tracks southward with cold, dry continental air, it causes intense temperature drops over south/southeast Asia (Wu and Chan, 1995). A northeasterly cold surge takes approximately two days to reach the South China Sea and results in temperature drops of 4 to 5 degrees Celsius in most parts of China (Wu and Chan, 1995). As a result, the northeasterly flow in the South China Sea is freshened, which can impose dramatic effects on synoptic- and planetary-scale convective patterns. The first effect is a general increase of deep convection over the maritime continent during the northern winter monsoon, as the cold surges seem to spawn near-equatorial cloud systems (Taylor, 1998). Over the equatorial region, strong cold surge events often lead to localized episodes of heavy rainfall and flooding. Secondly, northeasterly cold surges have an influence on associated convection and circulation patterns of the Australia summer monsoon and it's onset (Johnson and Houze, 1987).

Lastly, the northeasterly cold surge may also have a possible influence on the Southern Hemisphere tropical cyclone activity (Love, 1985).

The northeast monsoon pattern varies from early to late winter while northeasterly flow across the South China Sea is strongest and deepest in early winter and becomes weaker and shallower toward the end of the period. The peak convection of the Australia summer monsoon occurs in late February when the near equatorial trough lies between 10 and 15 degrees south (Johnson and Houze, 1987).

The purpose of this work is to investigate physical relationships between the global-scale MJO that varies on intraseasonal time scales and the synoptic-scale northeasterly cold surge. A composite analysis is employed.

II. DATA AND METHODOLOGY

Data used for this paper were the National Center for Environmental Prediction (NCEP) reanalysis 1000 hPa wind field at 2.5 x 2.5 degree resolution and outgoing longwave radiation (OLR) data that are also at 2.5 x 2.5 degree resolution. The OLR data were used to identify convection patterns. For both data sets, only daily averages were used. The period of this study was between 1979 and 1998 during the northern winter monsoon (December through March).

The area used for this study was 50N to 30S, 90E to 160W (Figure 1), which covers the tropical regions of the eastern Indian Ocean and western Pacific as well as the mid-latitude region where cold surges are initiated as a result of baroclinic forcing. The MJO is well defined in the pressure, wind, and convection patterns of the equatorial region shown in Figure 1 (Madden and Julian, 1994). Two area-averaged indices were defined; a convection index that was computed from the OLR fields and a cold-surge index that was computed from the 1000 hPa wind fields.

The convection index was calculated by converting the raw OLR data into radiance values (W/m^2). If the radiance value was greater than or equal to 230 W/m^2, then the radiance value was set to zero and not used. All radiance values, which were less than 230 W/m^2 were utilized in the convection index. Over tropical regions, these radiance values represent areas of convection that typically reach into the middle to upper troposphere.

To identify eastward-propagating cloud clusters associated with the MJO, the OLR data were band-pass filtered to isolate the 20 to 60 day signal of the MJO. Once the MJO was identified, it was divided into two phases. The active phase, also commonly

called the wet phase, contains large cloud clusters that propagate eastward in the equatorial region as part of the MJO signal. The inactive phase, also commonly called the dry phase, represents areas of clearing with little or no convection. The active phase and inactive phase are further divided as early (initial 50% of the active/inactive phase duration) or late (second 50% of the active/inactive phase duration). The filtered OLR data were examined for each of the 19 northern winter monsoon seasons from 1979 to 1998 to identify occurrences of MJO episodes. Over this period of interest, there were 26 MJO episodes.

The cold-surge index was calculated from the meridional (v) wind component of the 1000 hPa winds at 7.5N, 105E to 115E, which is the southern end of the South China Sea. The cold-surge index was used to define cold-surge events, and were composited according to the time relevant to the surge event. The beginning of a surge event is defined as day 0, which is when the northerly winds are at a minimum. A cold-surge event was identified if the northerly acceleration persisted for at least three days and reached approximately –4.5 m/s. There were 62 cold-surge events identified in conjunction with the MJO during the northern winter monsoon seasons from 1979 to 1998. Each surge event that occurred in conjunction with the MJO was further classified relative to the MJO active/inactive plus early/late phases of the MJO. For instance, the early-active phase represents surge events that occurred during the initial 50% of the MJO duration. For example, if the MJO has a period of 30 days and the surge event occurred in the first 15 days (initial 50%), then the surge was classified as early-active. If the surge event occurred in the latter 15 days (second 50%) of the MJO, then the surge was classified as late active. This same process applied to the inactive phase and was

divided into early/late inactive based on the same methodology described for the active phase. Composites of the 1000 hPa winds and convection fields were constructed daily for the 12 days following the beginning of a surge event associated with the MJO. The reason for further dividing the MJO into four phases rather than two will be discussed in a later chapter and will be the main focus for this study.

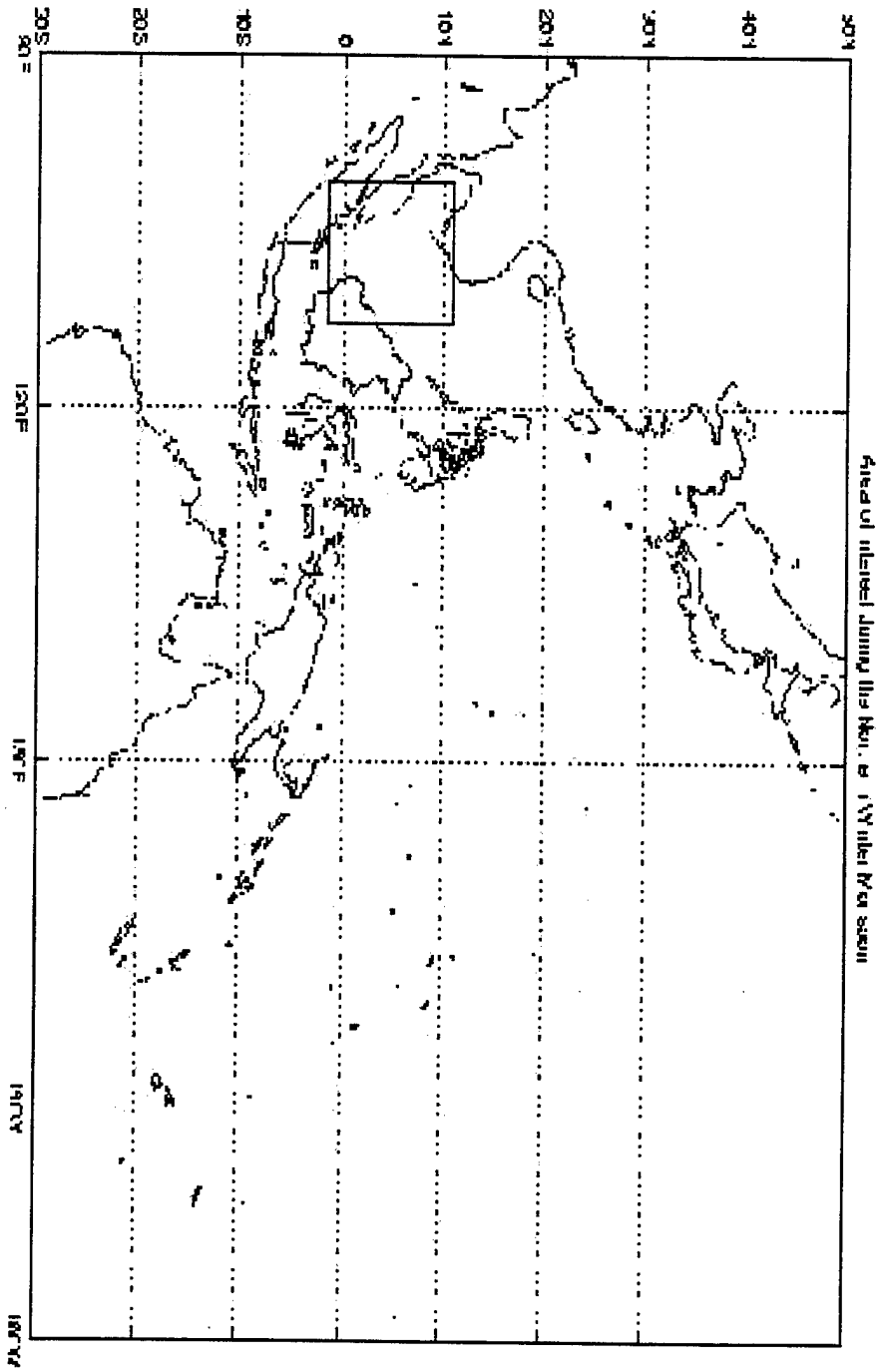

Figure 1. The region of interest for this study. Note that the South China Sea is defined by a square. This area is used to define and study cold surge events.

III. MEAN FLOW

Before the composite analysis of the MJO and northeasterly cold surges, the mean flow over the region as defined from 1979 to 1998 must be examined. The regime of the northern winter monsoon during December through March is examined over the eastern Indian Ocean and western Pacific (Figure 1). The mean 1000 hPa synoptic flow pattern as well as the pattern of convection from the convection index for OLR data are examined by simply averaging all the northern winter monsoon seasons over the 19-year period.

A. CIRCULATION PATTERN

In general, during the northern winter monsoon, the circulation and convection patterns indicate that the largest area of clouds are found to the north of the Southern Hemisphere monsoon trough axis from Sumatra across Indonesia to the southwest Pacific (Johnson and Houze, 1987). On average, northeasterly trade winds prevail over most of the eastern Indian Ocean and western Pacific between the equator and 20N as part of the northern winter monsoon (Figure 2). Over eastern Asia, the Mongolian-Siberian high, centered around 32N, 110E is well established. A strong north to south cross-equatorial flow is seen across the South China Sea region. In addition, there is also strong cross-equatorial flow to the east of the Philippines. The mid-latitudes are dominated by westerlies north of 30N.

There are two predominant circulation patterns that dominate the Southern Hemisphere. One is the strong cyclonic circulation in the SPCZ region south and southeast of New Guinea. The other dominant feature is the anticyclone/cyclone pair to the west of Australia between 10S and 30S. These patterns, which are established over

the eastern Indian Ocean and Western Pacific, are important components associated with northeasterly cold surges and will be vital in the composite analysis section covered in the next chapter.

As the Northern Hemisphere northeasterlies cross the equator, the flow turns westerly into the Australian summer monsoon trough located between 10S and 20S from 90E to Northern Australia. This cross-equatorial flow contributes to the ITCZ and SPCZ circulations. Both convergence zones occur in the Australian monsoon region between 90E to approximately 140E.

B. CONVECTION PATTERN

The OLR-based convection pattern for each northern winter monsoon season from 1979 to 1998 was averaged together to produce a 19-year mean convection chart (Figure 3). The strongest convection occurs south of the equator, which correspond to the summer hemisphere monsoon region. The ITCZ and SPCZ areas can be seen clearly with the ITCZ oriented zonally north of Australia and the SPCZ oriented from New Guinea to the southeast.

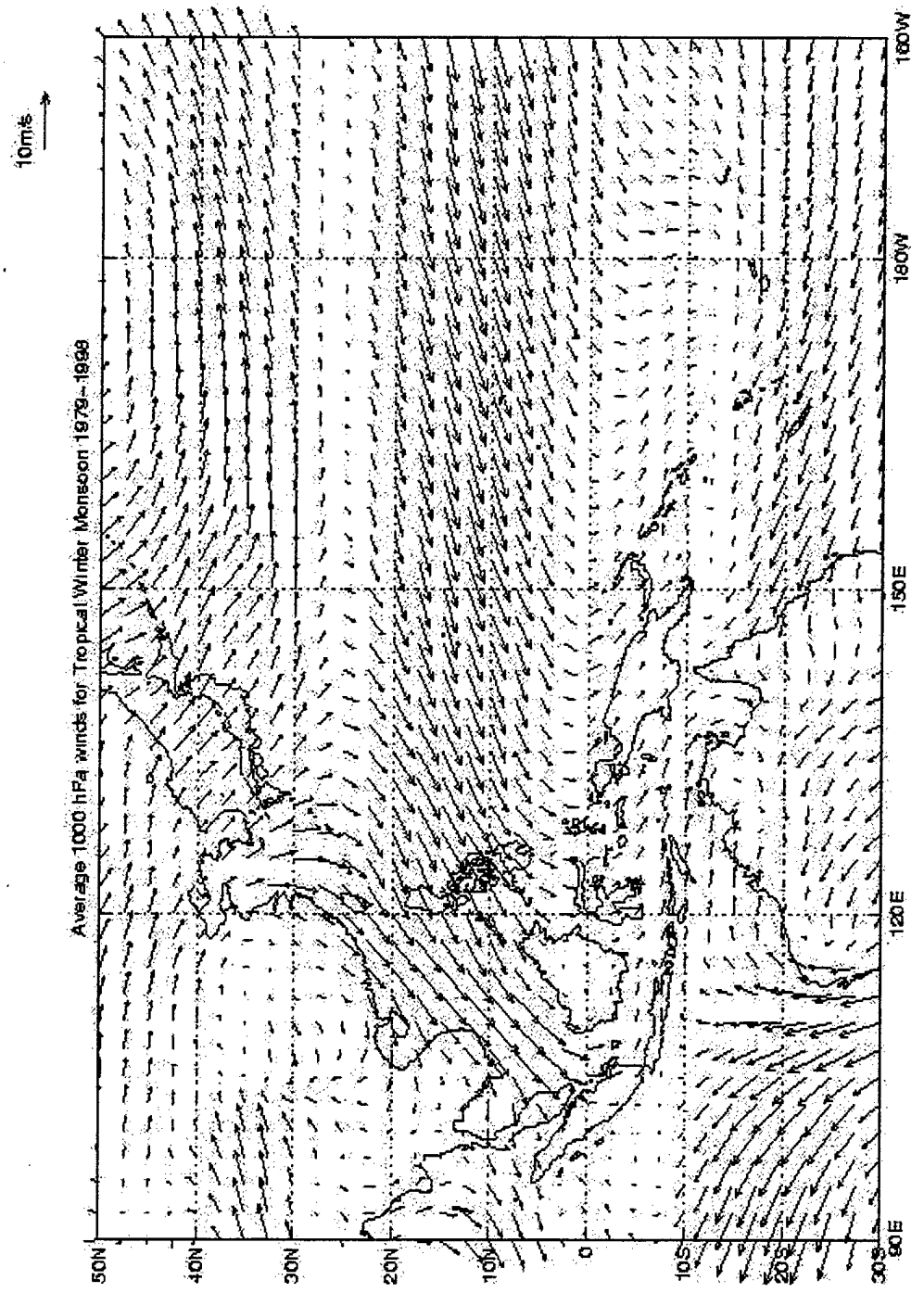

Figure 2. The 19-year average of 1000 hPa winds from 1979 to 1998.

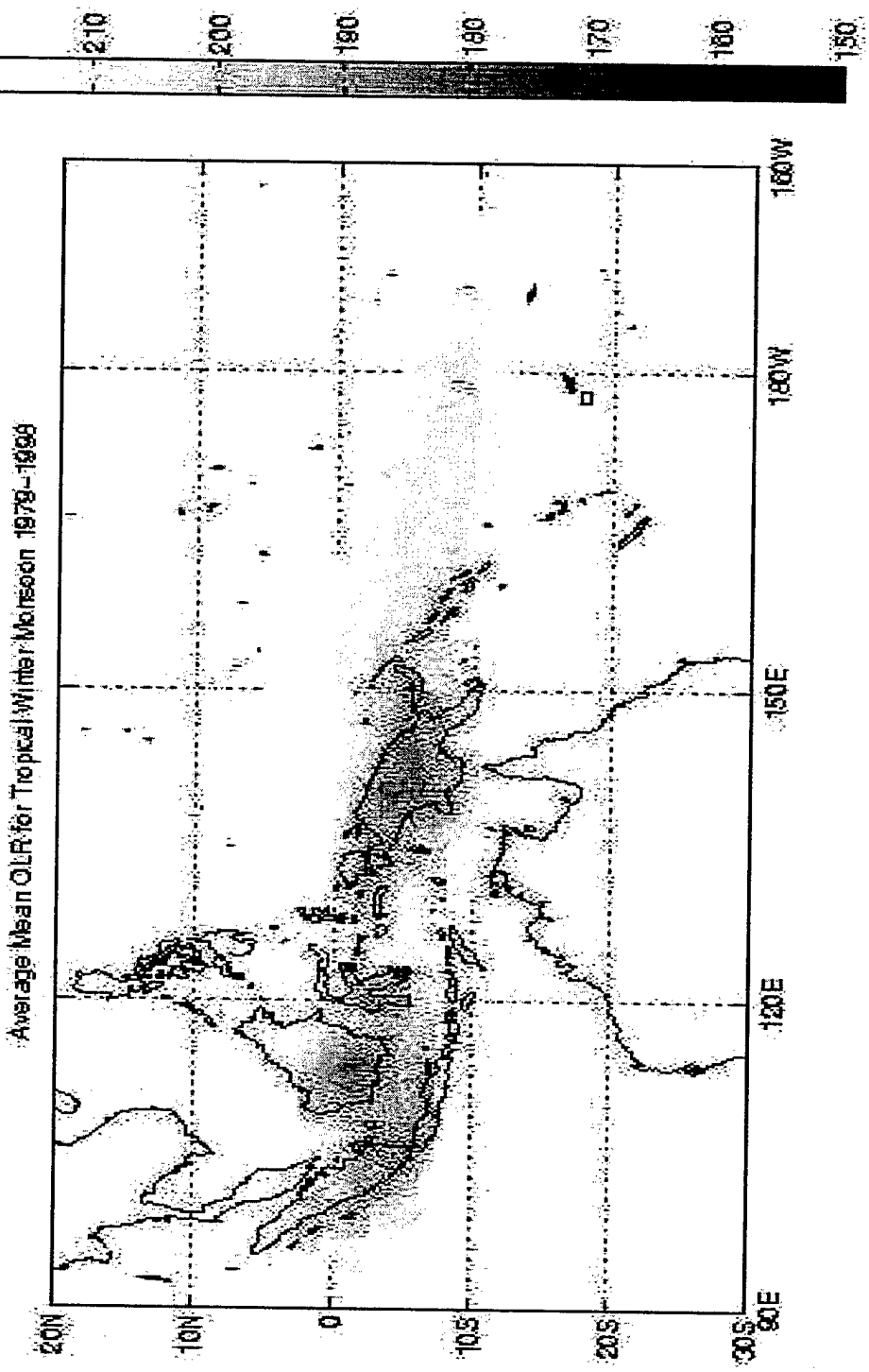

Figure 3. The 19-year average convection based on the OLR-based convective index from 1979-1998.

IV. ANALYSIS

Before the composite analysis of the interaction between northeasterly cold-surges and the MJO, individual pressure and circulation patterns associated with cold-surges and MJO events are identified. Following identification of the characteristics associated with each feature, the composite analysis (using the OLR-based convection index) is defined based on stratification of cold-surge events that occurred during specific periods within the MJO cycle.

A. MADDEN-JULIAN OSCILLATION BASED ON OLR DATA

The MJO is well defined in the equatorial region between the eastern Indian Ocean and the western Pacific during the northern winter monsoon (Madden and Julian 1994). Based on the theoretical and numerical analyses of the effects of anomalous heating along the equator (Gill 1980; Lau and Peng 1987), the "typical" circulation and convection patterns can be represented by a combination of Rossby and Kelvin mode responses (Figure 4). During the active phase when convection represents an anomalous heat source on the equator, a pattern of Rossby Gyres, northwest and southwest of the heat source, is generated off the equator over subtropical latitudes. Associated with these cyclonic circulations are enhanced equatorial westerlies to the west of the heat source. To the east of the heat source, a Kelvin wave response is generated. Associated with this mode are easterly winds along the equator. The combination of easterly winds east of the MJO convection and westerly winds to the west of the MJO convection contributes to convergence and persistence of the convection phase. Rui and Wang (1990) identified that the maximum convergence occurs slightly east of the main convection, which contributes to the eastward movement of the entire pattern. These circulation and

convection patterns will be used to hypothesize how the MJO pressure, wind, and convection patterns may influence a cold-surge event.

To identify MJO events during 1979-1998, the OLR data are band-pass filtered to isolate the 20 to 60 day signal of the MJO. The filtered OLR data that define the convection index are averaged between the equator to 15S. To identify the time evolution of the tropical convection associated with the MJO, time-longitude cross sections of the filtered OLR data are plotted (Figure 5), such that the MJO appears as eastward-propagating areas of convection. The active and inactive phases are further divided into early active/inactive (initial 50% of the MJO duration) and the late active/inactive (second 50% of the MJO duration).

There were 26 MJO episodes identified over the northern winter monsoon periods between 1979 and 1998. Due to interannual variability, the MJO appears as a strong signal one year but may be weak the next year. For example, Figure 4 defines strong MJO signals during the 1985, 1987, 1988, 1990, 1992, and the 1997 northern winter monsoon seasons. No MJO signals were present during the 1981, 1984, 1994, and 1996 northern winter monsoon seasons.

B. NORTHEASTERLY COLD SURGES OVER THE SOUTH CHINA SEA

Northeasterly cold-surges are characterized by cold, dry continental air that moves from eastern Asia equatorward. The sharp drop in temperature over south/southeast Asia is accompanied by a "surge" of the northeasterly wind into the East China Sea and the South China Sea (Wu and Chan 1995). Although previous studies (Taylor 1998) have shown that the zonal (u) and meridional (v) wind components are positively correlated (i.e., when there are strong easterlies, there are strong northerlies),

the primary cold-surge signal is contained in the v wind component. For this reason, the meridional (v) component is used to define cold-surge events. Figure 6 represents time series of the 1000 hPa v-wind component averaged along 7.5N, and between 105E to 115E (southern end of the South China Sea) during each northern winter monsoon period (December through March) between 1979 and 1998. Negative v-wind values represent northerly winds. Cold-surge events are identified when the northerly acceleration of winds persists for at least 3 days and reaches approximately –4.5 m/s. Day 0 is defined as the day when the northerly winds are at a minimum, which signifies the beginning of a cold-surge event. Over the 19-year period, 139 surge events were identified during the northern winter monsoon seasons. Table 1 of Appendix A labels each surge event from day 1 to day 12 for each northern winter monsoon period from 1979 to 1998. Table 1 also shows in which phase of the MJO the surge event occurred (bold is active phase). On average, there were 7 surge events per northern winter monsoon with a maximum of 9 surge events occurring during the 1981, 1982, and 1985 northern winter monsoon seasons, and a minimum of 5 surge events occurring during 1980 and 1992 northern winter monsoon seasons.

Typically, the intensification and southwestward movement of the low-level Siberian-Mongolian anticyclone (Wu and Chan, 1995; Compo et. al., 1999) initiates cold surges. The connection between typical synoptic-scale variability associated with the mid-latitude forcing of cold-surges is thought to be the primary reason for the observed interannual variability in the occurrence of cold-surges. In the remainder of this chapter, the relationships between cold-surges and intraseasonally varying MJO characteristics will be identified.

C. HYPOTHESIS ON THE INTERACTION OF SURGES AND THE MJO

Interactions between the MJO and cold-surge features are investigated by considering a superposition of the cold-surge on each phase of the MJO. The schematic MJO circulation and convection pattern of Figure 4 are modified in Figure 7 to represent the hypothesized effects of the superposition of the cold-surge on the MJO features. During the MJO active phase, enhanced convection over the equatorial region of the South China Sea produces lower pressure. The lower pressure will contribute to an increased pressure gradient between the mid-latitudes and the equatorial region, which may produce favorable conditions for the cold-surge (represented by solid arrows going into the area of convection on Figure 7). However, the pressure-wind pattern associated with the MJO (and represented by a open arrow in Figure 7) may produce an unfavorable situation for a surge event to occur because the cyclonic flow associated with the Rossby Gyres imposed by the heat source tends to oppose the direction of flow of the cold-surge.

During the inactive phase, the lack of convection contributes to higher pressure over the equatorial portion of the South China Sea. The reduced pressure gradient will not act to enhance a surge into the area (represented by solid arrows moving out of the dry region in Figure 7). However, the pressure-wind pattern may produce a favorable situation for an incoming surge (represented by an open arrow around the anticyclone in Figure 7). Therefore, it is hypothesized that during cold-surge events that are observed to occur during the MJO active phase, the effects of the MJO convection must dominate the effects of the MJO's pressure-wind pattern. Also, during the inactive phase, the effects of the MJO's pressure-wind pattern or the mid-latitude baroclinic forcing must dominate the effects of the lack of MJO convection for a surge event to occur.

There were 62 cold-surge events (Figure 6) identified in conjunction with the MJO (approximately 45% of the total number of surge events identified). Since there were 139 total surge events identified and only 62 were related to the MJO, it can be inferred that mid-latitude forcing dominates the initiation of a cold-surge. However, the MJO may have an effect on the surge intensity and duration extending into the equatorial region, which is the point of this study.

D. COMPOSITE ANALYSIS

All the cold surges that were related to the MJO are plotted on a histogram (Figure 8) with respect to the MJO phase in which each cold-surge event occurred. Of the 62 cold-surge events associated with an MJO, 42 occurred during the active phase and 20 occurred during the inactive phase. Therefore, it is inferred that the active phase is more favorable for the occurrence of a cold-surge event than the inactive phase. The observed distribution of surge events supports the hypothesis that the effects of the MJO convection would be favorable for surges during the active phase and unfavorable during the inactive phase. Recall, that the hypothesis is that the increased pressure gradient due to the convection pattern provides a favorable condition for extension of a surge to the southern portion of the South China Sea.

There were 20 surge events that occurred during the inactive phase. Although, the presence of the inactive phase of the MJO does not preclude cold-surges from occurring altogether, the number of surges is greatly reduced during the inactive phase. Therefore, it is hypothesized that the mid-latitudes and/or the pressure-wind pattern of the MJO must provide the dominant forcing for a surge event to occur during the inactive phase.

The reason for splitting the active phase and inactive phase into the early- and late-phases (based on the MJO duration) is that a surge that occurs in the early-active phase stays in the active phase for the typical duration of the surge. A surge that begins during the early-inactive phase stays in the inactive phase for the typical duration of the surge event. However, this is not the case with the late-active and late-inactive phases. A surge that occurs during the late-active phase transitions from the active phase to the inactive phase over its duration and a surge that occurs during the late-inactive phase transitions to the active phase over its duration.

Comparison of the early-active phase and the late-active phase reveals that a larger number of cold-surge events (18 early and 24 late) occur during the late-active phase. Recall that during the early-active phase, the areas of convection associated with the MJO are just beginning to enter the southern part of the South China Sea. However, during the late-active phase, the convection associated with the MJO is maximum over the southern end of the South China Sea. Therefore, it may be inferred that the pressure gradient becomes more enhanced as the MJO transitions from the early-active phase into the late-active phase over the southern end of the South China Sea. Thus producing a more favorable condition for the extension of a surge into the South China Sea. Comparison of the early-inactive phase and late-inactive phase reveals that the late-inactive phase had a larger number of cold-surge events (6 early and 14 late) than the early-inactive phase over the South China Sea. The lack of MJO convection over the equatorial portion of the South China Sea during the early-inactive phase is unfavorable for the extension of a surge equatorward. For a surge event to occur during the inactive

phase, the mid-latitudes and/or pressure-wind pattern of the MJO must be the dominant forcing of the cold-surge event.

The detailed characteristics associated with cold-surges during each of the four MJO phases are examined by construction of composite 1000 hPa winds and convection index fields from 1day to 12 days after day 0 (Appendix B). Different characteristics associated with the phases of the MJO are defined by comparisons between the early-inactive and early-active phases, and between the late-inactive and late-active phases. active and early-/late-inactive phases. Following examination of the daily composites, days 1 through 6 and days 7 through 12 were combined for each of the four phases.

A brief discussion of the comparison of the early-active and early-inactive phases is provided as a basis to the grouping and discussion of the days 1-6 and days 7-12 composites. The early-active and early-inactive phases are analyzed because the typical duration of a surge will occur solely within each phase. Also, the late-active and late-inactive phases are analyzed together due to the change of phase that occur over the duration of the surge event (late- active to early-inactive and late-inactive to early-active).

Analysis of daily charts for each phase of the MJO from day 1 to day 12 revealed that there was a change in the surge characteristics around day 7. For example, the early-inactive phase for day 1 to day 12 of a surge event (Figures B.1.a through B.1.l) provides a clear example of the change in surge characteristics over time. In Figure B.1.a, the Siberian-Mongolian anticyclone over eastern Asia is weak and the northeasterly flow remains near the Asian coastline. From day 2 to day 4 (Figures B.1.b-d), the Siberian-Mongolian anticyclone intensifies and a wider band of northeasterlies is identifiable over the extreme western Pacific. However, from day 5 to day 7 (Figures B.1.e-g), the

Siberian-Mongolian anticyclone migrates eastward and a noticeable weakening in the northeasterly flow occurs. This cycle repeats itself for day 8 through day 12 (i.e. day 8 is similar to the synoptic situation for day 1). Therefore, during the early-inactive phase, the composites indicate that surges vary over synoptic time scales, which last no longer than a week.

For the early-active phase, the characteristics of surge events exhibited little variation from day 1 to day 12. At day 1 (Figure B.2.a), the Siberian-Mongolian anticyclone is relatively weak and the northeasterly flow is narrow along the Asian coastline. When the Siberian-Mongolian anticyclone builds, the northeasterly flow intensifies from day 2 to day 9 (Figures B.2.b to B.2.i) and then begins to weaken such that by day 11 (Figure B.2.k), the synoptic pattern resembles day 1. During the early-active phase, there is an indication that surges last longer than the synoptic-scale surges of the early-inactive phase. Therefore, based on this chart, it is concluded that the persistence of the MJO convection over the equatorial region contributed to maintenance of the northeasterly flow for longer periods of time. Due to the identification of the synoptic-scale duration of typical surges in the day 1 to day 12 composites and in the time series of v-components (Figure 6), the individual day composites were averaged from day 1 to day 6 and day 7 to day 12 for each phase. Following the examination of these averaged composites, the differences between the early-active and early-inactive phases (day 1 to day 6 and day 7 to day 12) will be examined, as well as the differences between the late-active and late-inactive phases (day 1 to day 6 and day 7 to day 12).

The composites of the early-active and early-inactive phases averaged from day 1 to day 6 are examined first (Figure 9). During the early-active phase, the MJO

convection becomes established over the extreme southern portion of the South China Sea (Figure 9a). Northeasterly flow dominates the extreme western Pacific and the East and South China Seas. The Siberian-Mongolian anticyclone is well established and is located over eastern Asia. The composite of the early-inactive phase (Figure 9b) averaged from day 1 to day 6 defines a lack of convection over the South China Sea. The Siberian-Mongolian anticyclone is also established over eastern Asia with northeasterly flow persisting over the extreme western Pacific. The differences between the early-active and early-inactive phase (Figure 9.c) indicates that the northeasterly flow over the East and South China Seas is stronger during the early-active phase. This is attributed to the presence of enhanced convection due to the active MJO, which acts to produce an increased pressure gradient over the South China Sea and stronger northeasterly flow. The Siberian-Mongolian anticyclone is stronger for the early-inactive phase as defined by the cyclonic difference over eastern Asia. Although the northeasterly flow during the early-active phase is larger than during the early-inactive phase, the mid-latitude forcing of cold-surges is larger during the early-inactive phase. Therefore, it appears that the enhanced convection influences the surge winds to a greater extent than the mid-latitude forcing by the Siberian-Mongolian anticyclone.

Next, the composites of the early-active and early-inactive phases averaged from day 7 to day 12 are examined. During days 7-12 of the early-active phase (Figure 10a), there is considerably more convection over the South China Sea than during the day 1-6 average composite (Figure 9a). The Siberian-Mongolian anticyclone is still present over eastern Asia and the northeasterly flow over the western Pacific covers a larger area during days 1-6 (Figure 9a). During the early-inactive phase there is much reduced

convection over the South China Sea. Also, the Siberian-Mongolian anticyclone over eastern Asia is reduced from days 1-6 while flow along the Asian coastline also appears to have weakened. The difference (Figure 10.c) between the early-active and early-inactive phase averaged from day 7 to day 12 reveals much stronger northeasterly flow over the extreme western Pacific, and East and South China Seas during the day 7-12 early-active phase. The difference in convection over the region has also increased from day 7-12 (Figure 10.c) than that from day 1-6 (Figure 9.c). The strength of the Siberian-Mongolian anticyclone over eastern Asia appears to be similar during the two phases since the cyclonic differences over eastern Asia in Figure 9.c are no longer evident in Figure 10.c.

Comparison of the day 1-6 and day 7-12 composites suggests that the longer time scales of the MJO convection dominates the synoptic-scale variation of the Siberian-Mongolian anticyclone. The cyclonic difference over eastern Asia during the day 1-6 do not persist to day 7-12, while the difference in northeasterly flow over the South China Sea increase from day 1-6 to day 7-12. Therefore, surges during the early-active phase persist well into the second week. The persistence of MJO convection in the equatorial region contributes to the persistence of the northeasterly flow regime. During the early-inactive phase, surges persist on a synoptic time scale, which is no longer than a week.

The composites of the late-active and late-inactive phases averaged from day 1 to day 6 are examined (Figure 11a and 11b). During the late-active phase (Figure 11a), there is considerable convection over the South China Sea. The Siberian-Mongolian anticyclone over eastern Asia contributes to a broad band of northeasterly flow over the western Pacific, and the East and South China Seas. There is little or no convection over

the South China Sea during the late-inactive phase (Figure 11b). The Siberian-Mongolian anticyclone appears weak and as a result, the northeasterly flow is weak. The difference chart between the late-active and late-inactive phases (Figure 11.c) averaged from day 1 to day 6 indicates that the northeasterly flow over the South China Sea is stronger during the late-active phase. There is very little difference between the intensity of the Siberian-Mongolian anticyclone during the late-active and late-inactive phases. The subtropical ridge is much stronger during the late-inactive phase than the late-active phase since there is a cyclonic difference over a broad subtropical region.

The late-active and late-inactive phases (Figures 12a and 12b) averaged from day 7 to day 12 are examined. During the late-active phase day 7-12 (Figure 12a), the convection associated with the MJO has shifted to the east as the MJO signal propagates eastward. There is also a noticeable increase in northerly flow over the western Pacific between 120E and 180E. During the late-inactive phase day 7-12 (Figure 12b), the convection over the South China Sea has increased slightly as has northeasterly flow between 120E to 180E. However, only over the South China Sea did the northeasterly flow extend to the equator during the late-inactive phase (Figure 12b). The differences between the late-active and late-inactive phases (Figure 12.c) averaged from day 7 to day 12 define southwesterly flow over the South China Sea, which indicates that the northeasterly flow over this region associated with the late-inactive phase is stronger than the late-active phase. The Siberian-Mongolian anticyclone appears to be stronger during the late-inactive phase as indicated by cyclonic flow over eastern Asia. The difference in convection over the South China Sea appears to have decreased, while it has increased along the equator northeast of Australia.

From the difference charts for both the late-active and late-inactive phases from day 1 to day 6 and from day 7 to day 12, surges during the late-active phase are shorter in duration than those seen with the early-active phase. Therefore, the transition of the MJO from the late-active phase into the early-inactive phase results in a shortened surge duration. However, during the late-inactive phase, surges dominated by the mid-latitude forcing of the stronger Siberian-Mongolian anticyclone are longer in duration due to mid-latitude forcing and increased convection, as the late-inactive phase transitions into the early-active phase by the second week.

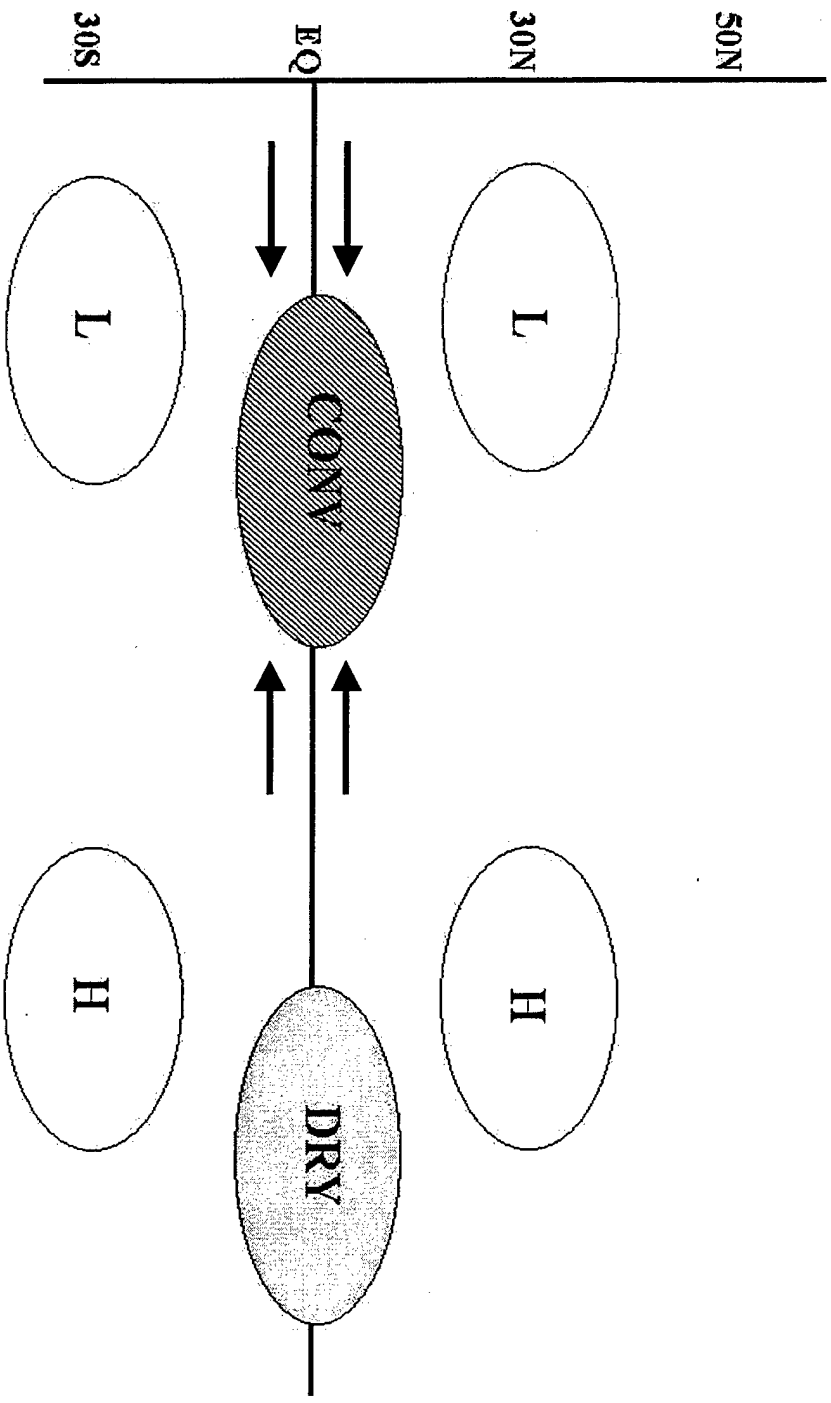

Figure 4. A schematic of the "typical" pressure-wind and convection pattern associated with the MJO during active and inactive phases.

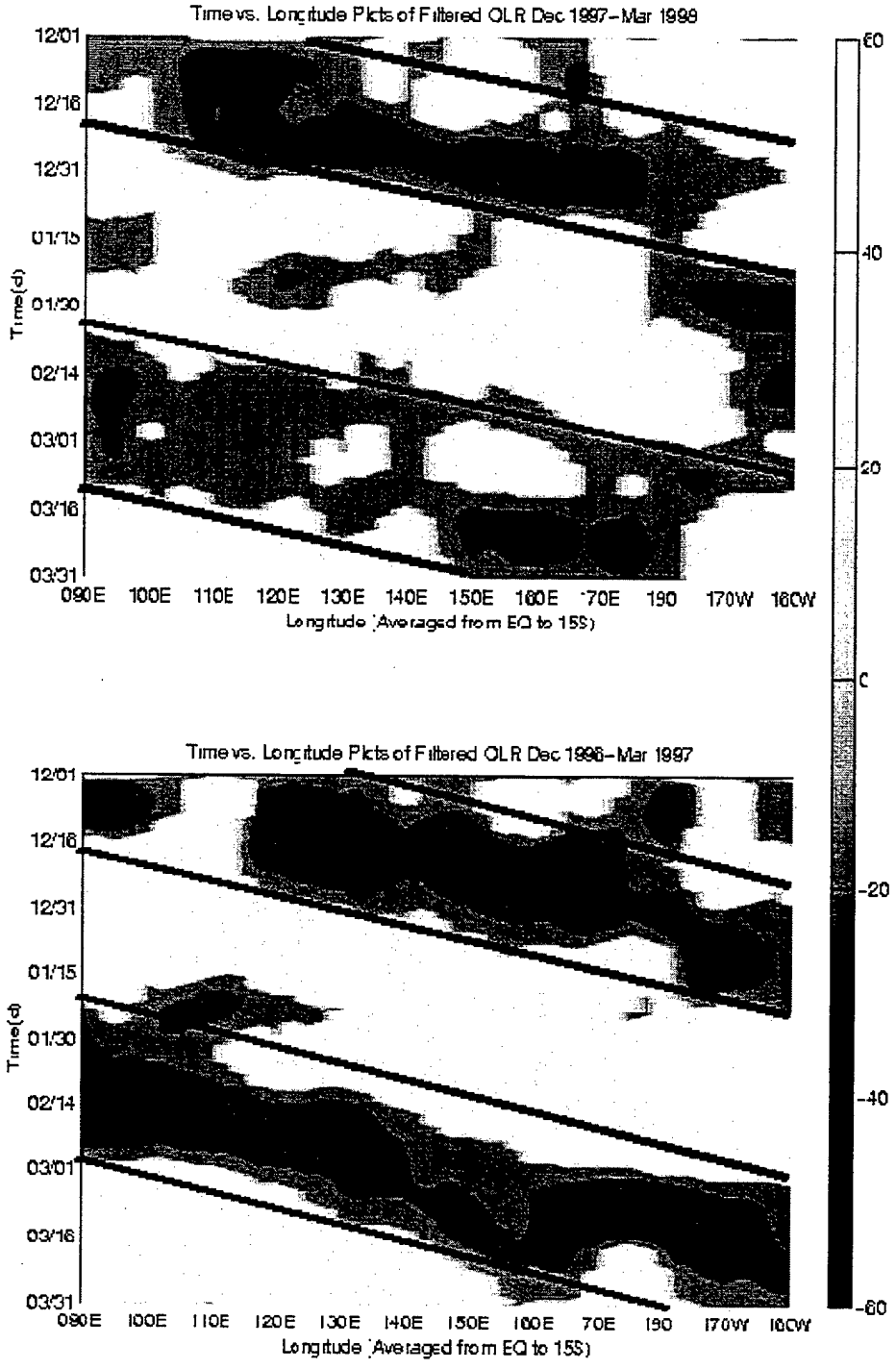

Figure 5. Time-Longitude plots of filtered convection index based on OLR data from 1979 to 1998 during the northern winter monsoon. The convection index was averaged between the equator and 15S. Units are in Wm^{-2}. Individual eastward-propagating MJO events are marked with diagonal black lines.

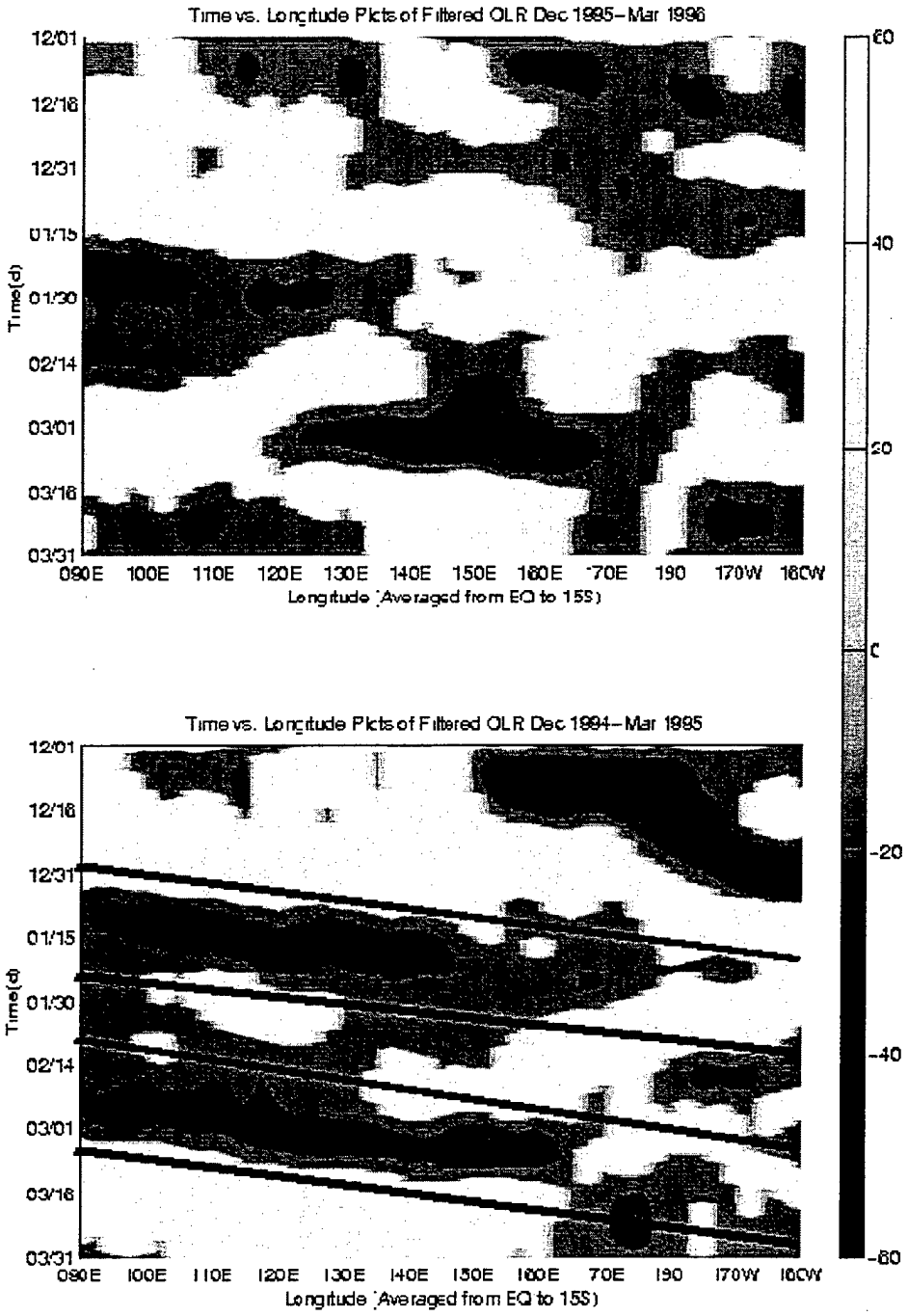

Figure 5. Continued.

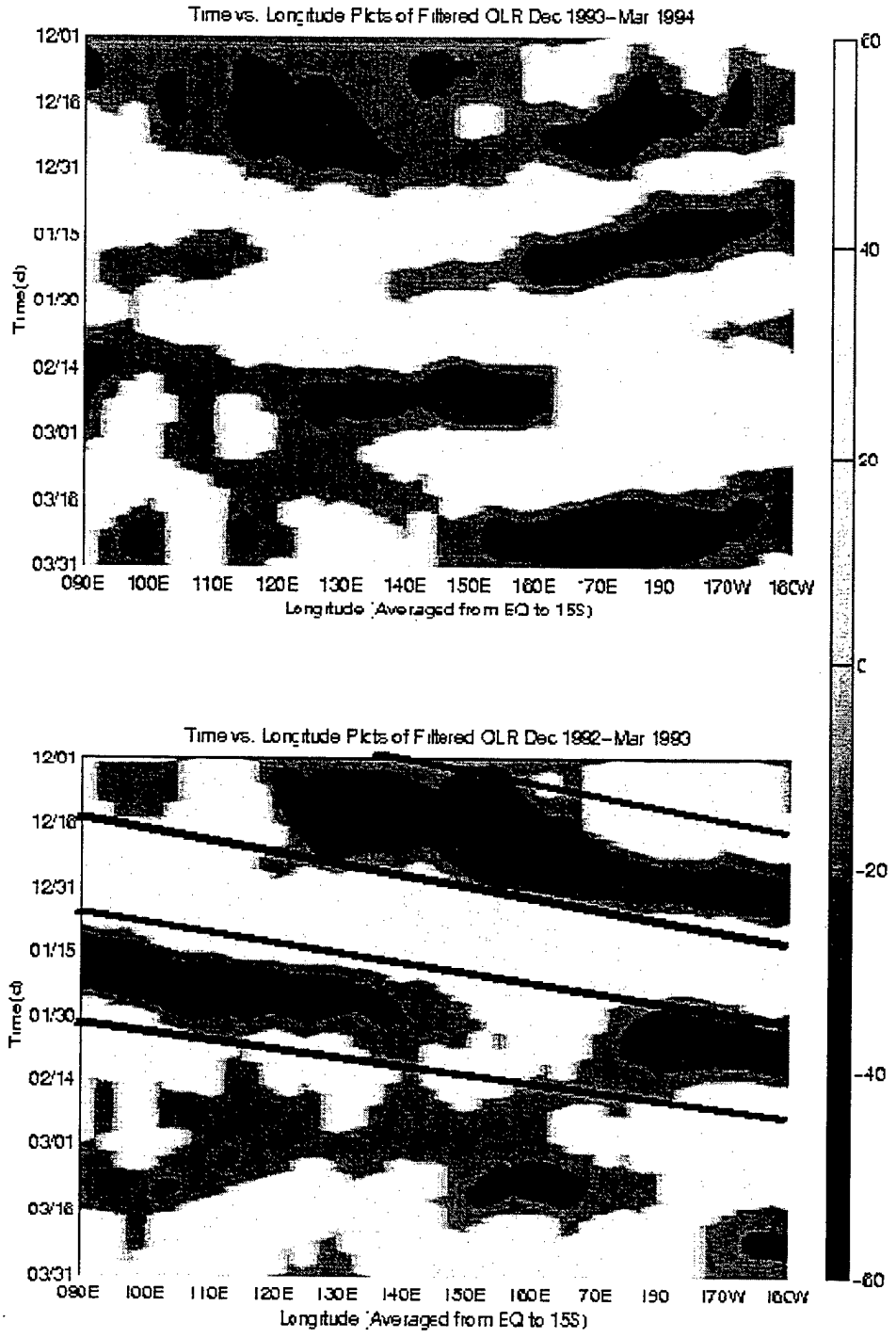

Figure 5. Continued.

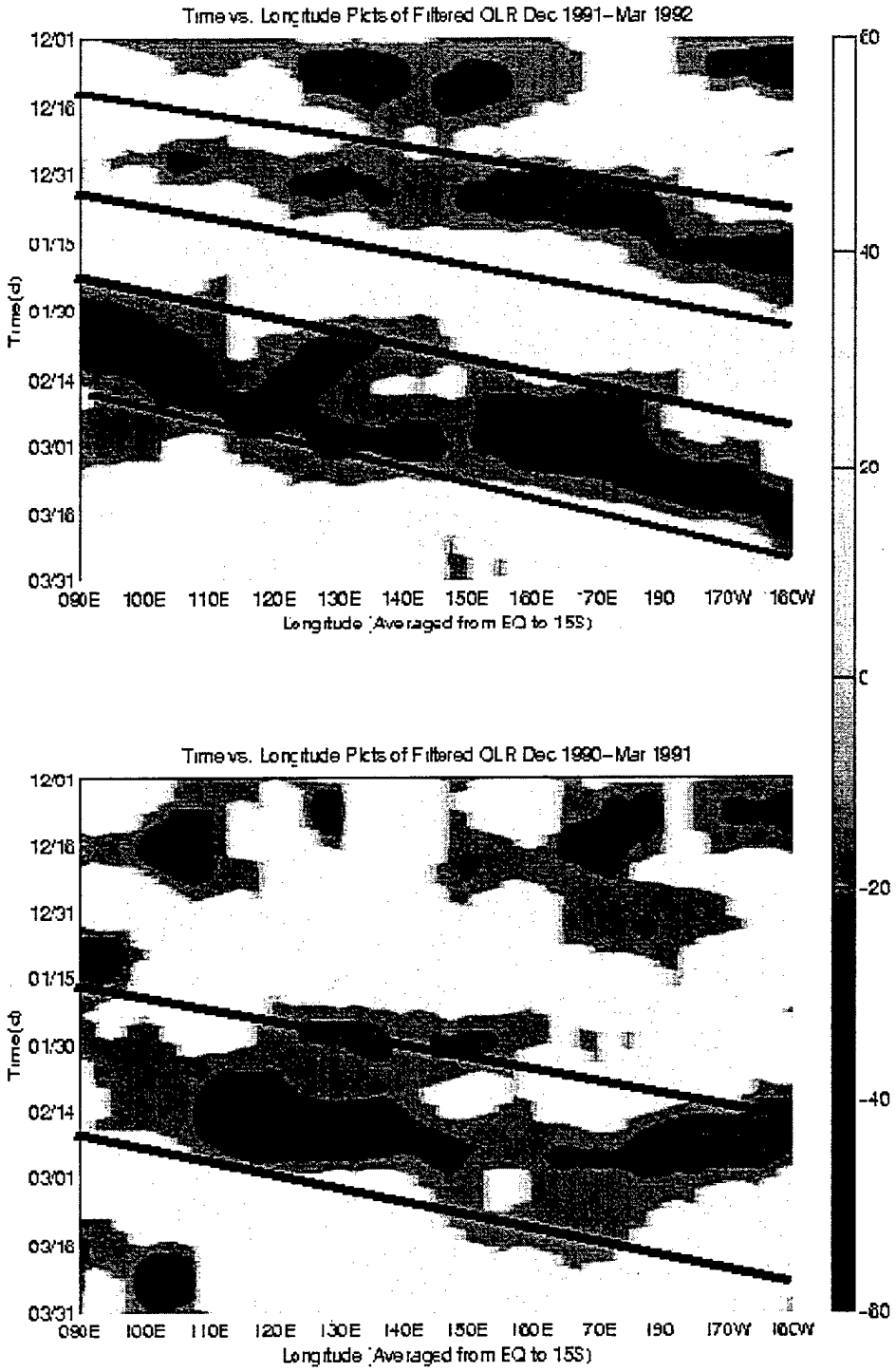

Figure 5. Continued.

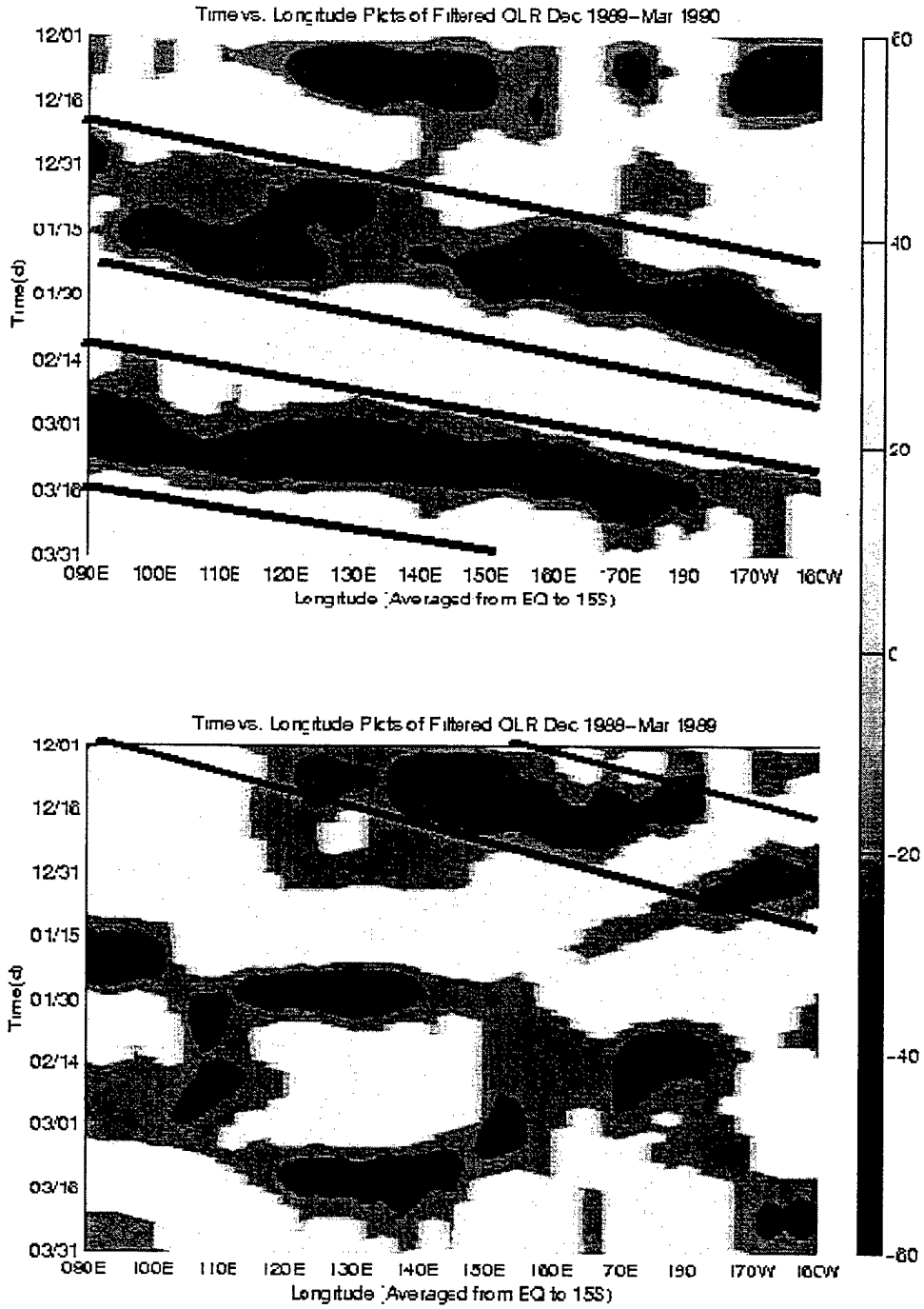

Figure 5. Continued.

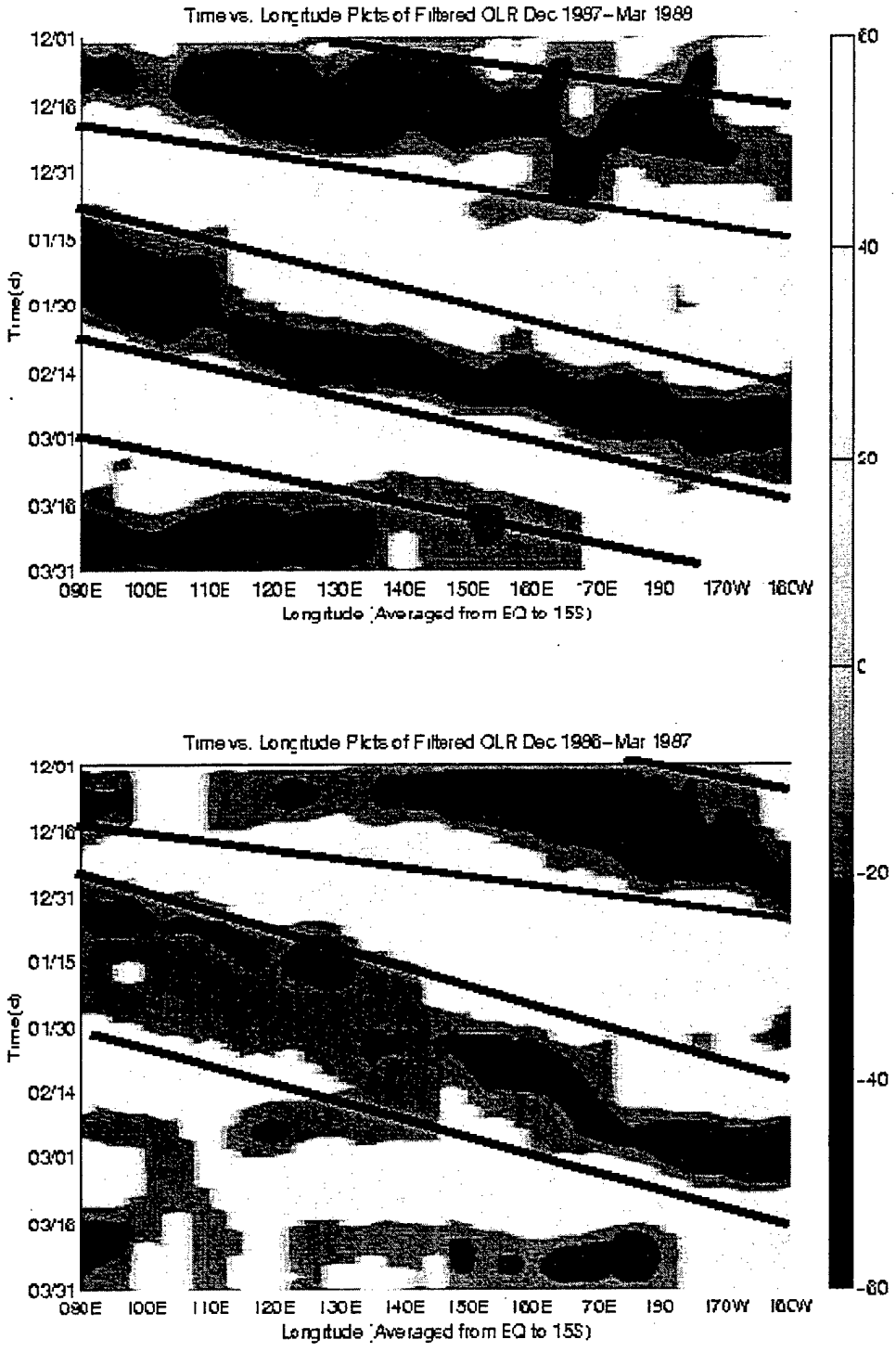

Figure 5. Continued.

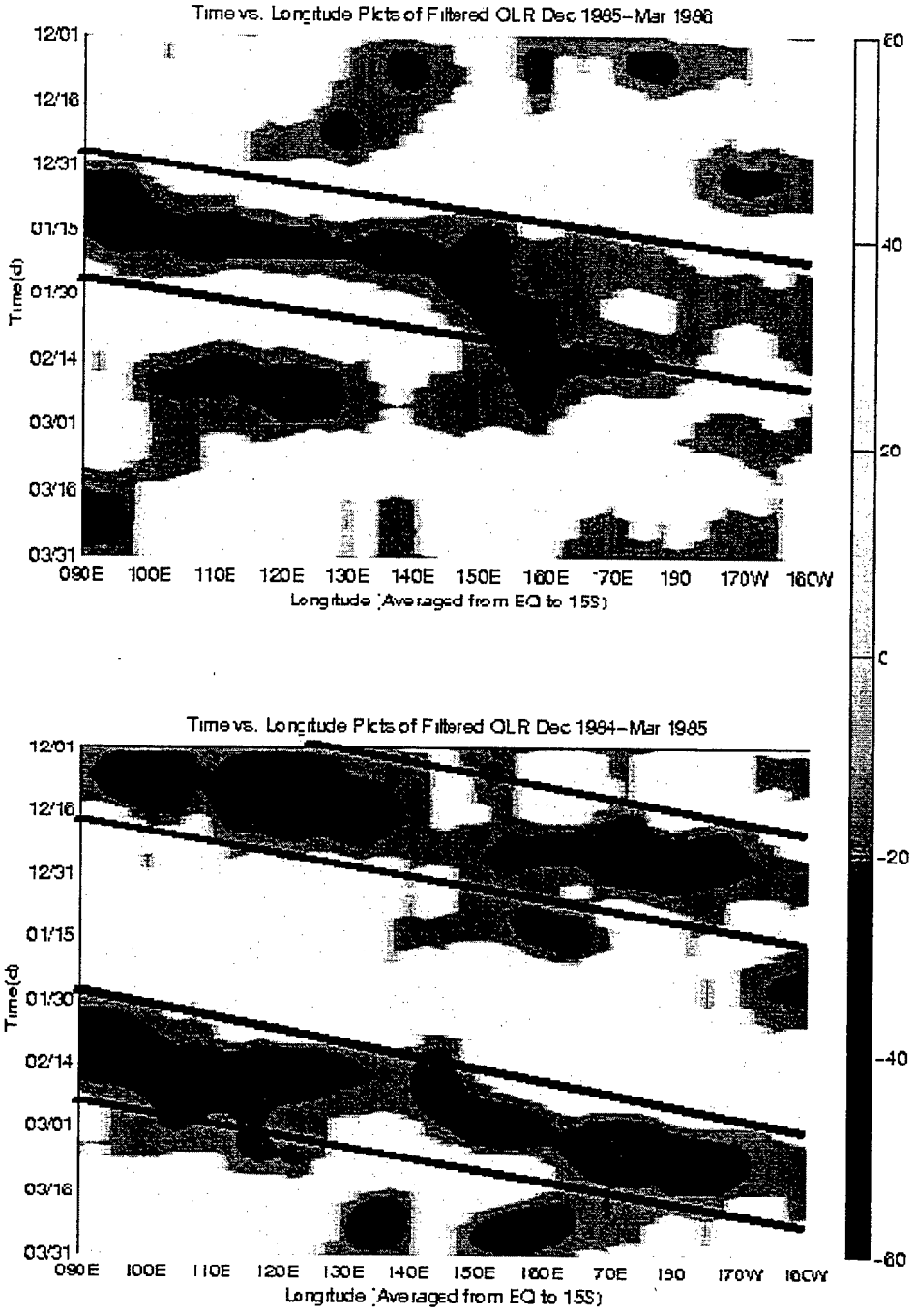

Figure 5. Continued.

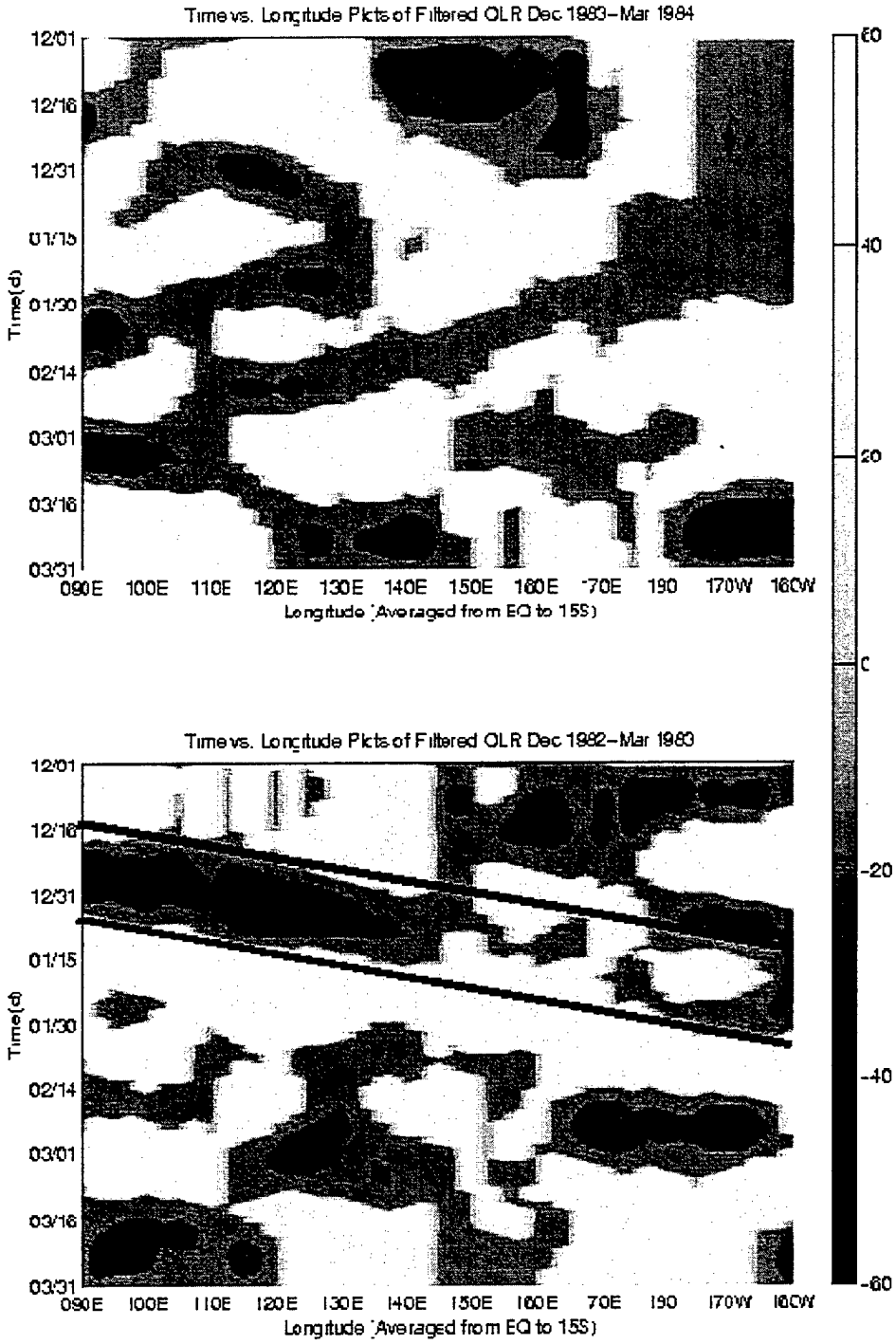

Figure 5. Continued.

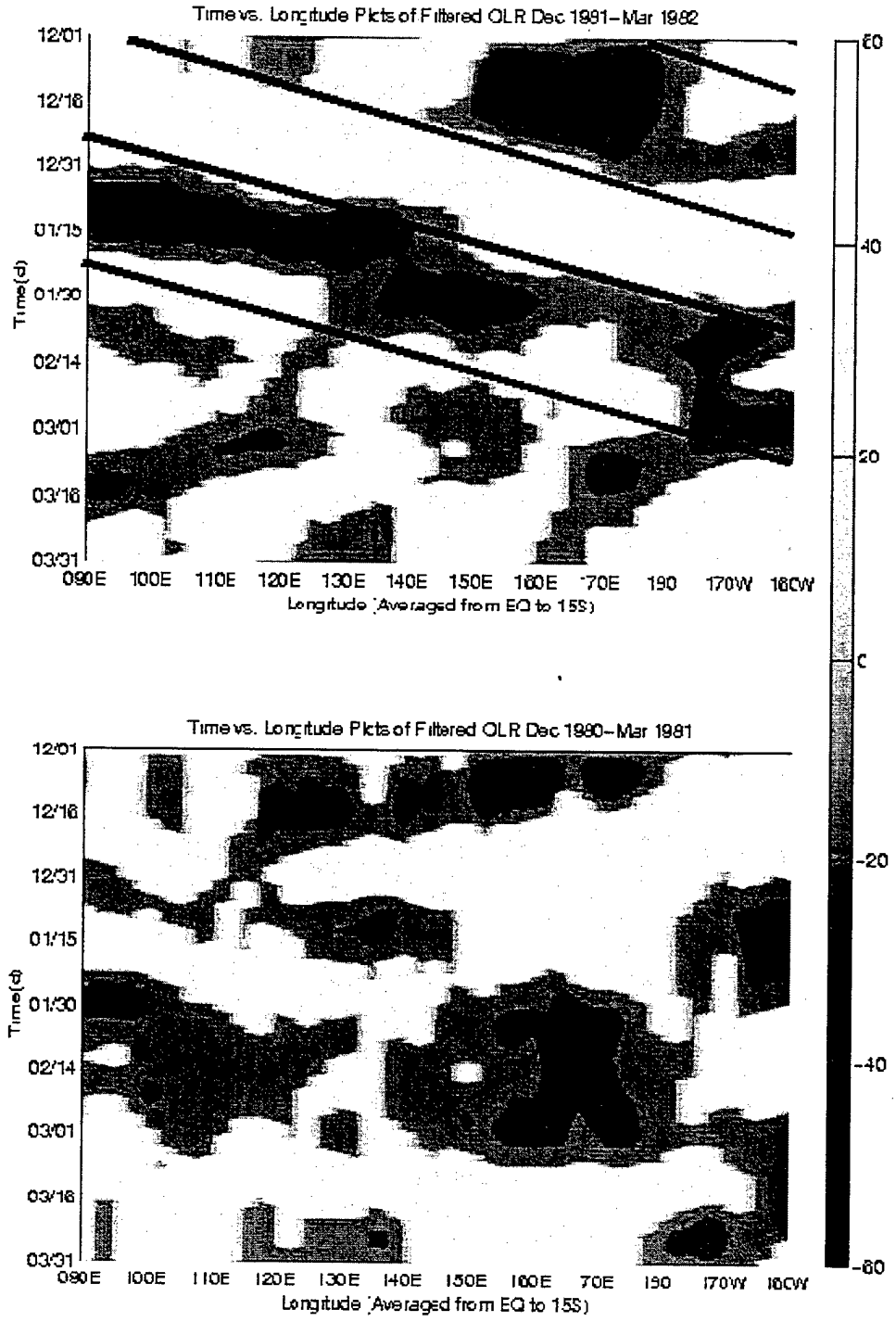

Figure 5. Continued.

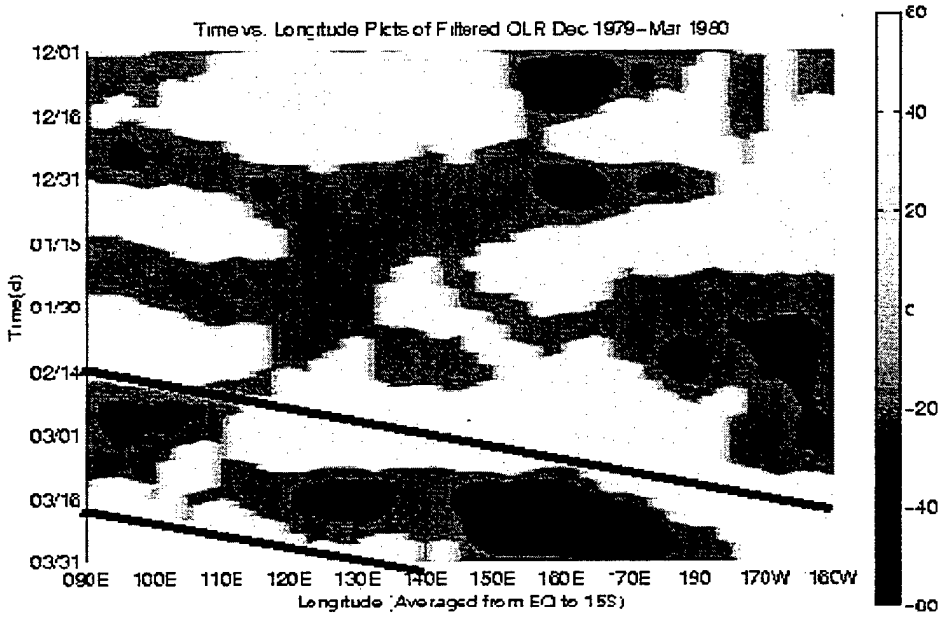

Figure 5. Continued.

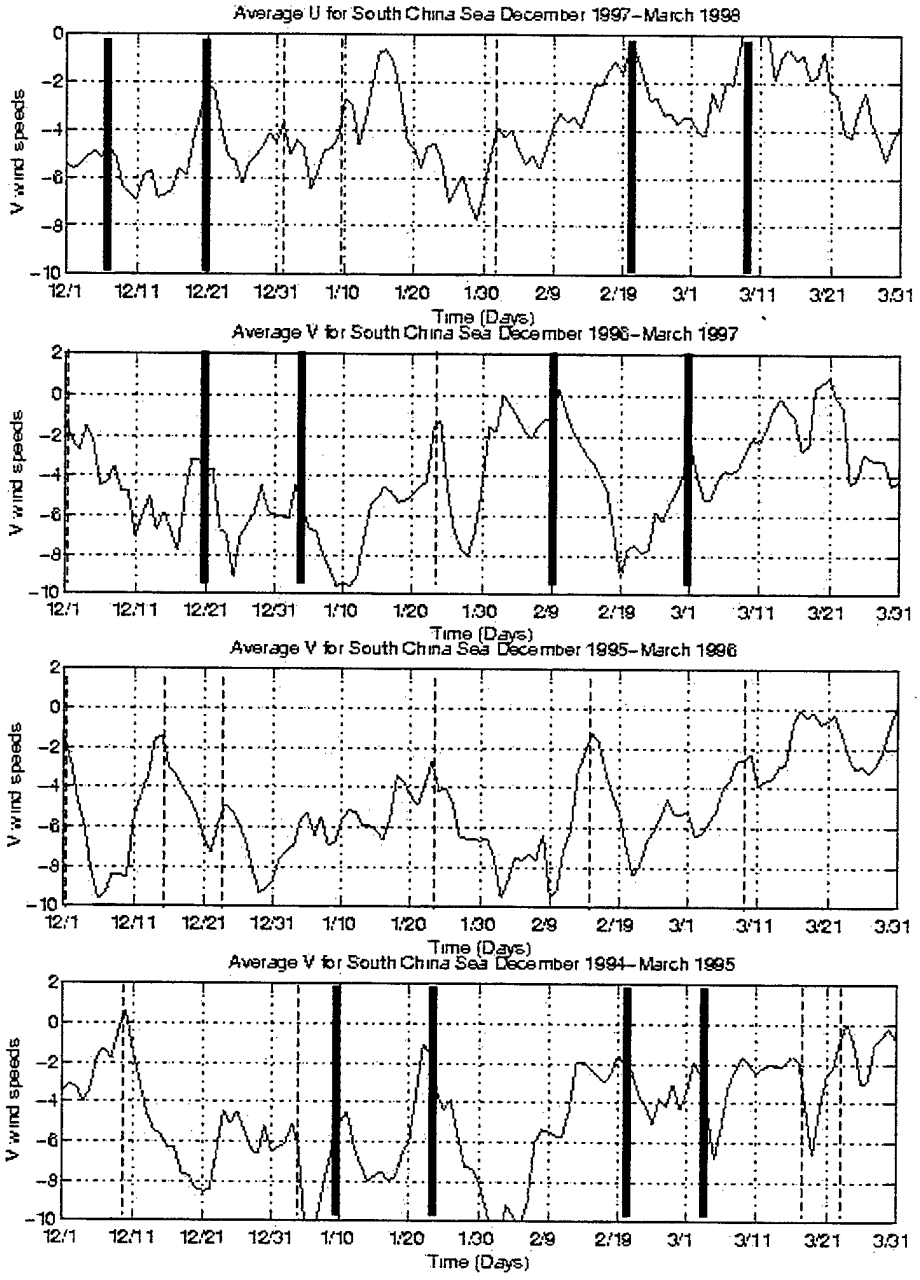

Figure 6. Time series of the v wind component averaged along 7.5N and between 105E-115E. Northeasterly winds are indicated by negative values. The solid line represents Day 0 of cold surge events associated with MJO and the dashed line represents Day 0 of cold surge events not associated with the MJO.

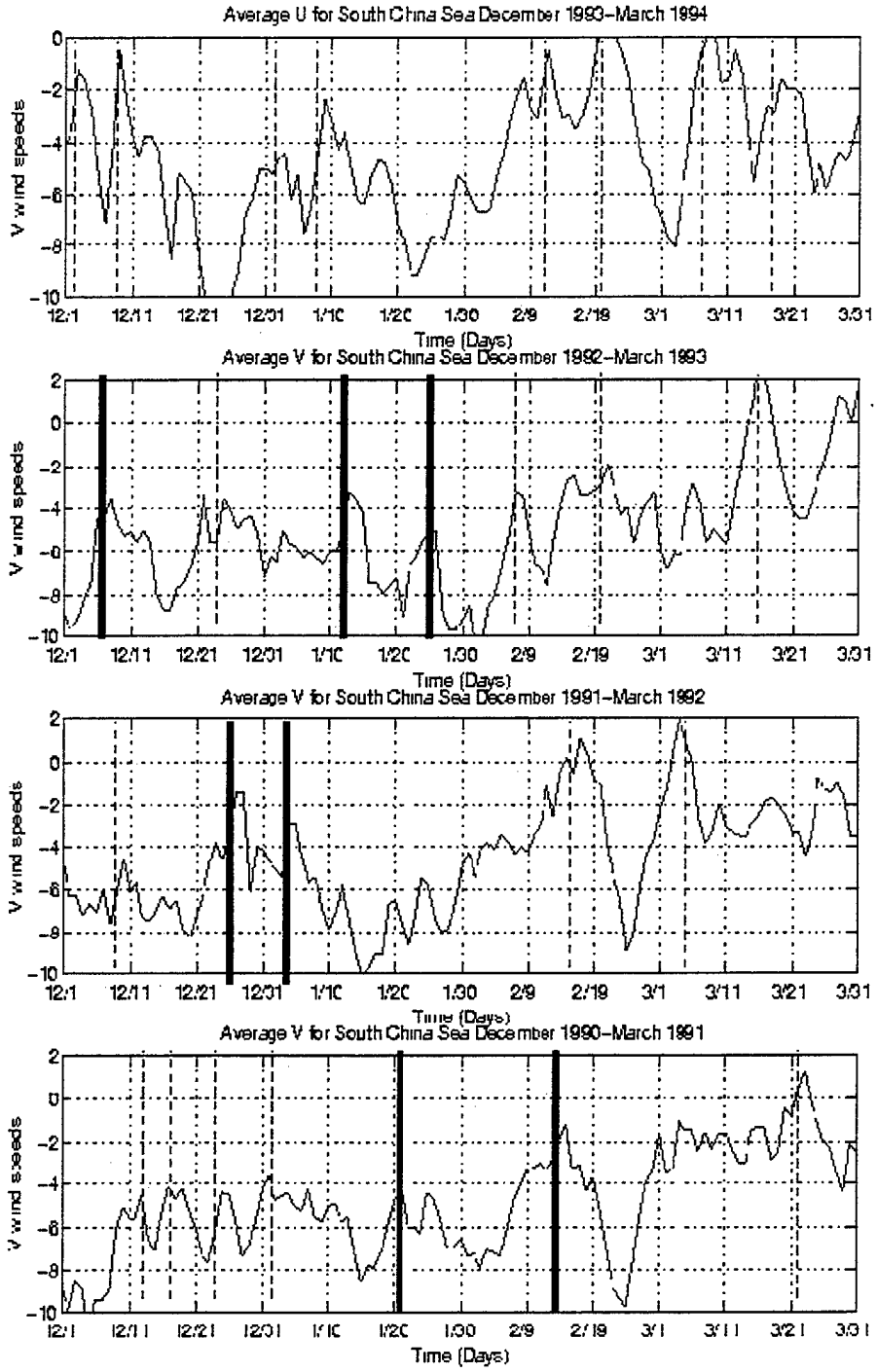

Figure 6. Continued.

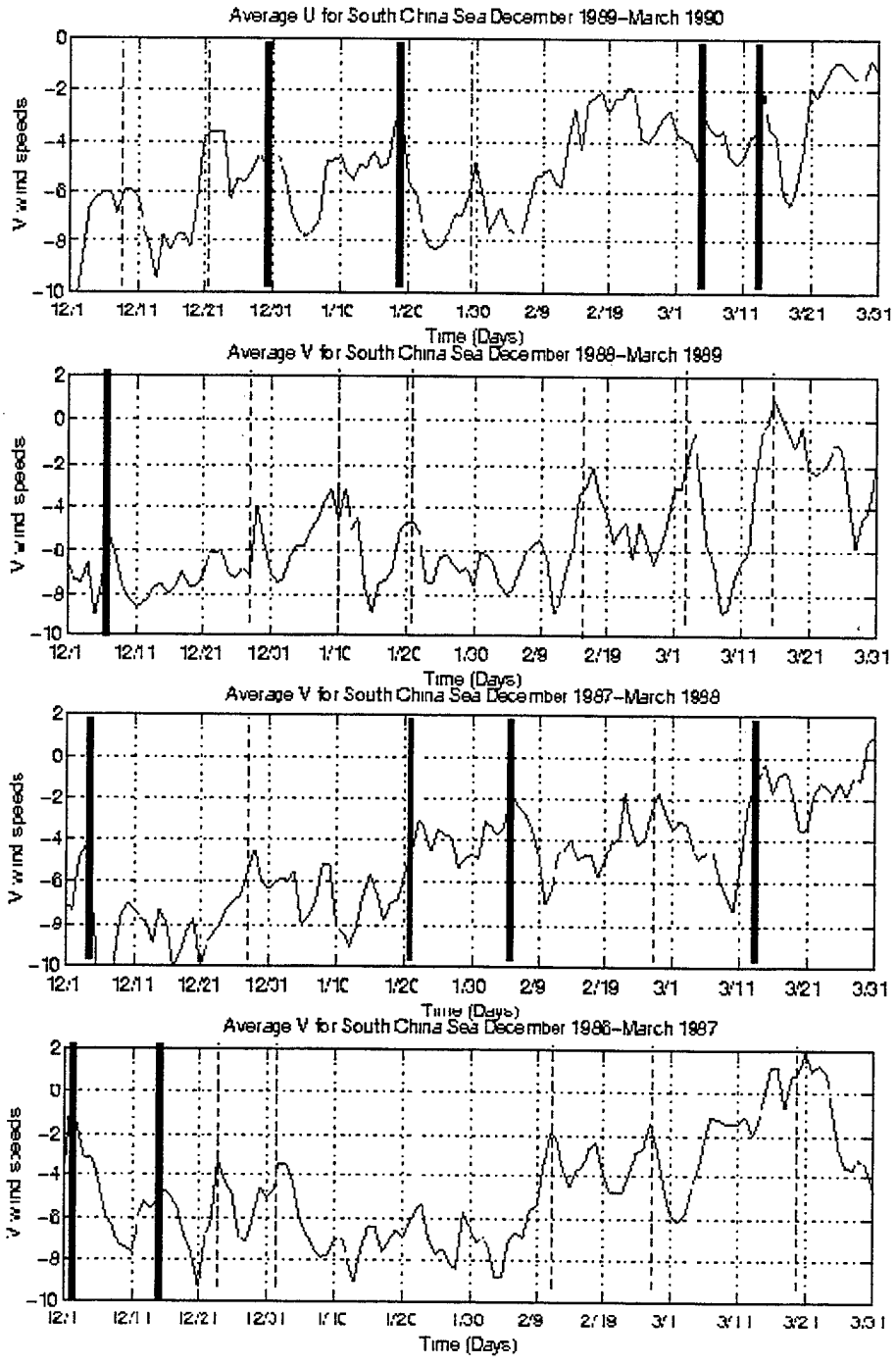

Figure 6. Continued.

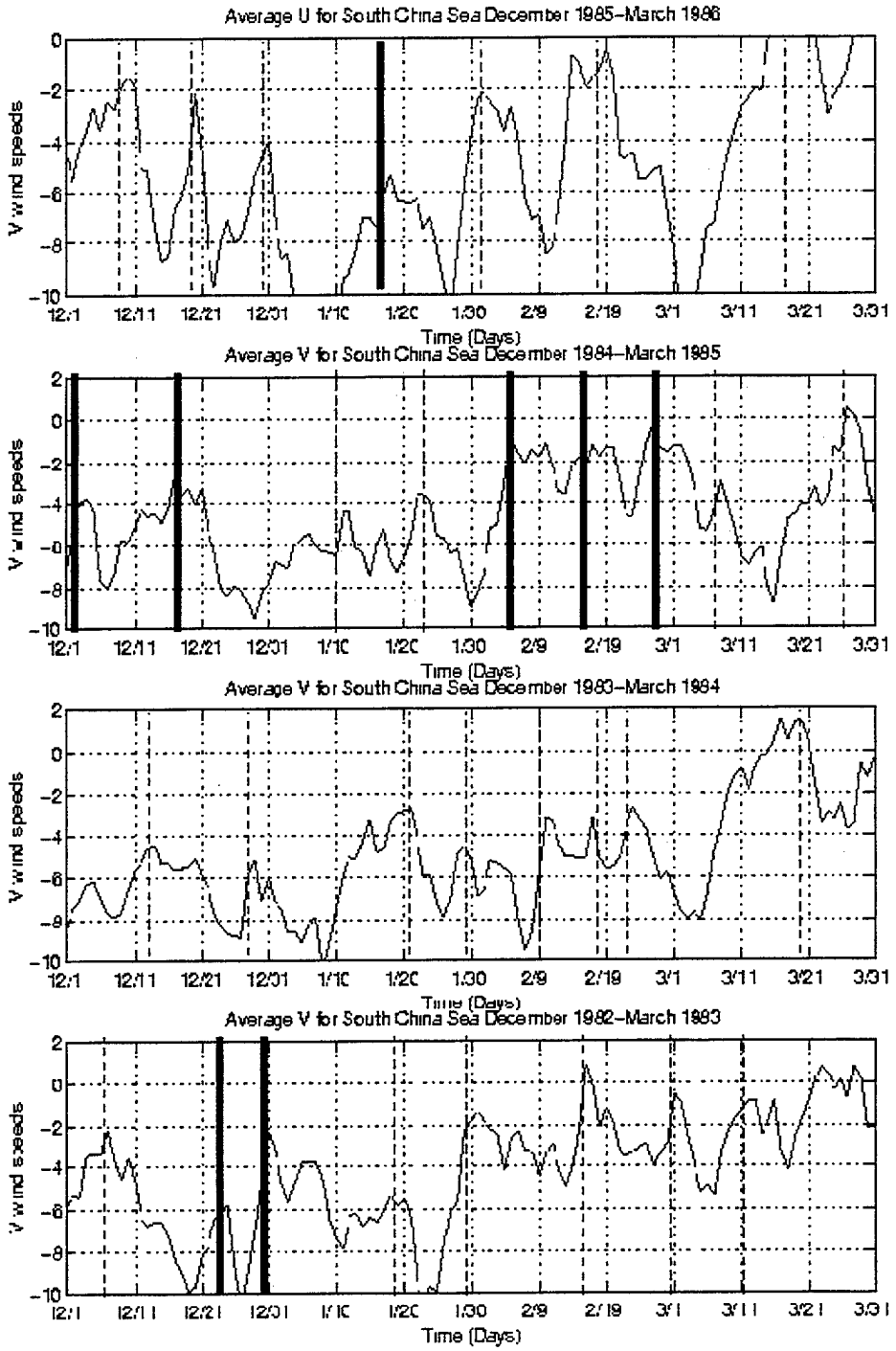

Figure 6. Continued.

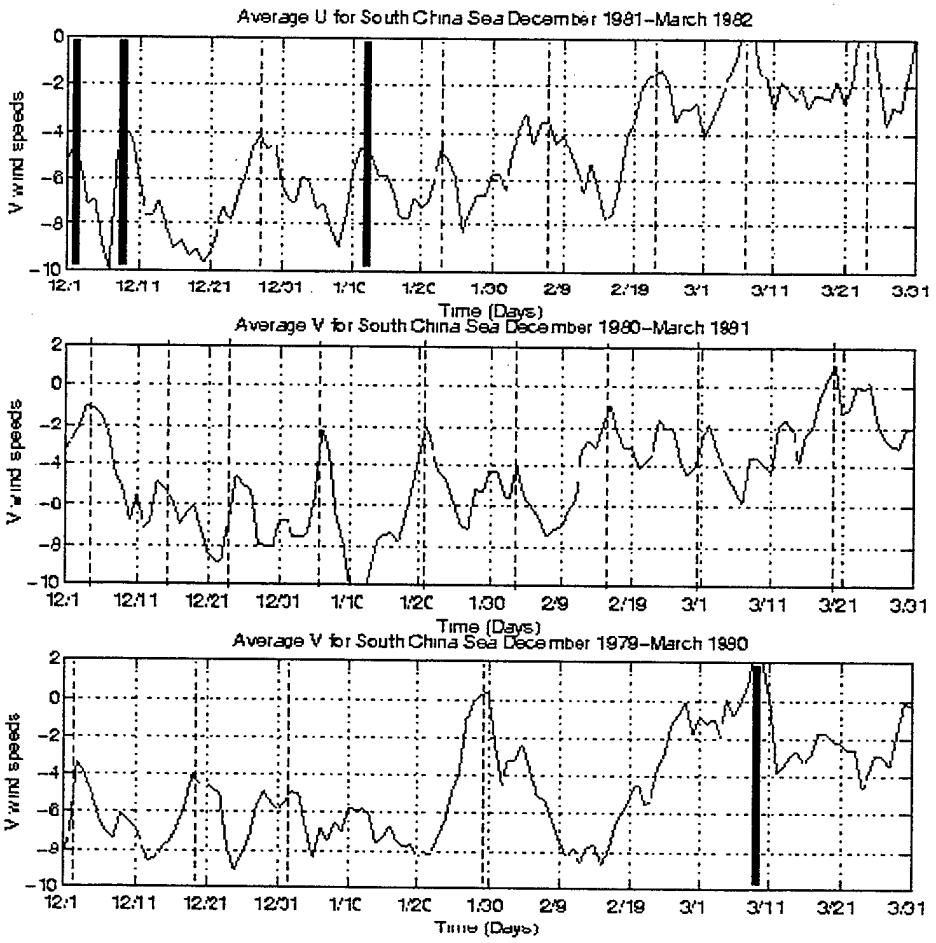

Figure 6. Continued.

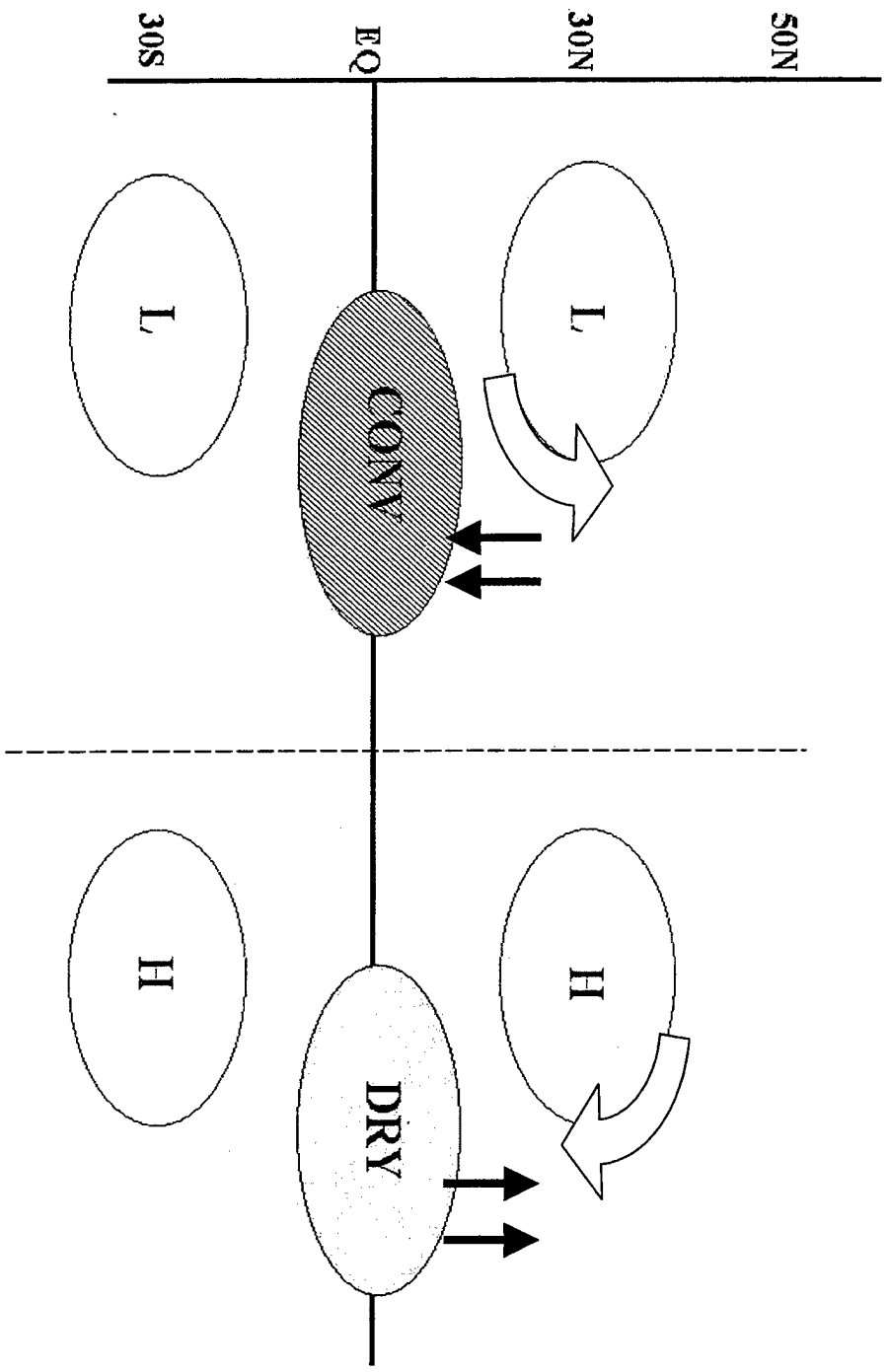

Figure 7. Schematic of the pressure-wind pattern and convection pattern for the MJO (as in Figure 4) modified to include the influence of MJO convection (bold solid arrows) and MJO pressure-wind pattern (open arrows) on cold-surge northerly winds that would be superimposed on the MJO features.

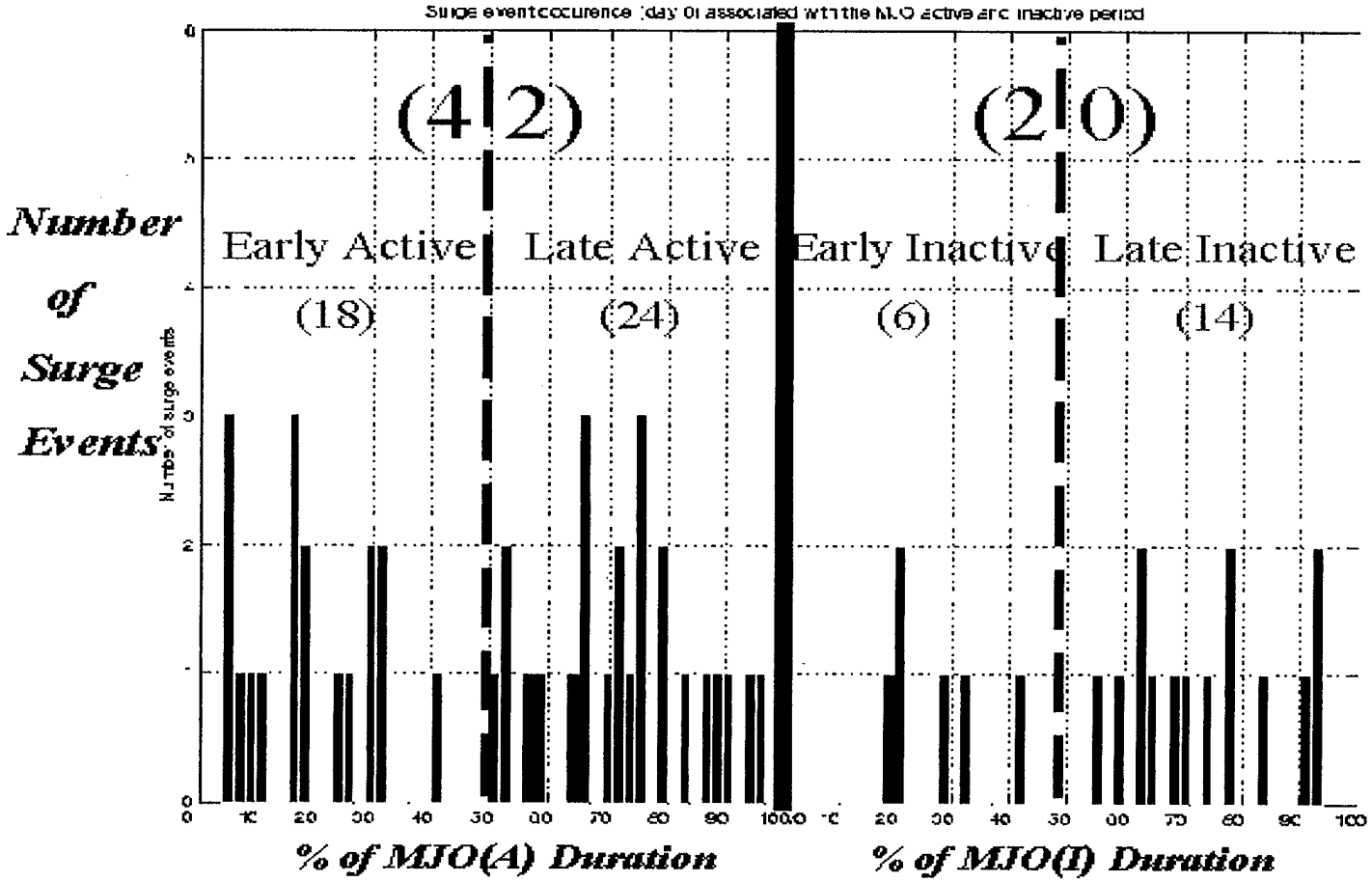

Figure 8. Histogram of surge events associated with the MJO.

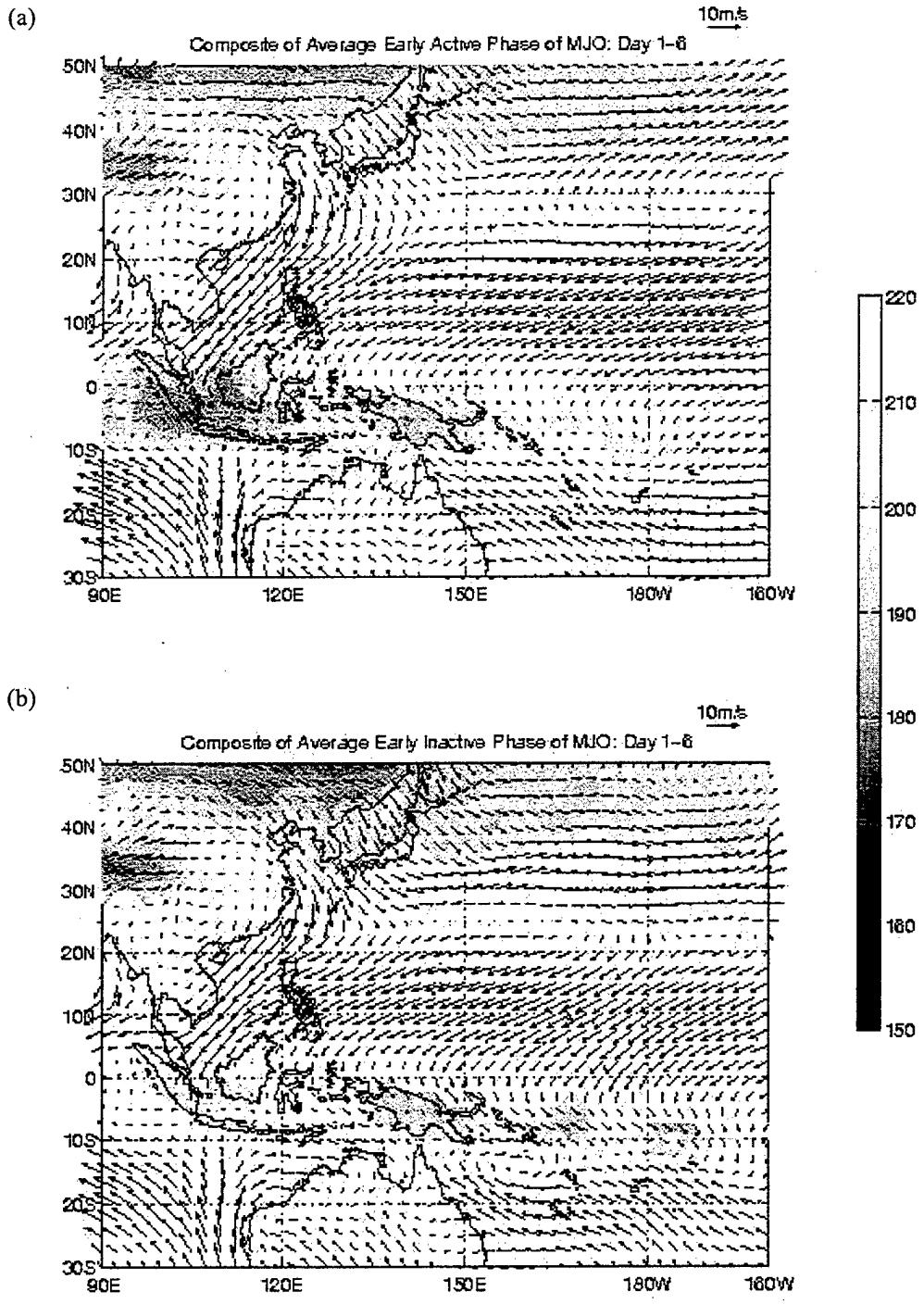

Figure 9. Composite analysis of averaged 1000 hPa winds and convection for surge events during the (a) early-active and the (b) early-inactive phases averaged from day 1 to day 6.

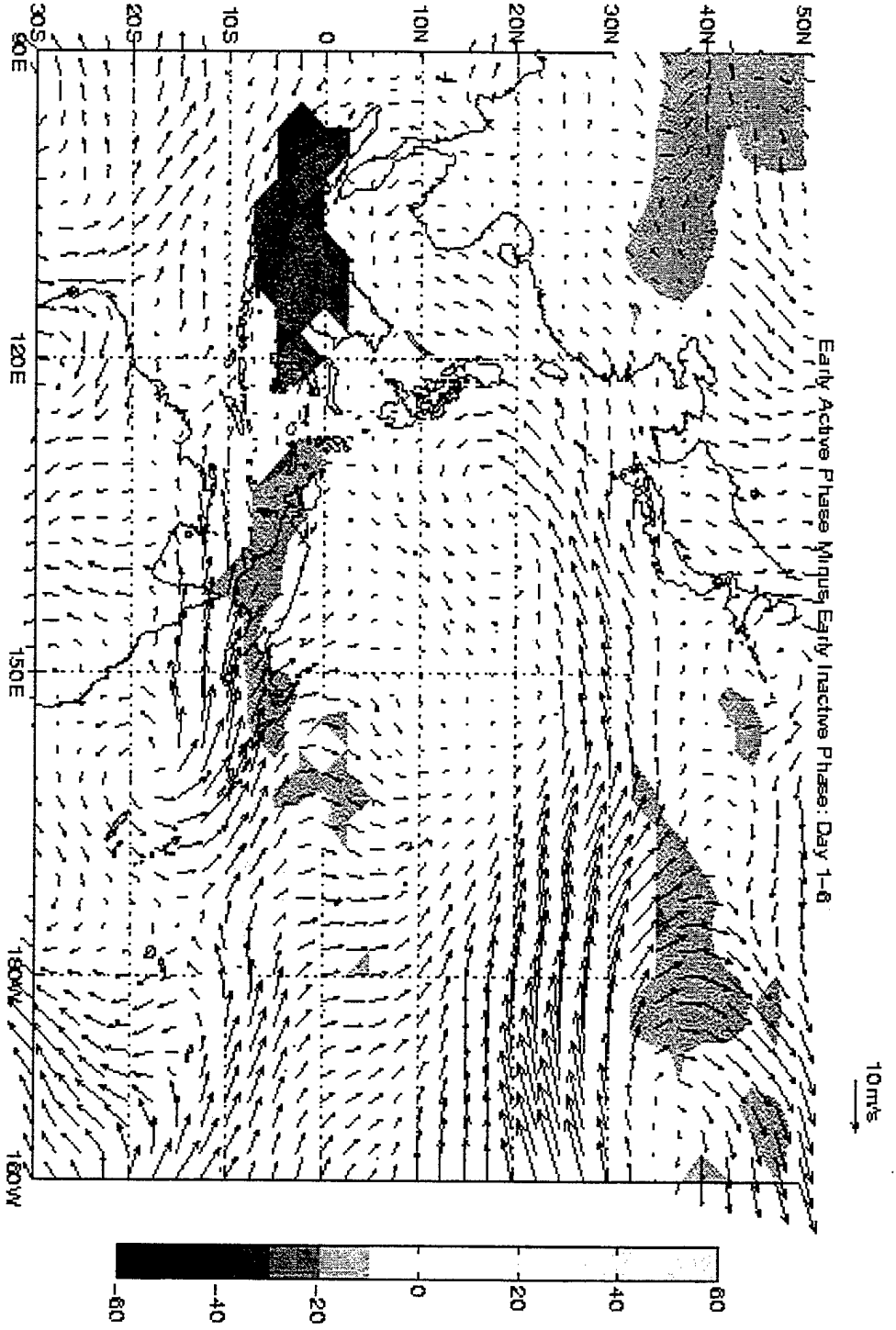

Figure 9.c. Difference between surge events during the early-active and early-inactive phases averaged from day 1 to day 6.

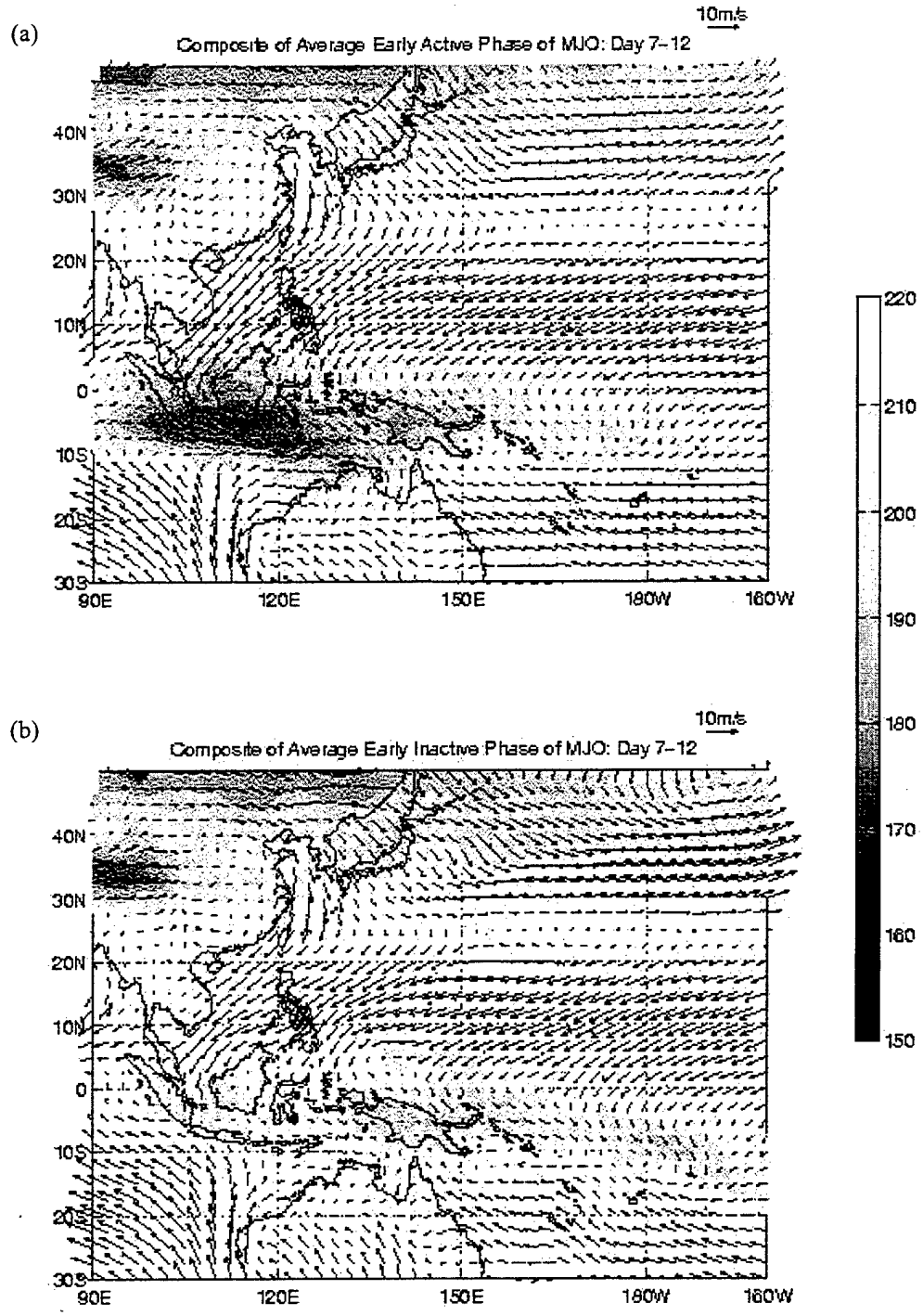

Figure 10. Composite analysis of averaged 1000 hPa winds and convection for surge events during the (a) early-active and the (b) early-inactive phases averaged from day 1 to day 7.

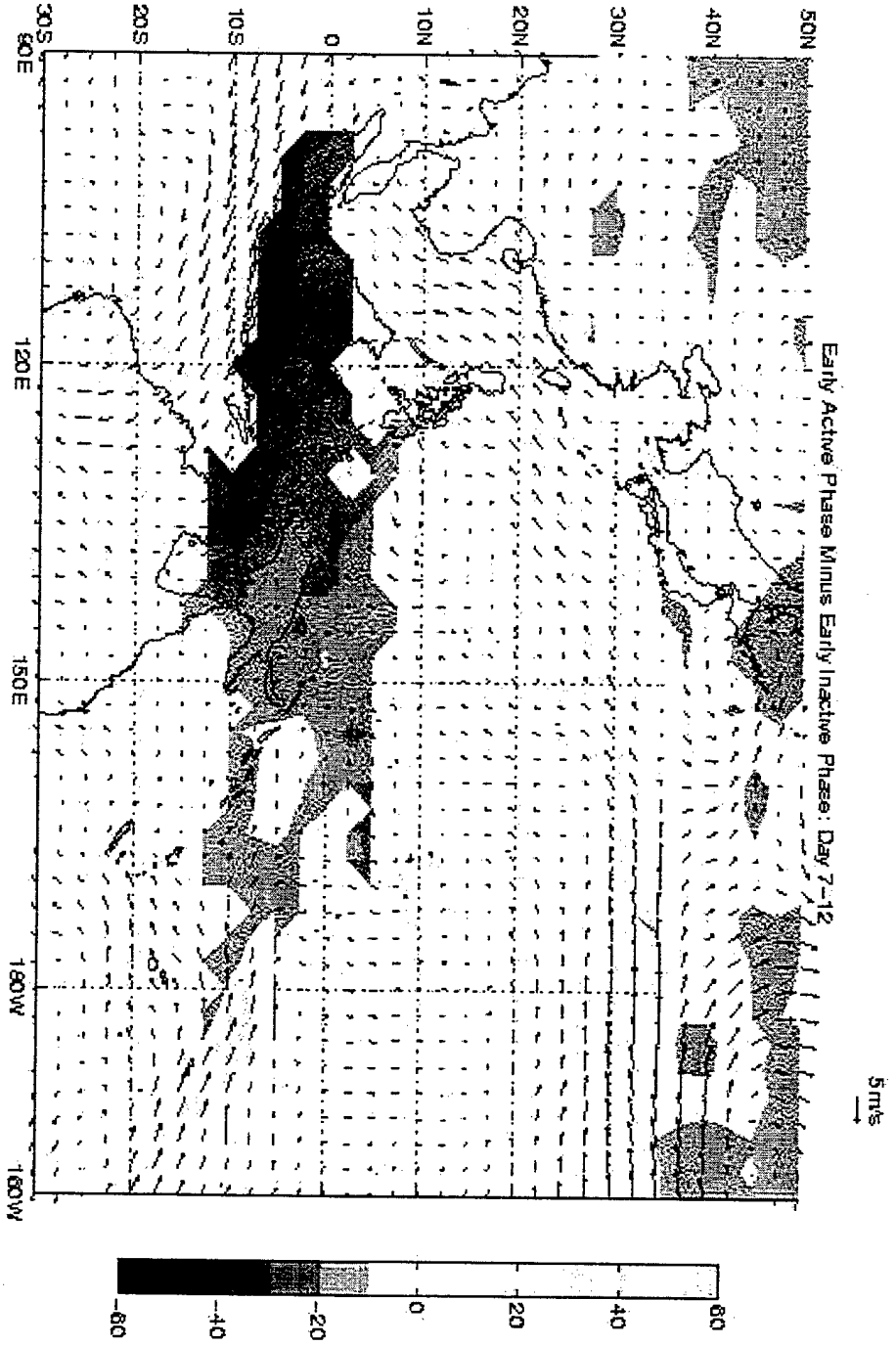

Figure 10.c. Difference between surge events during the early-active and early-inactive phases averaged from day 7 to day 12.

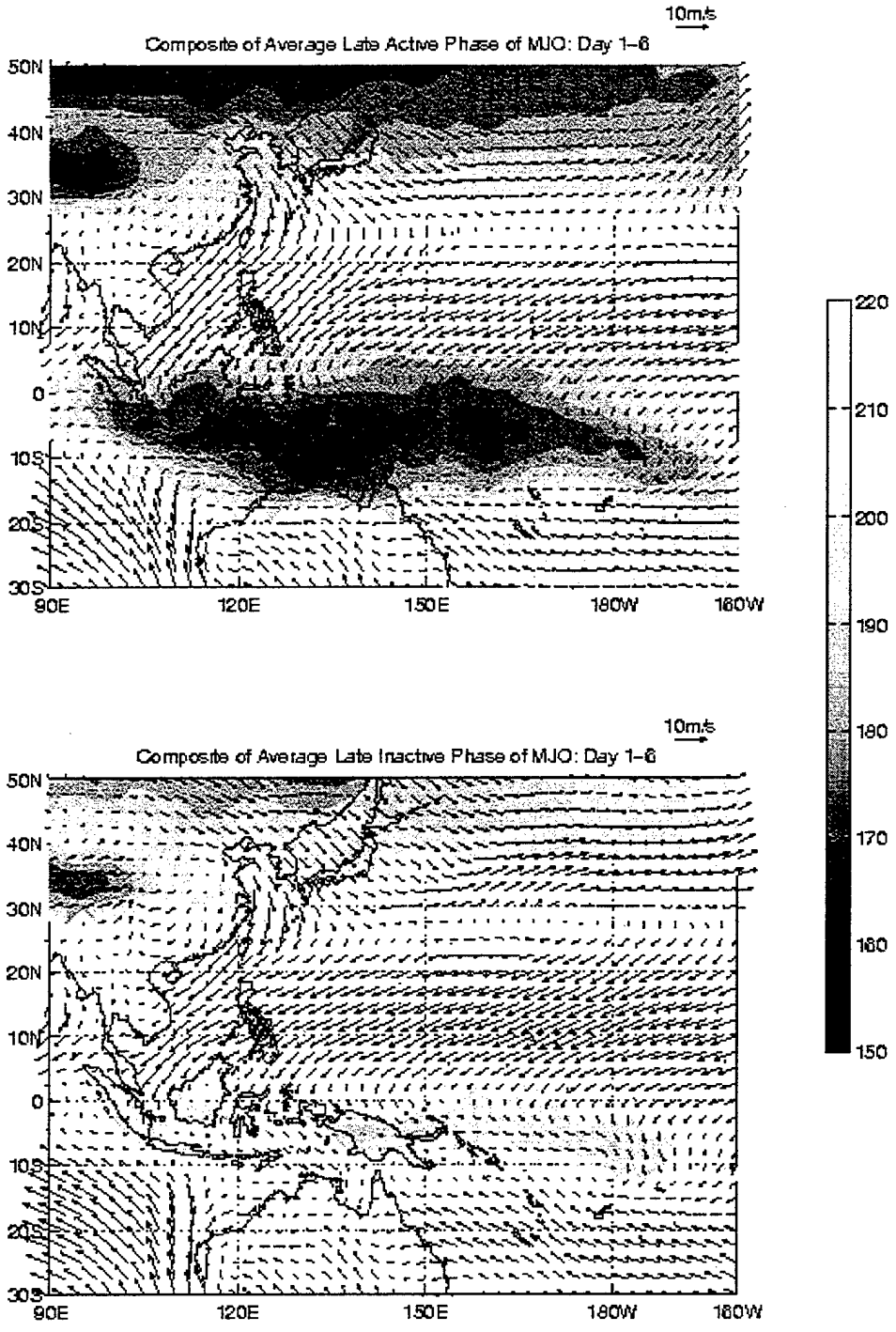

Figure 11. Composite analysis of averaged 1000 hPa winds and convection for surge events during the (a) late-active and the (b) late-inactive phases averaged from day 1 to day 6.

Figure 11.c. Difference between surge events during the late-active and late-inactive phases averaged from day 1 to day 6.

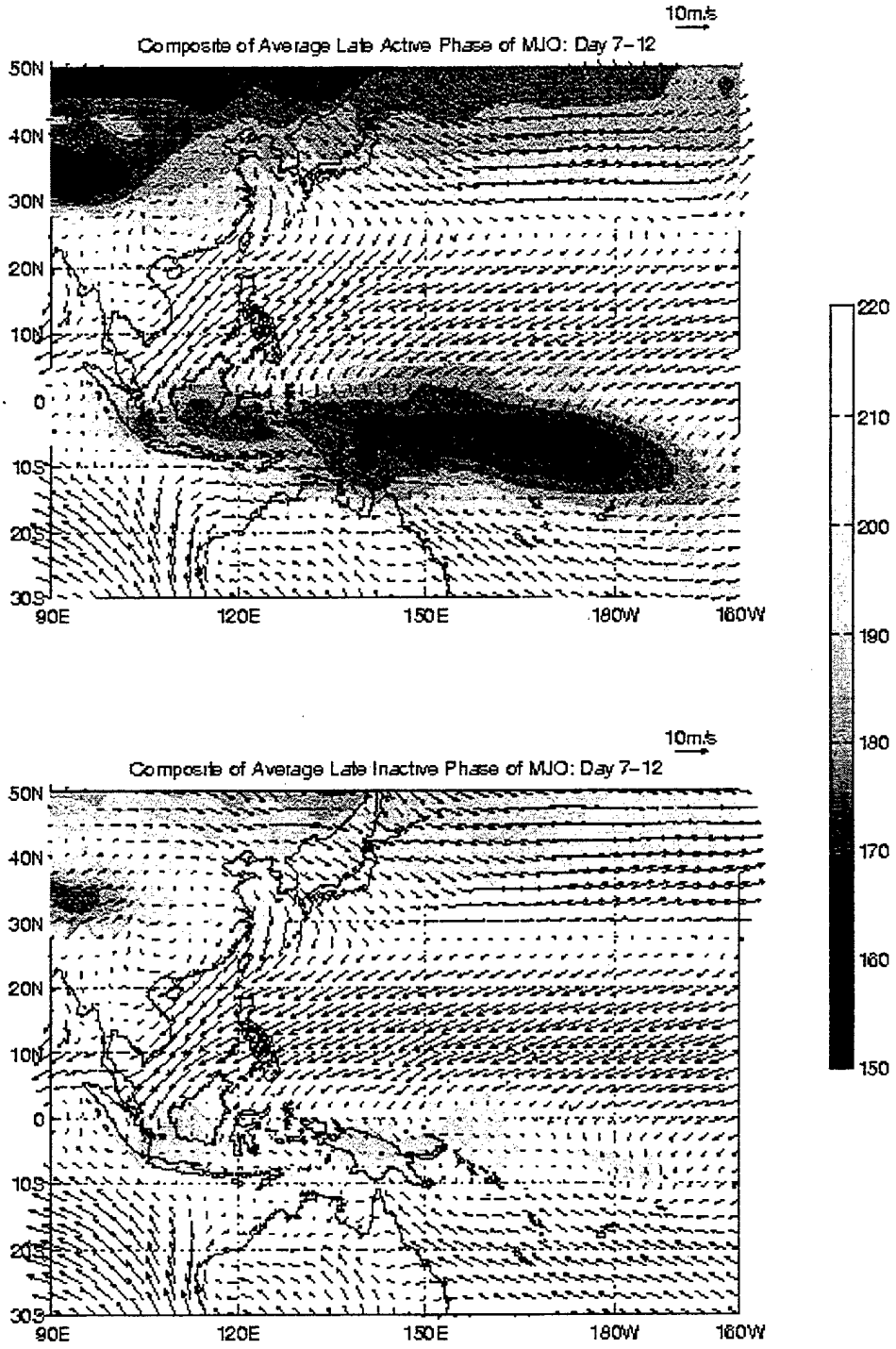

Figure 12. Composite analysis of averaged 1000 hPa winds and convection for surge events during the (a) late-active and the (b) late-inactive phases averaged from day 7 to day 12.

Figure 12.c. Difference between surge events during the late-active and late-inactive phases averaged from day 7 to day 12.

V. SUMMARY AND CONCLUSIONS

This study used NCEP 1000 hPa wind reanalysis and OLR-based convection fields to examine the interaction between the Madden-Julian Oscillation and northeasterly cold-surges over the South China Sea during the northern winter monsoon. The schematic MJO circulation and convection patterns of Figure 7 are modified in Figure 13 to represent the effects of the superposition of cold-surge events and MJO features over the South China Sea during the early-active and early-inactive phases for the averages from day 1 to day 6 and from day 7 to day 12. The dashed boxes correspond to the South China Sea and its position relative to the eastward-propagating MJO. During the early-active phase day 1-6, the area of convection associated with the MJO has just reached the longitude of the South China Sea. The MJO convection produces lower pressure over the region, which acts to increase the pressure gradient between the mid-latitude forcing of the Siberian-Mongolian anticyclone and the equatorial region. The pressure-wind pattern during the early-active phase would act to oppose northerly winds over eastern Asia. Opposite condition would occur during the early-inactive phase days 1-6. Based on the differences (Figure 9.c) between the early-active and early-inactive days 1-6, the magnitude of northerly winds south of 10° N over the South China Sea was nearly equal during the two phases (westerly differences). These differences indicate that during the early stages of each MJO phase there is a balance between competing effects.

When the early-active phase progresses to day 7-12 period, the MJO signal is located directly over the South China Sea. This leads to stronger convection and even lower pressure than that of the early-active phase day 1-6. The persistence of convection associated with the early-active phase of the MJO over the day 1-12 period results in

surges of longer duration than surges that occurred during the early-inactive phase. Surges during early-inactive phase are dominated by the synoptic-scale forcing from the mid-latitudes (Figure 9.c). Therefore, they typically do not last more than six days.

Recall that of the 42 surge events that occurred during the active phase, 18 surge events occurred during the early-active phase, while 24 surge events occurred during the late-active phase. The effects of the pressure-wind pattern of the MJO, especially days 1-6 of early-active phase, may act to limit the number of the surge events particularly if the mid-latitude forcing is weak. The MJO convection appears to dominate the effects of the pressure-wind pattern of the MJO during days 7-12 of the early-active phase. In particular, the slowly varying convection field acts to increase the duration of northerly winds over the South China Sea.

During the early-inactive phase day 1-6, there is little or no convection over the South China Sea, which contributes to higher pressure over the area. Of the 20 surge-events that occur during the inactive phase, only 6 occur during the early-inactive phase. The reduction in number of surge events during this phase suggests that mid-latitude forcing is solely responsible for the initiation of the surge. The forcing must be large enough to overcome the negative aspect of the MJO convection signal.

The schematic MJO circulation and convection pattern of Figure 7 are also modified in Figure 14 to represent the effects of the superposition of cold-surge events on the MJO features over the South China Sea during the late-active and late-inactive phases, averaged from day 1 to day 6 and day 7 to day 12. The dashed boxes also correspond to the location of the South China Sea and its position relative to the eastward-propagating MJO signal. During the late-active phase day 1-6, the MJO signal

lies directly over the South China Sea region. Therefore, the MJO convection causes an enhanced pressure gradient between the mid-latitudes and the equatorial region, which leads to strong northeasterly flow. During day 7-12 of the late-active phase, the MJO signal has passed through the South China Sea region and the area begins to enter the early-inactive phase (i.e., reduced convection). The effects of the eastward movement of the MJO convection weaken the favorable pressure gradient pattern over the South China Sea.

As an alternative to the schematic in Figure 14, it might be considered that during day 7-12, the eastward movement of the cyclonic circulations associated with the MJO convection might be oriented such that the western portion of the cyclonic cell is over the South China Sea. This would lead to an increase in northerly winds over the South China Sea. However, the composite analysis of chapter 4 indicates that surges associated with the late-inactive phase day 7-12 are larger than surges associated with the late-active phase day 7-12. This result leads to the conclusion that the influence of the MJO convection pattern dominates the MJO circulation pattern during all phases.

Conversely, surges during the late-inactive phase tend to last longer due to the favorable influences of the transition to the early-active phase. When the late-inactive phase day 1-6 transitions into the late-inactive phase day 7-12, the convection over the South China Sea begins to increase. The MJO signal is now beginning to create conditions as observed during the early-active phase day 1-6. Also, the pressure-wind pattern of the MJO is much more favorable and the combination with the increase of convection over the region leads to surges of longer duration during the late-inactive phase than during the late-active phase.

From these observations, the following can be concluded. The phase of the MJO over the South China Sea acts to either enhance or weaken a cold-surge that may have been originally forced by the mid-latitude Siberian-Mongolian anticyclone. When the MJO convection is located over the South China Sea, the surge is enhanced. The favorable convection pattern of the MJO dominates the unfavorable pressure-wind pattern of the MJO. When the MJO dry phase is over the South China Sea, greater mid-latitude baroclinic forcing is required to initiate a surge. The pressure-wind pattern of the MJO dominates the unfavorable convection pattern of the MJO. Lastly, the initiation of cold-surges over the South China Sea is either by MJO convection or by mid-latitude forcing, but not the pressure-wind pattern associated with the MJO.

The relationships between cold-surges and the MJO defined here may be further examined through inclusion of additional levels in the vertical. Also, the amount of forcing by mid-latitude mechanisms relative to the influences of the MJO circulation and convection patterns should be identified. Identification of whether a surge is being dominated by the mid-latitudes or MJO influences would provide some indication of potential surge extent and duration.

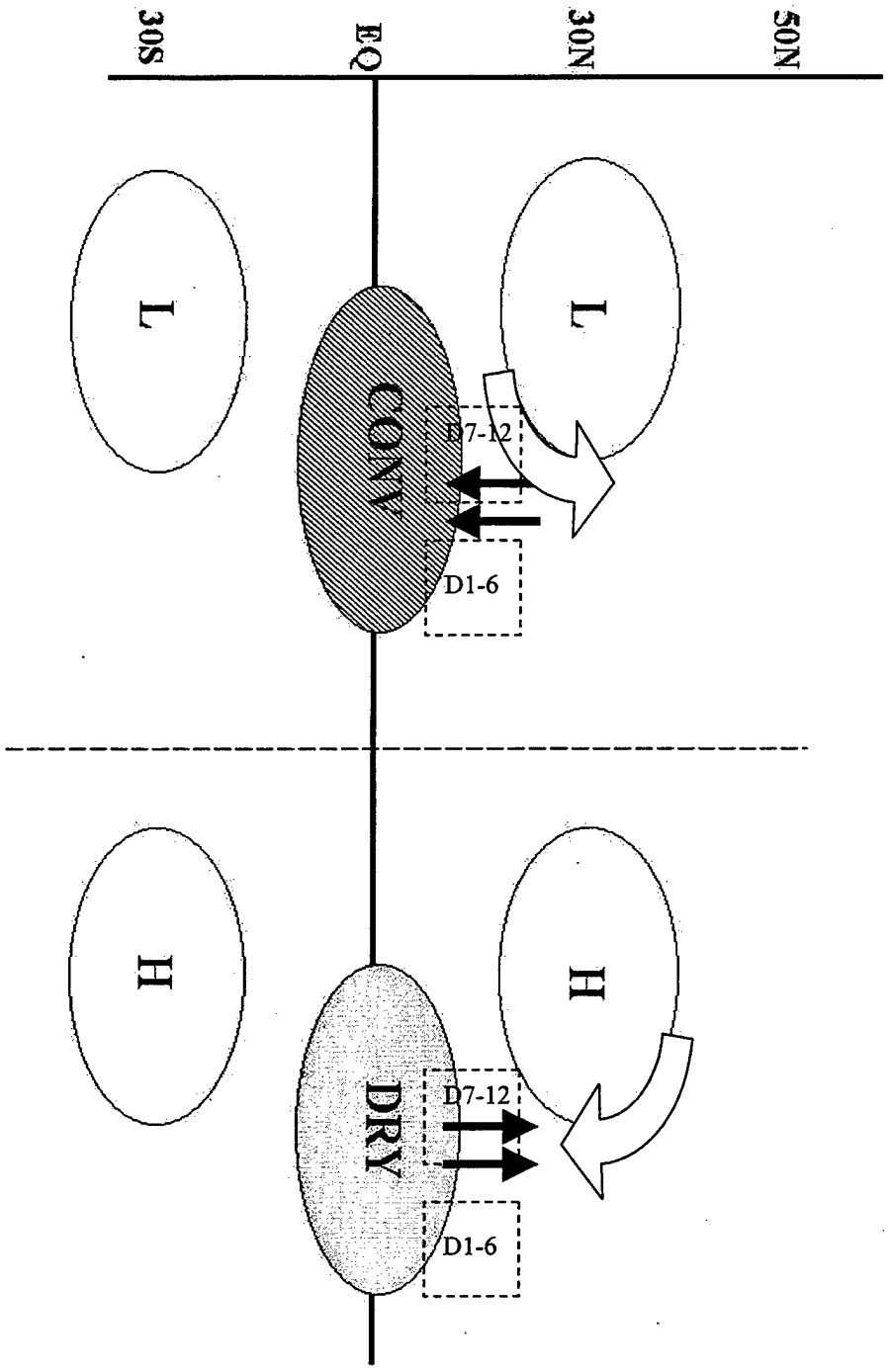

Figure 13. Schematic of the pressure-wind pattern and convection pattern for the MJO (as in Figure 4) modified to include the influence of MJO convection (bold solid arrows) and MJO pressure-wind pattern (open arrows) on cold-surge northerly winds that would be superimposed on the MJO features during the early-active and early-inactive phases. The locations of the South China Sea are defined by dashed boxes relative to each phase and each average period (days1-6 and days 7-12).

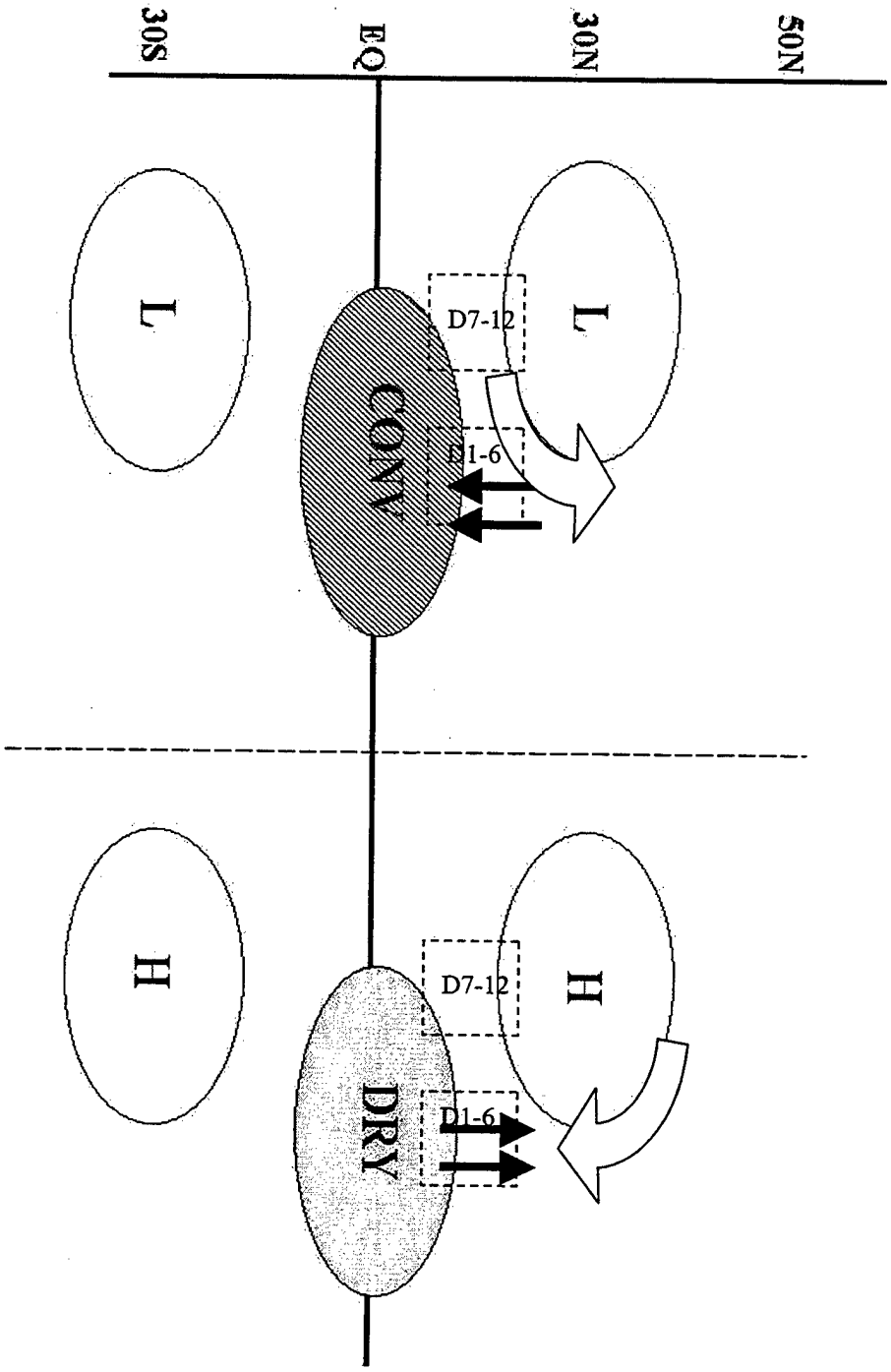

Figure 14. Schematic of the pressure-wind pattern and convection pattern for the MJO (as in Figure 4) modified to include the influence of MJO convection (bold solid arrows) and MJO pressure-wind pattern (open arrows) on cold-surge northerly winds that would be superimposed on the MJO features during the late-active and late-inactive phases. The locations of the South China Sea are defined by dashed boxes relative to each phase and each average period (days 1-6 and days 7-12).

APPENDIX A. NORTHERLY SURGE EVENTS BASED ON THE V-COMPONENT INDEX

Table A. contains a list (by date) of all surge events that occurred over the South China Sea and were associated with the MJO between 1979 and 1998. Sixty-two surge events associated with the MJO were identified during the northern winter monsoon over this period. Composites of 1000 hPa winds and convection were taken from day 1 to day 12. The surge events that occurred during the active phase are in bold. Note that no MJO occurred during the northern winter monsoon for 1981, 1984, 1994, and 1996.

Day	Category	Day	Category	Day	Category	Day	Category
01-Dec-79		01-Jan-80		01-Feb-80	2	01-Mar-80	
02-Dec-79		02-Jan-80		02-Feb-80	3	02-Mar-80	
03-Dec-79		03-Jan-80		03-Feb-80	4	03-Mar-80	
04-Dec-79		04-Jan-80		04-Feb-80	5	04-Mar-80	
05-Dec-79		05-Jan-80		05-Feb-80	6	05-Mar-80	
06-Dec-79		06-Jan-80		06-Feb-80	7	06-Mar-80	
07-Dec-79		07-Jan-80		07-Feb-80	8	07-Mar-80	
08-Dec-79		08-Jan-80		08-Feb-80	9	08-Mar-80	
09-Dec-79		09-Jan-80		09-Feb-80	10	09-Mar-80	1
10-Dec-79		10-Jan-80		10-Feb-80	11	10-Mar-80	2
11-Dec-79		11-Jan-80		11-Feb-80	12	11-Mar-80	3
12-Dec-79		12-Jan-80		12-Feb-80		12-Mar-80	4
13-Dec-79		13-Jan-80		13-Feb-80		13-Mar-80	5
14-Dec-79		14-Jan-80		14-Feb-80		14-Mar-80	6
15-Dec-79		15-Jan-80		15-Feb-80		15-Mar-80	7
16-Dec-79		16-Jan-80		16-Feb-80		16-Mar-80	8
17-Dec-79		17-Jan-80		17-Feb-80		17-Mar-80	9
18-Dec-79		18-Jan-80		18-Feb-80		18-Mar-80	10
19-Dec-79		19-Jan-80		19-Feb-80		19-Mar-80	11
20-Dec-79		20-Jan-80		20-Feb-80		20-Mar-80	12
21-Dec-79		21-Jan-80		21-Feb-80		21-Mar-80	
22-Dec-79		22-Jan-80		22-Feb-80		22-Mar-80	
23-Dec-79		23-Jan-80		23-Feb-80		23-Mar-80	
24-Dec-79		24-Jan-80		24-Feb-80		24-Mar-80	
25-Dec-79		25-Jan-80		25-Feb-80		25-Mar-80	
26-Dec-79		26-Jan-80		26-Feb-80		26-Mar-80	
27-Dec-79		27-Jan-80		27-Feb-80		27-Mar-80	
28-Dec-79		28-Jan-80		28-Feb-80		28-Mar-80	
29-Dec-79		29-Jan-80		29-Feb-80		29-Mar-80	
30-Dec-79		30-Jan-80				30-Mar-80	
31-Dec-79		31-Jan-80	1			31-Mar-80	

Table A.

Day	Category	Day	Category	Day	Category	Day	Category
01-Dec-81		01-Jan-82	4	01-Feb-82		01-Mar-82	
02-Dec-81	0	02-Jan-82	5	02-Feb-82		02-Mar-82	
03-Dec-81	1	03-Jan-82	6	03-Feb-82		03-Mar-82	
04-Dec-81	2	04-Jan-82	7	04-Feb-82		04-Mar-82	
05-Dec-81	3	05-Jan-82	8	05-Feb-82		05-Mar-82	
06-Dec-81	4	06-Jan-82	9	06-Feb-82	0	06-Mar-82	
07-Dec-81	5	07-Jan-82	10	07-Feb-82	1	07-Mar-82	
08-Dec-81	6	08-Jan-82	11	08-Feb-82	2	08-Mar-82	
09-Dec-81	7,1	09-Jan-82	12	09-Feb-82	3	09-Mar-82	
10-Dec-81	8,2	10-Jan-82		10-Feb-82	4	10-Mar-82	
11-Dec-81	9,3	11-Jan-82		11-Feb-82	5	11-Mar-82	
12-Dec-81	10,4	12-Jan-82		12-Feb-82	6	12-Mar-82	
13-Dec-81	11,5	13-Jan-82	1	13-Feb-82	7	13-Mar-82	
14-Dec-81	12,6	14-Jan-82	2	14-Feb-82	8	14-Mar-82	
15-Dec-81	7	15-Jan-82	3	15-Feb-82	9	15-Mar-82	
16-Dec-81	8	16-Jan-82	4	16-Feb-82	10	16-Mar-82	
17-Dec-81	9	17-Jan-82	5	17-Feb-82	11	17-Mar-82	
18-Dec-81	10	18-Jan-82	6	18-Feb-82	12	18-Mar-82	
19-Dec-81	11	19-Jan-82	7	19-Feb-82		19-Mar-82	
20-Dec-81	12	20-Jan-82	8	20-Feb-82		20-Mar-82	
21-Dec-81		21-Jan-82	9	21-Feb-82		21-Mar-82	
22-Dec-81		22-Jan-82	10	22-Feb-82		22-Mar-82	
23-Dec-81		23-Jan-82	11	23-Feb-82		23-Mar-82	
24-Dec-81		24-Jan-82	12	24-Feb-82		24-Mar-82	
25-Dec-81		25-Jan-82		25-Feb-82		25-Mar-82	
26-Dec-81		26-Jan-82		26-Feb-82		26-Mar-82	
27-Dec-81		27-Jan-82		27-Feb-82		27-Mar-82	
28-Dec-81		28-Jan-82		28-Feb-82		28-Mar-82	
29-Dec-81	1	29-Jan-82				29-Mar-82	
30-Dec-81	2	30-Jan-82				30-Mar-82	
31-Dec-81	3	31-Jan-82				31-Mar-82	

Table A. Continued.

Day	Category	Day	Category	Day	Category	Day	Category
01-Dec-82		01-Jan-83	**7,1**	01-Feb-83		01-Mar-83	
02-Dec-82		02-Jan-83	**8,2**	02-Feb-83		02-Mar-83	
03-Dec-82		03-Jan-83	**9,3**	03-Feb-83		03-Mar-83	
04-Dec-82		04-Jan-83	**10,4**	04-Feb-83		04-Mar-83	
05-Dec-82		05-Jan-83	**11,5**	05-Feb-83		05-Mar-83	
06-Dec-82		06-Jan-83	**12,6**	06-Feb-83		06-Mar-83	
07-Dec-82		07-Jan-83	**7**	07-Feb-83		07-Mar-83	
08-Dec-82	1	08-Jan-83	**8**	08-Feb-83		08-Mar-83	
09-Dec-82	2	09-Jan-83	**9**	09-Feb-83		09-Mar-83	
10-Dec-82	3	10-Jan-83	**10**	10-Feb-83		10-Mar-83	
11-Dec-82	4	11-Jan-83	**11**	11-Feb-83		11-Mar-83	
12-Dec-82	5	12-Jan-83	**12**	12-Feb-83		12-Mar-83	
13-Dec-82	6	13-Jan-83		13-Feb-83		13-Mar-83	
14-Dec-82	7	14-Jan-83		14-Feb-83		14-Mar-83	
15-Dec-82	8	15-Jan-83		15-Feb-83		15-Mar-83	
16-Dec-82	9	16-Jan-83		16-Feb-83		16-Mar-83	
17-Dec-82	10	17-Jan-83		17-Feb-83		17-Mar-83	
18-Dec-82	11	18-Jan-83		18-Feb-83		18-Mar-83	
19-Dec-82	12	19-Jan-83		19-Feb-83		19-Mar-83	
20-Dec-82		20-Jan-83		20-Feb-83		20-Mar-83	
21-Dec-82		21-Jan-83		21-Feb-83		21-Mar-83	
22-Dec-82		22-Jan-83		22-Feb-83		22-Mar-83	
23-Dec-82		23-Jan-83		23-Feb-83		23-Mar-83	
24-Dec-82		24-Jan-83		24-Feb-83		24-Mar-83	
25-Dec-82		25-Jan-83		25-Feb-83		25-Mar-83	
26-Dec-82	**1**	26-Jan-83		26-Feb-83		26-Mar-83	
27-Dec-82	**2**	27-Jan-83		27-Feb-83		27-Mar-83	
28-Dec-82	**3**	28-Jan-83		28-Feb-83		28-Mar-83	
29-Dec-82	**4**	29-Jan-83				29-Mar-83	
30-Dec-82	**5**	30-Jan-83				30-Mar-83	
31-Dec-82	**6**	31-Jan-83				31-Mar-83	

Table A. Continued.

Day	Category	Day	Category	Day	Category	Day	Category
01-Dec-84		01-Jan-85		01-Feb-85	10	01-Mar-85	12,3
02-Dec-84		02-Jan-85		02-Feb-85	11	02-Mar-85	4
03-Dec-84		03-Jan-85		03-Feb-85	12	03-Mar-85	5
04-Dec-84		04-Jan-85		04-Feb-85		04-Mar-85	6
05-Dec-84	1	05-Jan-85		05-Feb-85		05-Mar-85	7
06-Dec-84	2	06-Jan-85		06-Feb-85	1	06-Mar-85	8
07-Dec-84	3	07-Jan-85		07-Feb-85	2	07-Mar-85	9
08-Dec-84	4	08-Jan-85		08-Feb-85	3	08-Mar-85	10
09-Dec-84	5	09-Jan-85		09-Feb-85	4	09-Mar-85	11
10-Dec-84	6	10-Jan-85		10-Feb-85	5	10-Mar-85	12
11-Dec-84	7	11-Jan-85		11-Feb-85	6	11-Mar-85	
12-Dec-84	8	12-Jan-85		12-Feb-85	7	12-Mar-85	
13-Dec-84	9	13-Jan-85	1	13-Feb-85	8	13-Mar-85	
14-Dec-84	10	14-Jan-85	2	14-Feb-85	9	14-Mar-85	
15-Dec-84	11	15-Jan-85	3	15-Feb-85	10	15-Mar-85	
16-Dec-84	12	16-Jan-85	4	16-Feb-85	11	16-Mar-85	
17-Dec-84		17-Jan-85	5	17-Feb-85	12	17-Mar-85	
18-Dec-84	1	18-Jan-85	6	18-Feb-85	1	18-Mar-85	
19-Dec-84	2	19-Jan-85	7	19-Feb-85	2	19-Mar-85	
20-Dec-84	3	20-Jan-85	8	20-Feb-85	3	20-Mar-85	
21-Dec-84	4	21-Jan-85	9	21-Feb-85	4	21-Mar-85	
22-Dec-84	5	22-Jan-85	10	22-Feb-85	5	22-Mar-85	
23-Dec-84	6	23-Jan-85	11,1	23-Feb-85	6	23-Mar-85	
24-Dec-84	7	24-Jan-85	12,2	24-Feb-85	7	24-Mar-85	
25-Dec-84	8	25-Jan-85	3	25-Feb-85	8	25-Mar-85	
26-Dec-84	9	26-Jan-85	4	26-Feb-85	9	26-Mar-85	
27-Dec-84	10	27-Jan-85	5	27-Feb-85	10,1	27-Mar-85	
28-Dec-84	11	28-Jan-85	6	28-Feb-85	11,2	28-Mar-85	1
29-Dec-84	12	29-Jan-85	7			29-Mar-85	2
30-Dec-84		30-Jan-85	8			30-Mar-85	3
31-Dec-84		31-Jan-85	9			31-Mar-85	4

Table A. Continued.

Day	Category	Day	Category	Day	Category	Day	Category
01-Dec-85		01-Jan-86	12	01-Feb-86		01-Mar-86	
02-Dec-85		02-Jan-86		02-Feb-86		02-Mar-86	
03-Dec-85		03-Jan-86		03-Feb-86		03-Mar-86	
04-Dec-85		04-Jan-86		04-Feb-86		04-Mar-86	
05-Dec-85		05-Jan-86		05-Feb-86		05-Mar-86	
06-Dec-85		06-Jan-86		06-Feb-86		06-Mar-86	
07-Dec-85		07-Jan-86		07-Feb-86		07-Mar-86	
08-Dec-85		08-Jan-86		08-Feb-86		08-Mar-86	
09-Dec-85		09-Jan-86		09-Feb-86		09-Mar-86	
10-Dec-85		10-Jan-86		10-Feb-86		10-Mar-86	
11-Dec-85	1	11-Jan-86		11-Feb-86		11-Mar-86	
12-Dec-85	2	12-Jan-86		12-Feb-86		12-Mar-86	
13-Dec-85	3	13-Jan-86		13-Feb-86		13-Mar-86	
14-Dec-85	4	14-Jan-86		14-Feb-86		14-Mar-86	
15-Dec-85	5	15-Jan-86		15-Feb-86		15-Mar-86	
16-Dec-85	6	16-Jan-86		16-Feb-86		16-Mar-86	
17-Dec-85	7	17-Jan-86		17-Feb-86		17-Mar-86	
18-Dec-85	8	18-Jan-86		18-Feb-86		18-Mar-86	
19-Dec-85	9	19-Jan-86	1	19-Feb-86		19-Mar-86	
20-Dec-85	10	20-Jan-86	2	20-Feb-86		20-Mar-86	
21-Dec-85	11,1	21-Jan-86	3	21-Feb-86		21-Mar-86	
22-Dec-85	12,2	22-Jan-86	4	22-Feb-86		22-Mar-86	
23-Dec-85	3	23-Jan-86	5	23-Feb-86		23-Mar-86	
24-Dec-85	4	24-Jan-86	6	24-Feb-86		24-Mar-86	
25-Dec-85	5	25-Jan-86	7	25-Feb-86		25-Mar-86	
26-Dec-85	6	26-Jan-86	8	26-Feb-86		26-Mar-86	
27-Dec-85	7	27-Jan-86	9	27-Feb-86		27-Mar-86	
28-Dec-85	8	28-Jan-86	10	28-Feb-86		28-Mar-86	
29-Dec-85	9	29-Jan-86	11			29-Mar-86	
30-Dec-85	10	30-Jan-86	12			30-Mar-86	
31-Dec-85	11	31-Jan-86				31-Mar-86	

Table A. Continued.

Day	Category	Day	Category	Day	Category	Day	Category
01-Dec-86		01-Jan-87		01-Feb-87		01-Mar-87	3
02-Dec-86		02-Jan-87		02-Feb-87		02-Mar-87	4
03-Dec-86	1	03-Jan-87		03-Feb-87		03-Mar-87	5
04-Dec-86	2	04-Jan-87		04-Feb-87		04-Mar-87	6
05-Dec-86	3	05-Jan-87		05-Feb-87		05-Mar-87	7
06-Dec-86	4	06-Jan-87		06-Feb-87		06-Mar-87	8
07-Dec-86	5	07-Jan-87		07-Feb-87		07-Mar-87	9
08-Dec-86	6	08-Jan-87		08-Feb-87		08-Mar-87	10
09-Dec-86	7	09-Jan-87		09-Feb-87		09-Mar-87	11
10-Dec-86	8	10-Jan-87		10-Feb-87		10-Mar-87	12
11-Dec-86	9	11-Jan-87		11-Feb-87		11-Mar-87	
12-Dec-86	10	12-Jan-87		12-Feb-87		12-Mar-87	
13-Dec-86	11	13-Jan-87		13-Feb-87		13-Mar-87	
14-Dec-86	12	14-Jan-87		14-Feb-87		14-Mar-87	
15-Dec-86		15-Jan-87		15-Feb-87		15-Mar-87	
16-Dec-86		16-Jan-87		16-Feb-87		16-Mar-87	
17-Dec-86	1	17-Jan-87		17-Feb-87		17-Mar-87	
18-Dec-86	2	18-Jan-87		18-Feb-87		18-Mar-87	
19-Dec-86	3	19-Jan-87		19-Feb-87		19-Mar-87	
20-Dec-86	4	20-Jan-87		20-Feb-87		20-Mar-87	
21-Dec-86	5	21-Jan-87		21-Feb-87		21-Mar-87	
22-Dec-86	6	22-Jan-87		22-Feb-87		22-Mar-87	1
23-Dec-86	7	23-Jan-87		23-Feb-87		23-Mar-87	2
24-Dec-86	8	24-Jan-87		24-Feb-87		24-Mar-87	3
25-Dec-86	9	25-Jan-87		25-Feb-87		25-Mar-87	4
26-Dec-86	10	26-Jan-87		26-Feb-87		26-Mar-87	5
27-Dec-86	11	27-Jan-87		27-Feb-87	1	27-Mar-87	6
28-Dec-86	12	28-Jan-87		28-Feb-87	2	28-Mar-87	7
29-Dec-86		29-Jan-87				29-Mar-87	8
30-Dec-86		30-Jan-87				30-Mar-87	9
31-Dec-86		31-Jan-87				31-Mar-87	10

Table A. Continued.

Day	Category	Day	Category	Day	Category	Day	Category
01-Dec-87		01-Jan-88		01-Feb-88	10	01-Mar-88	
02-Dec-87		02-Jan-88		02-Feb-88	11	02-Mar-88	
03-Dec-87		03-Jan-88		03-Feb-88	12	03-Mar-88	
04-Dec-87		04-Jan-88		04-Feb-88		04-Mar-88	
05-Dec-87	1	05-Jan-88		05-Feb-88		05-Mar-88	
06-Dec-87	2	06-Jan-88		06-Feb-88	1	06-Mar-88	
07-Dec-87	3	07-Jan-88		07-Feb-88	2	07-Mar-88	
08-Dec-87	4	08-Jan-88		08-Feb-88	3	08-Mar-88	
09-Dec-87	5	09-Jan-88		09-Feb-88	4	09-Mar-88	
10-Dec-87	6	10-Jan-88		10-Feb-88	5	10-Mar-88	
11-Dec-87	7	11-Jan-88		11-Feb-88	6	11-Mar-88	
12-Dec-87	8	12-Jan-88		12-Feb-88	7	12-Mar-88	
13-Dec-87	9	13-Jan-88		13-Feb-88	8	13-Mar-88	
14-Dec-87	10	14-Jan-88		14-Feb-88	9	14-Mar-88	
15-Dec-87	11	15-Jan-88		15-Feb-88	10	15-Mar-88	1
16-Dec-87	12	16-Jan-88		16-Feb-88	11	16-Mar-88	2
17-Dec-87		17-Jan-88		17-Feb-88	12	17-Mar-88	3
18-Dec-87		18-Jan-88		18-Feb-88		18-Mar-88	4
19-Dec-87		19-Jan-88		19-Feb-88		19-Mar-88	5
20-Dec-87		20-Jan-88		20-Feb-88		20-Mar-88	6
21-Dec-87		21-Jan-88		21-Feb-88		21-Mar-88	7
22-Dec-87		22-Jan-88		22-Feb-88		22-Mar-88	8
23-Dec-87		23-Jan-88	1	23-Feb-88		23-Mar-88	9
24-Dec-87		24-Jan-88	2	24-Feb-88		24-Mar-88	10
25-Dec-87		25-Jan-88	3	25-Feb-88		25-Mar-88	11
26-Dec-87		26-Jan-88	4	26-Feb-88		26-Mar-88	12
27-Dec-87		27-Jan-88	5	27-Feb-88		27-Mar-88	
28-Dec-87		28-Jan-88	6	28-Feb-88		28-Mar-88	
29-Dec-87		29-Jan-88	7	29-Feb-88		29-Mar-88	
30-Dec-87		30-Jan-88	8			30-Mar-88	
31-Dec-87		31-Jan-88	9			31-Mar-88	

Table A. Continued.

Day	Category	Day	Category	Day	Category	Day	Category
01-Dec-88		01-Jan-89		01-Feb-89		01-Mar-89	
02-Dec-88		02-Jan-89		02-Feb-89		02-Mar-89	
03-Dec-88		03-Jan-89		03-Feb-89		03-Mar-89	
04-Dec-88		04-Jan-89		04-Feb-89		04-Mar-89	
05-Dec-88		05-Jan-89		05-Feb-89		05-Mar-89	
06-Dec-88		06-Jan-89		06-Feb-89		06-Mar-89	
07-Dec-88		07-Jan-89		07-Feb-89		07-Mar-89	
08-Dec-88	1	08-Jan-89		08-Feb-89		08-Mar-89	
09-Dec-88	2	09-Jan-89		09-Feb-89		09-Mar-89	
10-Dec-88	3	10-Jan-89		10-Feb-89		10-Mar-89	
11-Dec-88	4	11-Jan-89		11-Feb-89		11-Mar-89	
12-Dec-88	5	12-Jan-89		12-Feb-89		12-Mar-89	
13-Dec-88	6	13-Jan-89		13-Feb-89		13-Mar-89	
14-Dec-88	7	14-Jan-89		14-Feb-89		14-Mar-89	
15-Dec-88	8	15-Jan-89		15-Feb-89		15-Mar-89	
16-Dec-88	9	16-Jan-89		16-Feb-89		16-Mar-89	
17-Dec-88	10	17-Jan-89		17-Feb-89		17-Mar-89	
18-Dec-88	11	18-Jan-89		18-Feb-89		18-Mar-89	
19-Dec-88	12	19-Jan-89		19-Feb-89		19-Mar-89	
20-Dec-88		20-Jan-89		20-Feb-89		20-Mar-89	
21-Dec-88		21-Jan-89		21-Feb-89		21-Mar-89	
22-Dec-88		22-Jan-89		22-Feb-89		22-Mar-89	
23-Dec-88		23-Jan-89		23-Feb-89		23-Mar-89	
24-Dec-88		24-Jan-89		24-Feb-89		24-Mar-89	
25-Dec-88		25-Jan-89		25-Feb-89		25-Mar-89	
26-Dec-88		26-Jan-89		26-Feb-89		26-Mar-89	
27-Dec-88		27-Jan-89		27-Feb-89		27-Mar-89	
28-Dec-88		28-Jan-89		28-Feb-89		28-Mar-89	
29-Dec-88		29-Jan-89				29-Mar-89	
30-Dec-88		30-Jan-89				30-Mar-89	
31-Dec-88		31-Jan-89				31-Mar-89	

Table A. Continued.

Day	Category	Day	Category	Day	Category	Day	Category
01-Dec-89		01-Jan-90	1	01-Feb-90		01-Mar-90	
02-Dec-89		02-Jan-90	2	02-Feb-90		02-Mar-90	
03-Dec-89		03-Jan-90	3	03-Feb-90		03-Mar-90	
04-Dec-89		04-Jan-90	4	04-Feb-90		04-Mar-90	
05-Dec-89		05-Jan-90	5	05-Feb-90		05-Mar-90	
06-Dec-89		06-Jan-90	6	06-Feb-90		06-Mar-90	1
07-Dec-89		07-Jan-90	7	07-Feb-90		07-Mar-90	2
08-Dec-89		08-Jan-90	8	08-Feb-90		08-Mar-90	3
09-Dec-89		09-Jan-90	9	09-Feb-90		09-Mar-90	4
10-Dec-89		10-Jan-90	10	10-Feb-90		10-Mar-90	5
11-Dec-89	1	11-Jan-90	11	11-Feb-90		11-Mar-90	6
12-Dec-89	2	12-Jan-90	12	12-Feb-90		12-Mar-90	7
13-Dec-89	3	13-Jan-90		13-Feb-90		13-Mar-90	8
14-Dec-89	4	14-Jan-90		14-Feb-90		14-Mar-90	9
15-Dec-89	5	15-Jan-90		15-Feb-90		15-Mar-90	10,1
16-Dec-89	6	16-Jan-90		16-Feb-90		16-Mar-90	11,2
17-Dec-89	7	17-Jan-90		17-Feb-90		17-Mar-90	12,3
18-Dec-89	8	18-Jan-90		18-Feb-90		18-Mar-90	4
19-Dec-89	9	19-Jan-90		19-Feb-90		19-Mar-90	5
20-Dec-89	10	20-Jan-90	1	20-Feb-90		20-Mar-90	6
21-Dec-89	11	21-Jan-90	2	21-Feb-90		21-Mar-90	7
22-Dec-89	12	22-Jan-90	3	22-Feb-90		22-Mar-90	8
23-Dec-89		23-Jan-90	4	23-Feb-90		23-Mar-90	9
24-Dec-89		24-Jan-90	5	24-Feb-90		24-Mar-90	10
25-Dec-89		25-Jan-90	6	25-Feb-90		25-Mar-90	11
26-Dec-89		26-Jan-90	7	26-Feb-90		26-Mar-90	12
27-Dec-89		27-Jan-90	8	27-Feb-90		27-Mar-90	
28-Dec-89		28-Jan-90	9	28-Feb-90		28-Mar-90	
29-Dec-89		29-Jan-90	10			29-Mar-90	
30-Dec-89		30-Jan-90	11			30-Mar-90	
31-Dec-89		31-Jan-90	12			31-Mar-90	

Table A. Continued.

Day	Category	Day	Category	Day	Category	Day	Category
01-Dec-90		01-Jan-91		01-Feb-91	11	01-Mar-91	
02-Dec-90		02-Jan-91		02-Feb-91	12	02-Mar-91	
03-Dec-90		03-Jan-91		03-Feb-91		03-Mar-91	
04-Dec-90		04-Jan-91		04-Feb-91		04-Mar-91	
05-Dec-90		05-Jan-91		05-Feb-91		05-Mar-91	
06-Dec-90		06-Jan-91		06-Feb-91		06-Mar-91	
07-Dec-90		07-Jan-91		07-Feb-91		07-Mar-91	
08-Dec-90		08-Jan-91		08-Feb-91		08-Mar-91	
09-Dec-90		09-Jan-91		09-Feb-91		09-Mar-91	
10-Dec-90		10-Jan-91		10-Feb-91		10-Mar-91	
11-Dec-90		11-Jan-91		11-Feb-91		11-Mar-91	
12-Dec-90		12-Jan-91		12-Feb-91		12-Mar-91	
13-Dec-90		13-Jan-91		13-Feb-91		13-Mar-91	
14-Dec-90		14-Jan-91		14-Feb-91		14-Mar-91	
15-Dec-90		15-Jan-91		15-Feb-91		15-Mar-91	
16-Dec-90		16-Jan-91		16-Feb-91	1	16-Mar-91	
17-Dec-90		17-Jan-91		17-Feb-91	2	17-Mar-91	
18-Dec-90		18-Jan-91		18-Feb-91	3	18-Mar-91	
19-Dec-90		19-Jan-91		19-Feb-91	4	19-Mar-91	
20-Dec-90		20-Jan-91		20-Feb-91	5	20-Mar-91	
21-Dec-90		21-Jan-91		21-Feb-91	6	21-Mar-91	
22-Dec-90		22-Jan-91	1	22-Feb-91	7	22-Mar-91	
23-Dec-90		23-Jan-91	2	23-Feb-91	8	23-Mar-91	
24-Dec-90		24-Jan-91	3	24-Feb-91	9	24-Mar-91	1
25-Dec-90		25-Jan-91	4	25-Feb-91	10	25-Mar-91	2
26-Dec-90		26-Jan-91	5	26-Feb-91	11	26-Mar-91	3
27-Dec-90		27-Jan-91	6	27-Feb-91	12	27-Mar-91	4
28-Dec-90		28-Jan-91	7	28-Feb-91		28-Mar-91	5
29-Dec-90		29-Jan-91	8			29-Mar-91	6
30-Dec-90		30-Jan-91	9			30-Mar-91	7
31-Dec-90		31-Jan-91	10			31-Mar-91	8

Table A. Continued.

Day	Category	Day	Category	Day	Category	Day	Category
01-Dec-91		01-Jan-92	4	01-Feb-92		01-Mar-92	
02-Dec-91		02-Jan-92	5	02-Feb-92		02-Mar-92	
03-Dec-91		03-Jan-92	6	03-Feb-92		03-Mar-92	
04-Dec-91		04-Jan-92	7	04-Feb-92		04-Mar-92	
05-Dec-91		05-Jan-92	8	05-Feb-92		05-Mar-92	
06-Dec-91		06-Jan-92	9,1	06-Feb-92		06-Mar-92	
07-Dec-91		07-Jan-92	10,2	07-Feb-92		07-Mar-92	
08-Dec-91		08-Jan-92	11,3	08-Feb-92		08-Mar-92	
09-Dec-91		09-Jan-92	12,4	09-Feb-92		09-Mar-92	
10-Dec-91		10-Jan-92	5	10-Feb-92		10-Mar-92	
11-Dec-91		11-Jan-92	6	11-Feb-92		11-Mar-92	
12-Dec-91		12-Jan-92	7	12-Feb-92		12-Mar-92	
13-Dec-91		13-Jan-92	8	13-Feb-92		13-Mar-92	
14-Dec-91		14-Jan-92	9	14-Feb-92		14-Mar-92	
15-Dec-91		15-Jan-92	10	15-Feb-92		15-Mar-92	
16-Dec-91		16-Jan-92	11	16-Feb-92		16-Mar-92	
17-Dec-91		17-Jan-92	12	17-Feb-92		17-Mar-92	
18-Dec-91		18-Jan-92		18-Feb-92		18-Mar-92	
19-Dec-91		19-Jan-92		19-Feb-92		19-Mar-92	
20-Dec-91		20-Jan-92		20-Feb-92		20-Mar-92	
21-Dec-91		21-Jan-92		21-Feb-92		21-Mar-92	
22-Dec-91		22-Jan-92		22-Feb-92		22-Mar-92	
23-Dec-91		23-Jan-92		23-Feb-92		23-Mar-92	
24-Dec-91		24-Jan-92		24-Feb-92		24-Mar-92	
25-Dec-91		25-Jan-92		25-Feb-92		25-Mar-92	
26-Dec-91		26-Jan-92		26-Feb-92		26-Mar-92	
27-Dec-91		27-Jan-92		27-Feb-92		27-Mar-92	
28-Dec-91		28-Jan-92		28-Feb-92		28-Mar-92	
29-Dec-91	1	29-Jan-92		29-Feb-92		29-Mar-92	
30-Dec-91	2	30-Jan-92				30-Mar-92	
31-Dec-91	3	31-Jan-92				31-Mar-92	

Table A. Continued.

Day	Category	Day	Category	Day	Category	Day	Category
01-Dec-92		01-Jan-93		01-Feb-93	6	01-Mar-93	
02-Dec-92		02-Jan-93		02-Feb-93	7	02-Mar-93	
03-Dec-92		03-Jan-93		03-Feb-93	8	03-Mar-93	
04-Dec-92		04-Jan-93		04-Feb-93	9	04-Mar-93	
05-Dec-92		05-Jan-93		05-Feb-93	10	05-Mar-93	
06-Dec-92		06-Jan-93		06-Feb-93	11	06-Mar-93	
07-Dec-92		07-Jan-93		07-Feb-93	12	07-Mar-93	
08-Dec-92		08-Jan-93		08-Feb-93		08-Mar-93	
09-Dec-92	1	09-Jan-93		09-Feb-93		09-Mar-93	
10-Dec-92	2	10-Jan-93		10-Feb-93		10-Mar-93	
11-Dec-92	3	11-Jan-93		11-Feb-93		11-Mar-93	
12-Dec-92	4	12-Jan-93		12-Feb-93		12-Mar-93	
13-Dec-92	5	13-Jan-93		13-Feb-93		13-Mar-93	
14-Dec-92	6	14-Jan-93	1	14-Feb-93		14-Mar-93	
15-Dec-92	7	15-Jan-93	2	15-Feb-93		15-Mar-93	
16-Dec-92	8	16-Jan-93	3	16-Feb-93		16-Mar-93	
17-Dec-92	9	17-Jan-93	4	17-Feb-93		17-Mar-93	
18-Dec-92	10	18-Jan-93	5	18-Feb-93		18-Mar-93	
19-Dec-92	11	19-Jan-93	6	19-Feb-93		19-Mar-93	
20-Dec-92	12	20-Jan-93	7	20-Feb-93		20-Mar-93	
21-Dec-92		21-Jan-93	8	21-Feb-93		21-Mar-93	
22-Dec-92		22-Jan-93	9	22-Feb-93		22-Mar-93	
23-Dec-92		23-Jan-93	10	23-Feb-93		23-Mar-93	
24-Dec-92		24-Jan-93	11	24-Feb-93		24-Mar-93	
25-Dec-92		25-Jan-93	12	25-Feb-93		25-Mar-93	
26-Dec-92		26-Jan-93		26-Feb-93		26-Mar-93	
27-Dec-92		27-Jan-93	1	27-Feb-93		27-Mar-93	
28-Dec-92		28-Jan-93	2	28-Feb-93		28-Mar-93	
29-Dec-92		29-Jan-93	3			29-Mar-93	
30-Dec-92		30-Jan-93	4			30-Mar-93	
31-Dec-92		31-Jan-93	5			31-Mar-93	

Table A. Continued.

Day	Category	Day	Category	Day	Category	Day	Category
01-Dec-94		01-Jan-95		01-Feb-95	10	01-Mar-95	10
02-Dec-94		02-Jan-95		02-Feb-95	11	02-Mar-95	11
03-Dec-94		03-Jan-95		03-Feb-95	12	03-Mar-95	12,1
04-Dec-94		04-Jan-95		04-Feb-95		04-Mar-95	2
05-Dec-94		05-Jan-95		05-Feb-95		05-Mar-95	3
06-Dec-94		06-Jan-95		06-Feb-95		06-Mar-95	4
07-Dec-94		07-Jan-95		07-Feb-95		07-Mar-95	5
08-Dec-94		08-Jan-95		08-Feb-95		08-Mar-95	6
09-Dec-94		09-Jan-95		09-Feb-95		09-Mar-95	7
10-Dec-94		10-Jan-95		10-Feb-95		10-Mar-95	8
11-Dec-94	1	11-Jan-95	1	11-Feb-95		11-Mar-95	9
12-Dec-94	2	12-Jan-95	2	12-Feb-95		12-Mar-95	10
13-Dec-94	3	13-Jan-95	3	13-Feb-95		13-Mar-95	11
14-Dec-94	4	14-Jan-95	4	14-Feb-95		14-Mar-95	12
15-Dec-94	5	15-Jan-95	5	15-Feb-95		15-Mar-95	
16-Dec-94	6	16-Jan-95	6	16-Feb-95		16-Mar-95	
17-Dec-94	7	17-Jan-95	7	17-Feb-95		17-Mar-95	1
18-Dec-94	8	18-Jan-95	8	18-Feb-95		18-Mar-95	2
19-Dec-94	9	19-Jan-95	9	19-Feb-95		19-Mar-95	3
20-Dec-94	10	20-Jan-95	10	20-Feb-95	1	20-Mar-95	4
21-Dec-94	11	21-Jan-95	11	21-Feb-95	2	21-Mar-95	5
22-Dec-94	12	22-Jan-95	12	22-Feb-95	3	22-Mar-95	6
23-Dec-94		23-Jan-95	1	23-Feb-95	4	23-Mar-95	7
24-Dec-94		24-Jan-95	2	24-Feb-95	5	24-Mar-95	8
25-Dec-94		25-Jan-95	3	25-Feb-95	6	25-Mar-95	9,1
26-Dec-94		26-Jan-95	4	26-Feb-95	7	26-Mar-95	10,2
27-Dec-94		27-Jan-95	5	27-Feb-95	8	27-Mar-95	11,3
28-Dec-94		28-Jan-95	6	28-Feb-95	9	28-Mar-95	12,4
29-Dec-94		29-Jan-95	7			29-Mar-95	5
30-Dec-94		30-Jan-95	8			30-Mar-95	6
31-Dec-94		31-Jan-95	9			31-Mar-95	7

Table A. Continued.

Day	Category	Day	Category	Day	Category	Day	Category
01-Dec-96		01-Jan-97		01-Feb-97		01-Mar-97	
02-Dec-96	1	02-Jan-97		02-Feb-97		02-Mar-97	1
03-Dec-96	2	03-Jan-97		03-Feb-97		03-Mar-97	2
04-Dec-96	3	04-Jan-97	1	04-Feb-97		04-Mar-97	3
05-Dec-96	4	05-Jan-97	2	05-Feb-97		05-Mar-97	4
06-Dec-96	5	06-Jan-97	3	06-Feb-97		06-Mar-97	5
07-Dec-96	6	07-Jan-97	4	07-Feb-97		07-Mar-97	6
08-Dec-96	7	08-Jan-97	5	08-Feb-97		08-Mar-97	7
09-Dec-96	8	09-Jan-97	6	09-Feb-97		09-Mar-97	8
10-Dec-96	9	10-Jan-97	7	10-Feb-97		10-Mar-97	9
11-Dec-96	10	11-Jan-97	8	11-Feb-97	1	11-Mar-97	10
12-Dec-96	11	12-Jan-97	9	12-Feb-97	2	12-Mar-97	11
13-Dec-96	12	13-Jan-97	10	13-Feb-97	3	13-Mar-97	12
14-Dec-96		14-Jan-97	11	14-Feb-97	4	14-Mar-97	
15-Dec-96		15-Jan-97	12	15-Feb-97	5	15-Mar-97	
16-Dec-96		16-Jan-97		16-Feb-97	6	16-Mar-97	
17-Dec-96		17-Jan-97		17-Feb-97	7	17-Mar-97	
18-Dec-96		18-Jan-97		18-Feb-97	8	18-Mar-97	
19-Dec-96		19-Jan-97		19-Feb-97	9	19-Mar-97	
20-Dec-96	1	20-Jan-97		20-Feb-97	10	20-Mar-97	
21-Dec-96	2	21-Jan-97		21-Feb-97	11	21-Mar-97	1
22-Dec-96	3	22-Jan-97		22-Feb-97	12	22-Mar-97	2
23-Dec-96	4	23-Jan-97		23-Feb-97		23-Mar-97	3
24-Dec-96	5	24-Jan-97		24-Feb-97		24-Mar-97	4
25-Dec-96	6	25-Jan-97		25-Feb-97		25-Mar-97	5
26-Dec-96	7	26-Jan-97		26-Feb-97		26-Mar-97	6
27-Dec-96	8	27-Jan-97		27-Feb-97		27-Mar-97	7
28-Dec-96	9	28-Jan-97		28-Feb-97		28-Mar-97	8
29-Dec-96	10	29-Jan-97				29-Mar-97	9
30-Dec-96	11	30-Jan-97				30-Mar-97	10
31-Dec-96	12	31-Jan-97				31-Mar-97	11

Table A. Continued.

Day	Category	Day	Category	Day	Category	Day	Category
01-Dec-97		01-Jan-98	11	01-Feb-98		01-Mar-98	9
02-Dec-97		02-Jan-98	12	02-Feb-98		02-Mar-98	10
03-Dec-97		03-Jan-98		03-Feb-98		03-Mar-98	11
04-Dec-97		04-Jan-98		04-Feb-98		04-Mar-98	12
05-Dec-97		05-Jan-98		05-Feb-98		05-Mar-98	
06-Dec-97		06-Jan-98		06-Feb-98		06-Mar-98	
07-Dec-97		07-Jan-98		07-Feb-98		07-Mar-98	
08-Dec-97	1	08-Jan-98		08-Feb-98		08-Mar-98	
09-Dec-97	2	09-Jan-98		09-Feb-98		09-Mar-98	
10-Dec-97	3	10-Jan-98		10-Feb-98		10-Mar-98	
11-Dec-97	4	11-Jan-98	1	11-Feb-98		11-Mar-98	1
12-Dec-97	5	12-Jan-98	2	12-Feb-98		12-Mar-98	2
13-Dec-97	6	13-Jan-98	3	13-Feb-98		13-Mar-98	3
14-Dec-97	7	14-Jan-98	4	14-Feb-98		14-Mar-98	4
15-Dec-97	8	15-Jan-98	5	15-Feb-98		15-Mar-98	5
16-Dec-97	9	16-Jan-98	6,1	16-Feb-98		16-Mar-98	6
17-Dec-97	10	17-Jan-98	7,2	17-Feb-98		17-Mar-98	7
18-Dec-97	11	18-Jan-98	8,3	18-Feb-98		18-Mar-98	8
19-Dec-97	12	19-Jan-98	9,4	19-Feb-98		19-Mar-98	9
20-Dec-97		20-Jan-98	10,5	20-Feb-98		20-Mar-98	10
21-Dec-97		21-Jan-98	11,6	21-Feb-98	1	21-Mar-98	11
22-Dec-97	1	22-Jan-98	12,7	22-Feb-98	2	22-Mar-98	12
23-Dec-97	2	23-Jan-98	8	23-Feb-98	3	23-Mar-98	
24-Dec-97	3	24-Jan-98	9	24-Feb-98	4	24-Mar-98	
25-Dec-97	4	25-Jan-98	10	25-Feb-98	5	25-Mar-98	
26-Dec-97	5	26-Jan-98	11	26-Feb-98	6	26-Mar-98	
27-Dec-97	6	27-Jan-98	12	27-Feb-98	7	27-Mar-98	
28-Dec-97	7	28-Jan-98		28-Feb-98	8	28-Mar-98	
29-Dec-97	8	29-Jan-98				29-Mar-98	
30-Dec-97	9	30-Jan-98				30-Mar-98	
31-Dec-97	10	31-Jan-98				31-Mar-98	

Table A. Continued.

APPENDIX B. DAILY COMPOSITES FOR FOUR PHASES OF MJO

Appendix B. contains daily composites of 1000 hPa winds and OLR-based convection index for all phases of the MJO during the early-inactive phase (a-l), early-active phase (a-l), late-inactive phase (a-l), and the late-active phase (a-l).

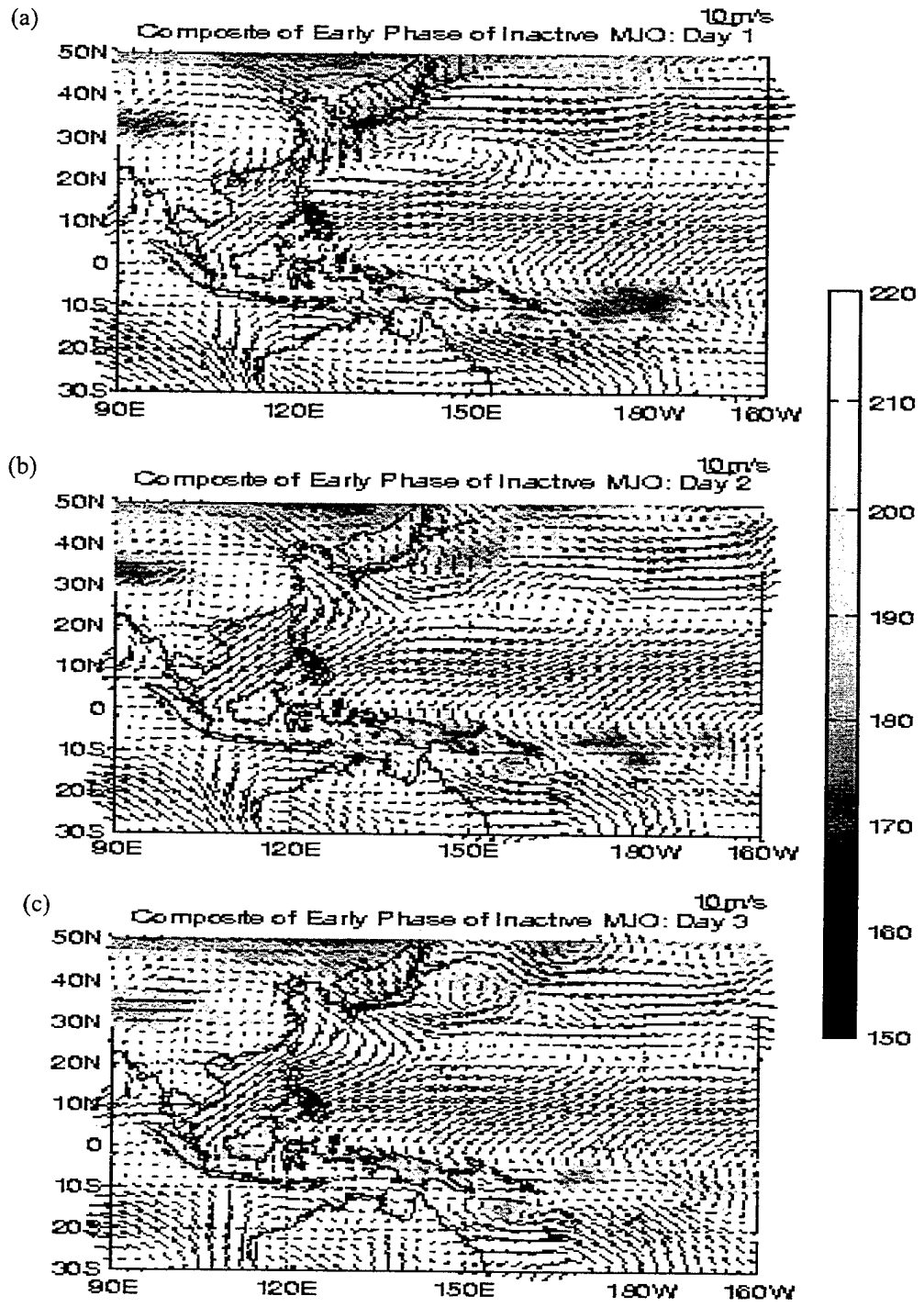

Figure B-1. Composite analysis of 1000 hPa winds and convection for surge events during the early-inactive phase, Day 1 to Day 12 (a-l).

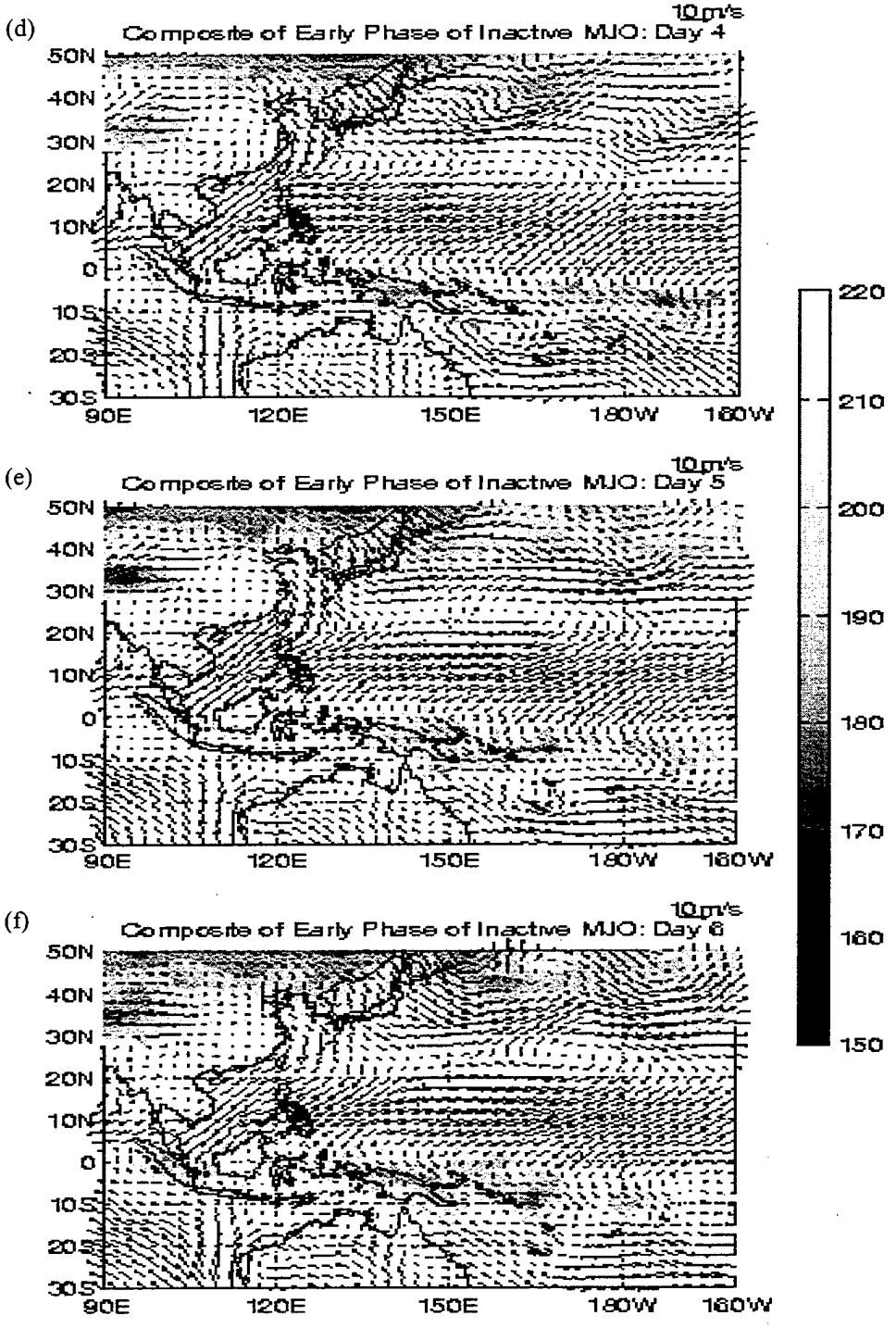

Figure B-1. Continued.

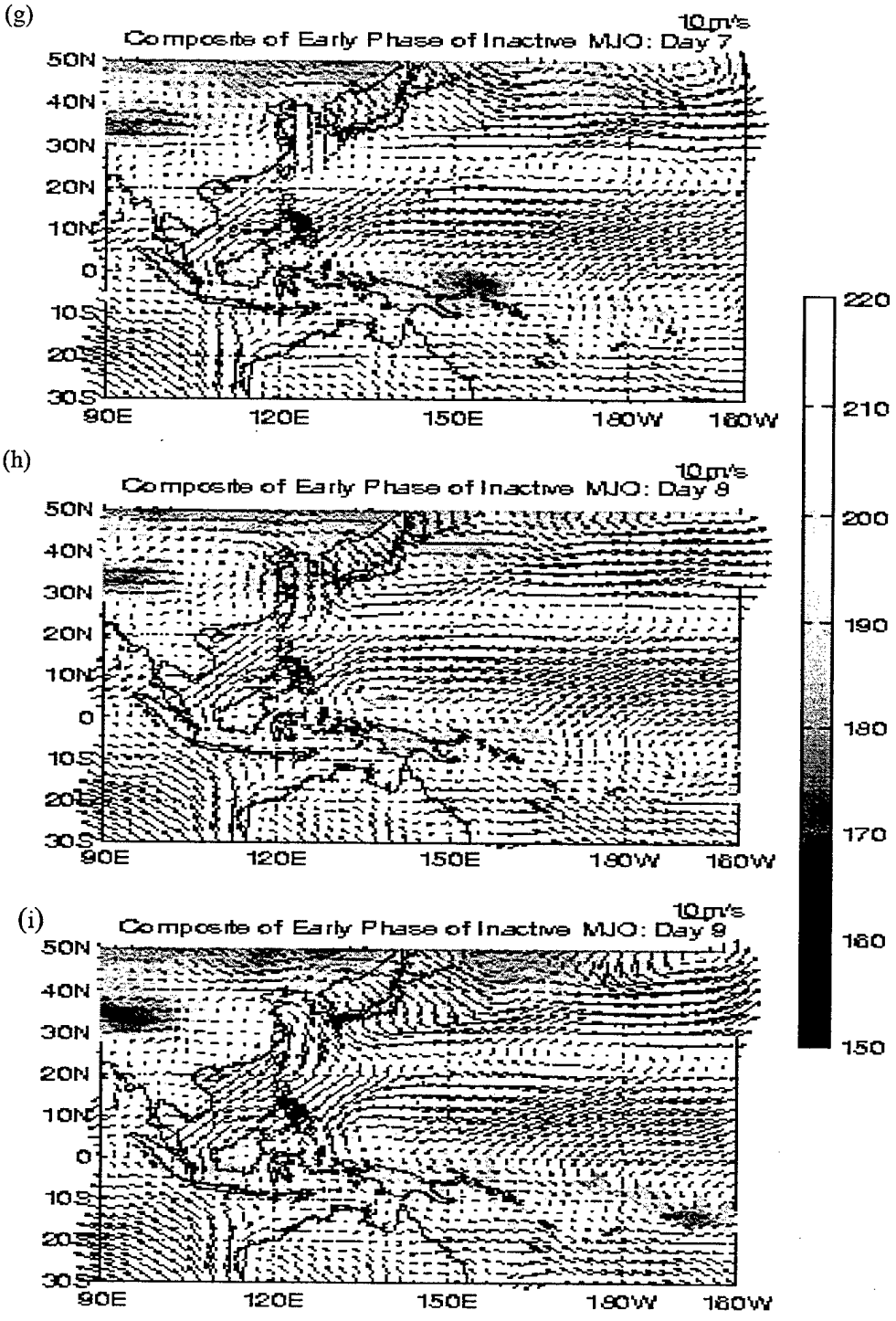

Figure B-1. Continued.

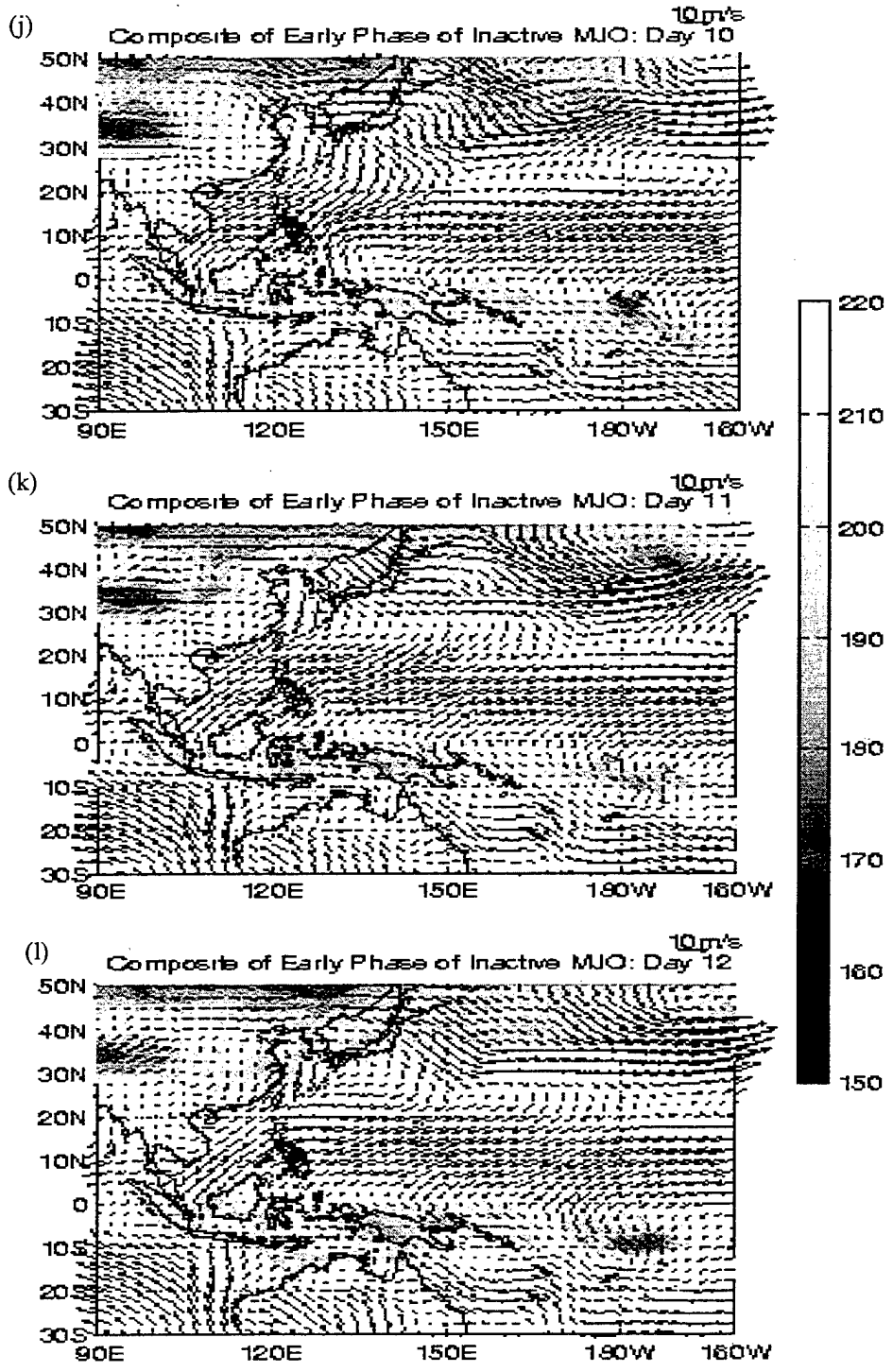

Figure B-1. Continued.

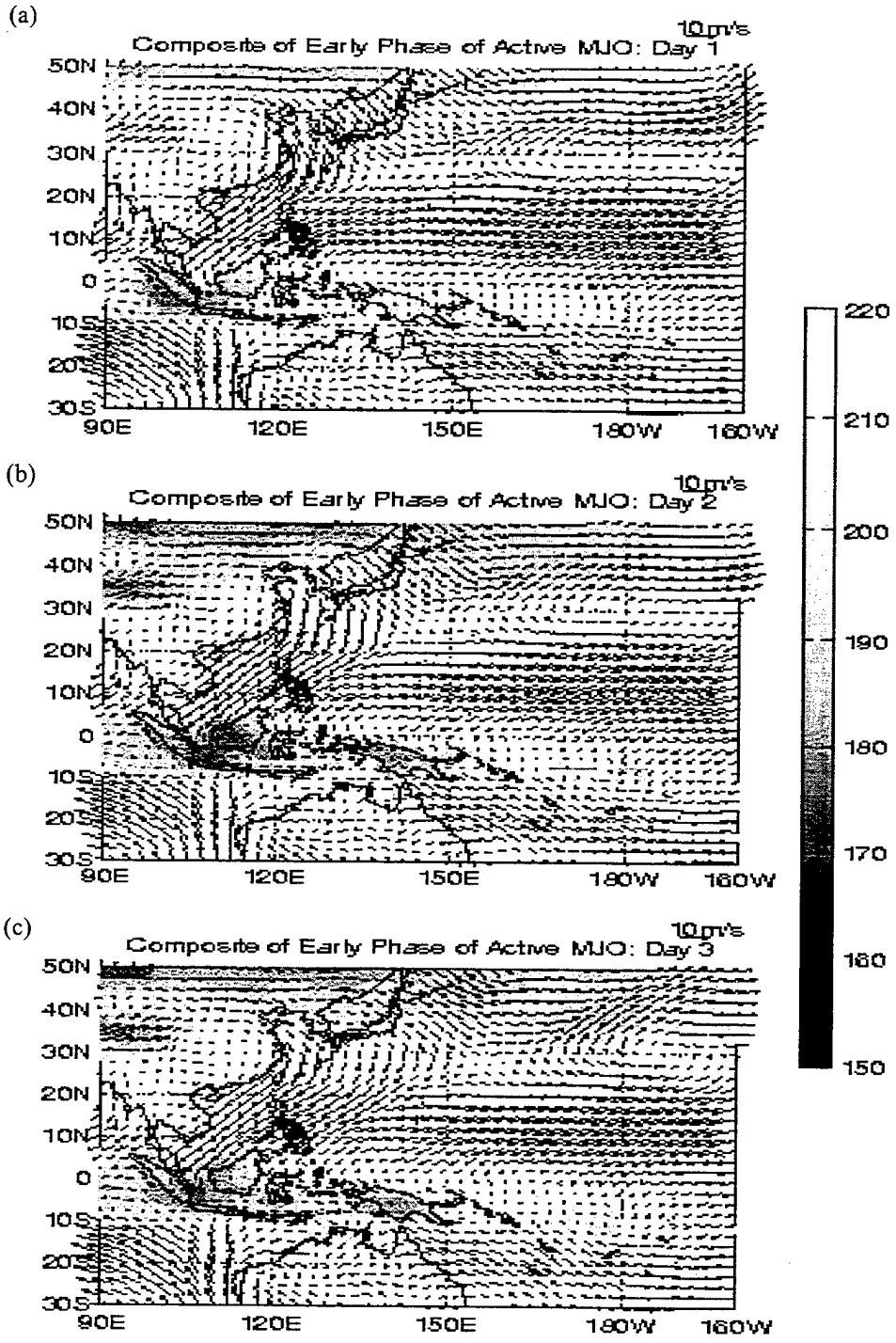

Figure B-2. Composite analysis of 1000 hPa winds and convection for surge events during the early-active phase, Day 1 to Day 12 (a-l).

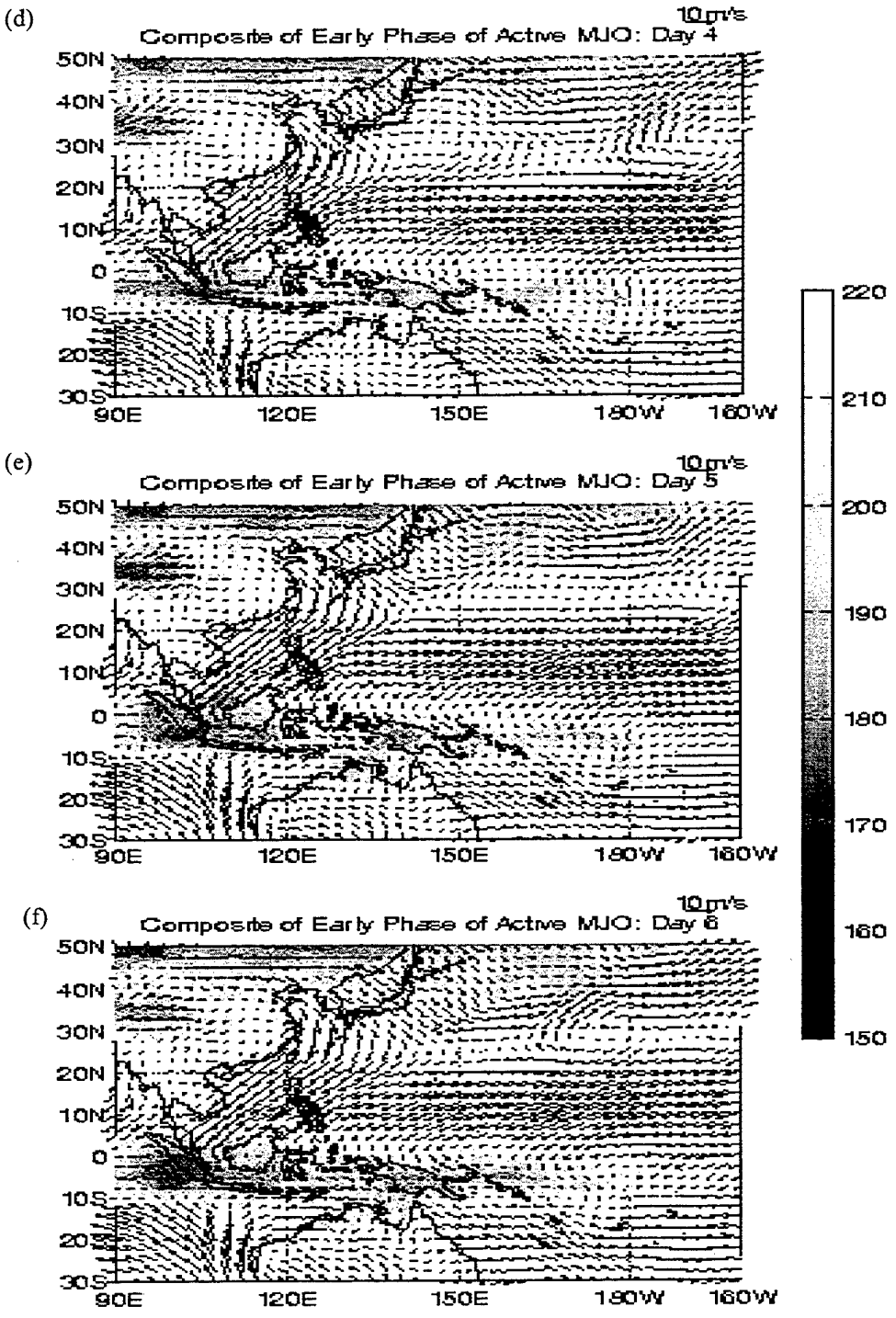

Figure B-2. Continued.

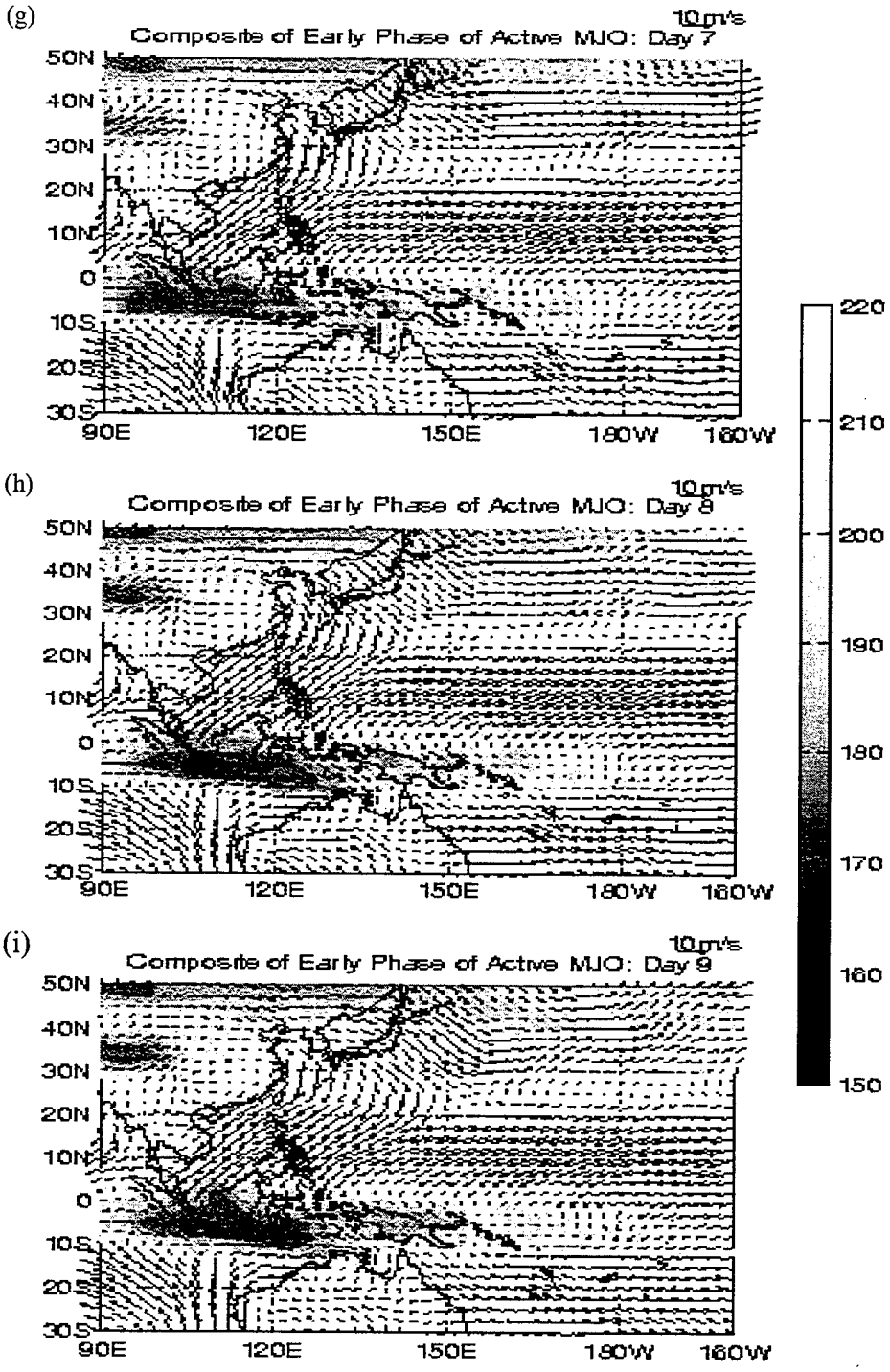

Figure B-2. Continued.

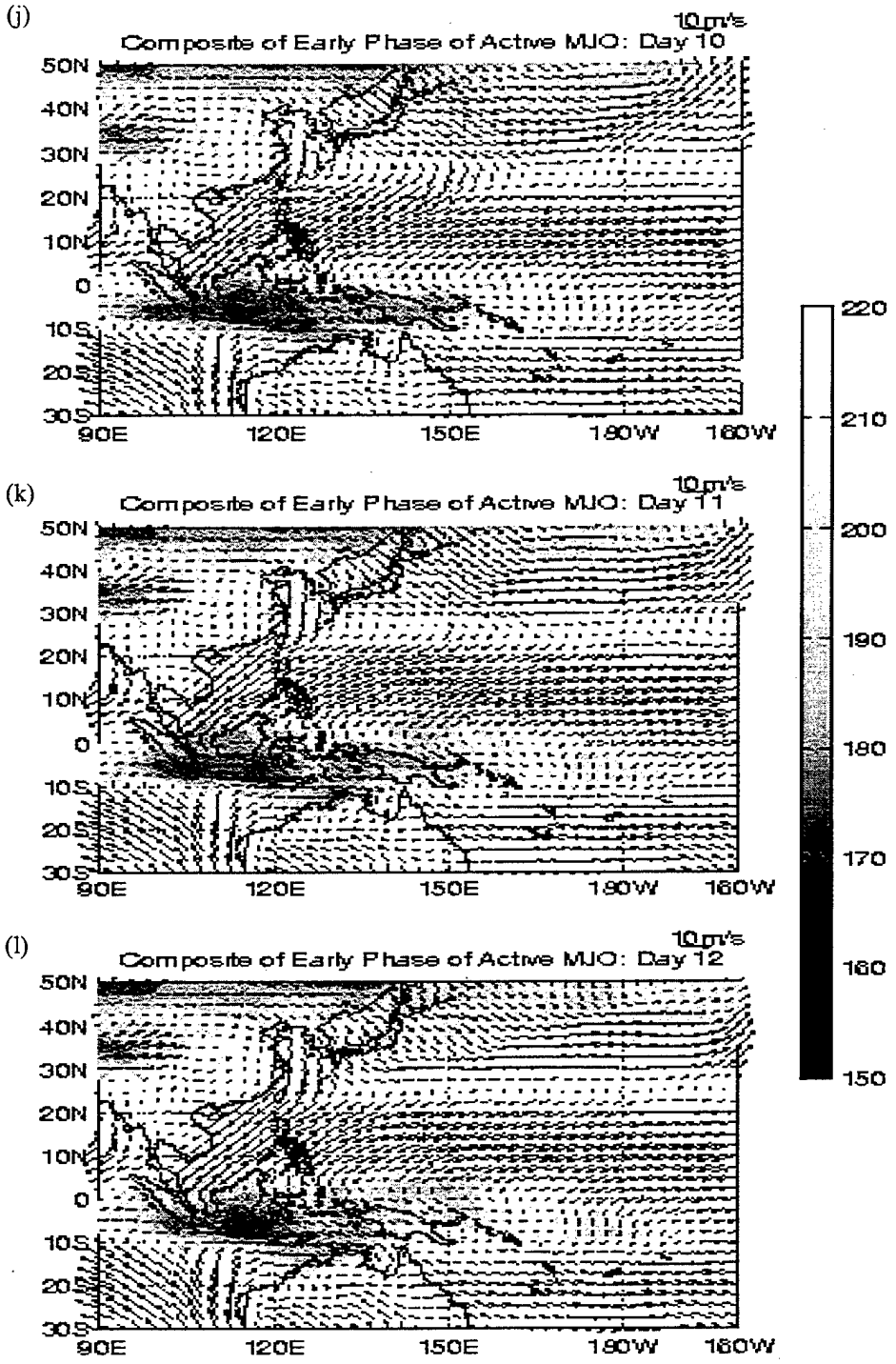

Figure B-2. Continued.

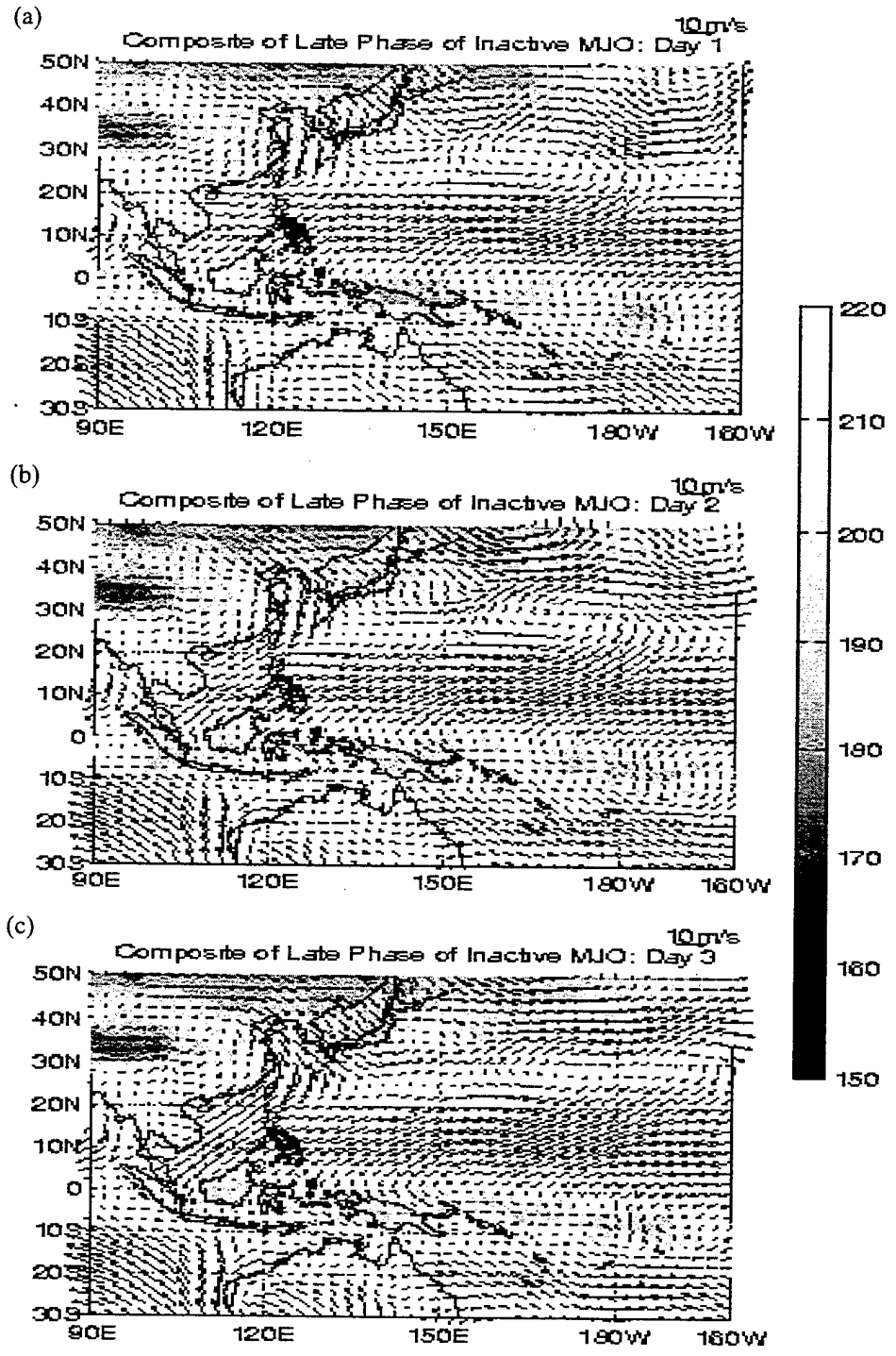

Figure B-3. Composite analysis of 1000 hPa winds and convection for surge events during the late-inactive phase, Day 1 to Day 12 (a-l).

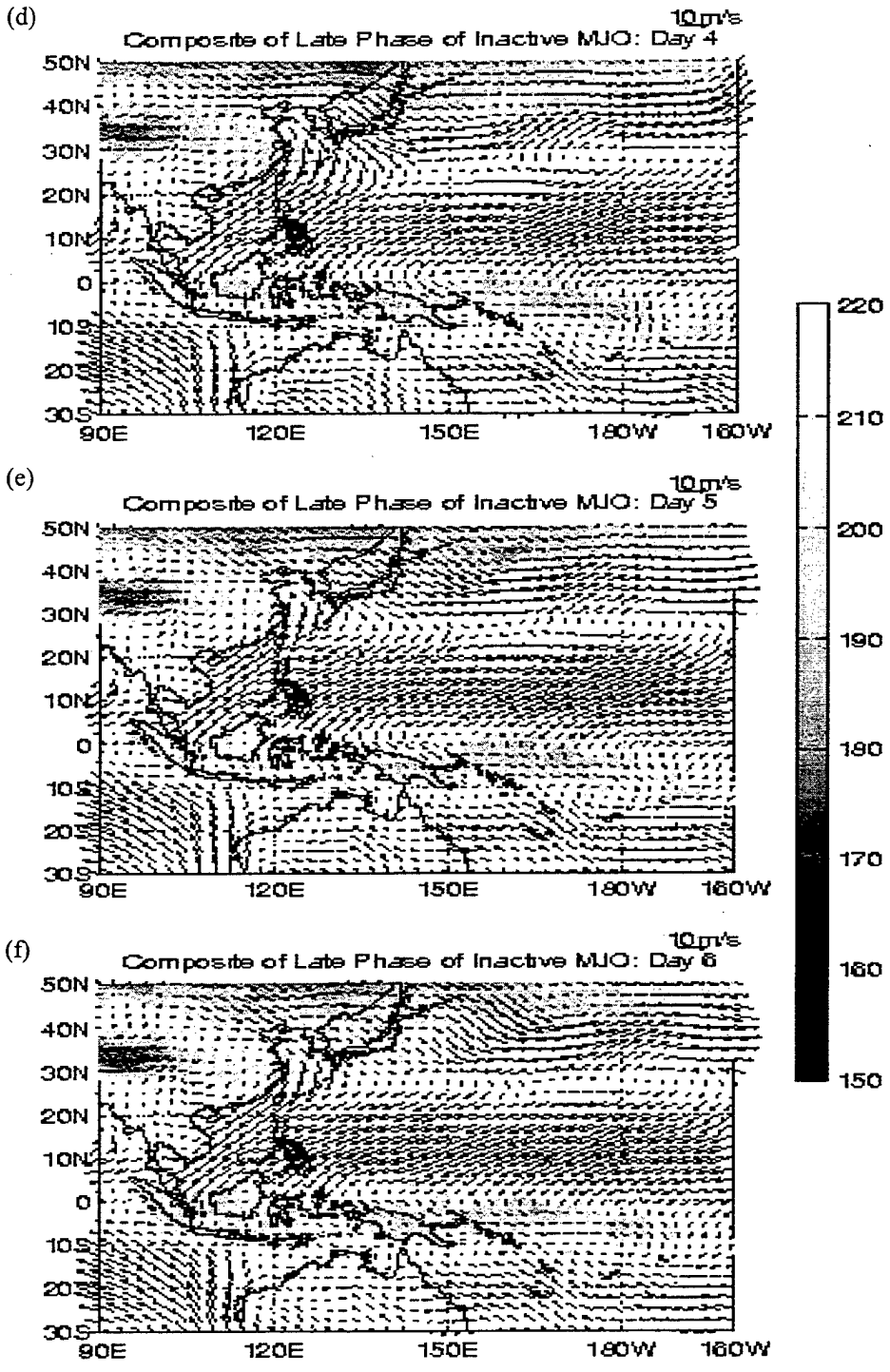

Figure B-3. Continued.

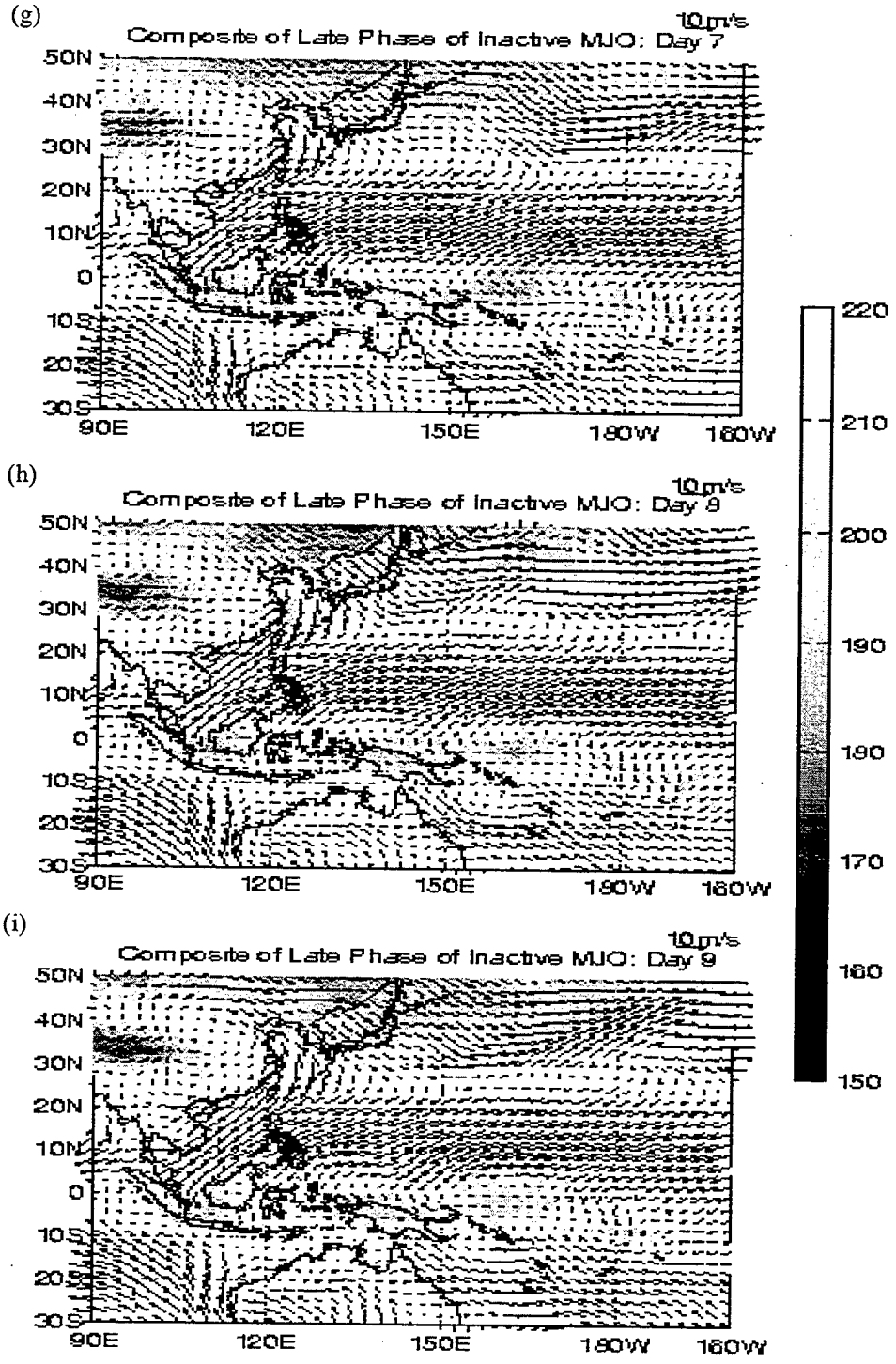

Figure B-3. Continued.

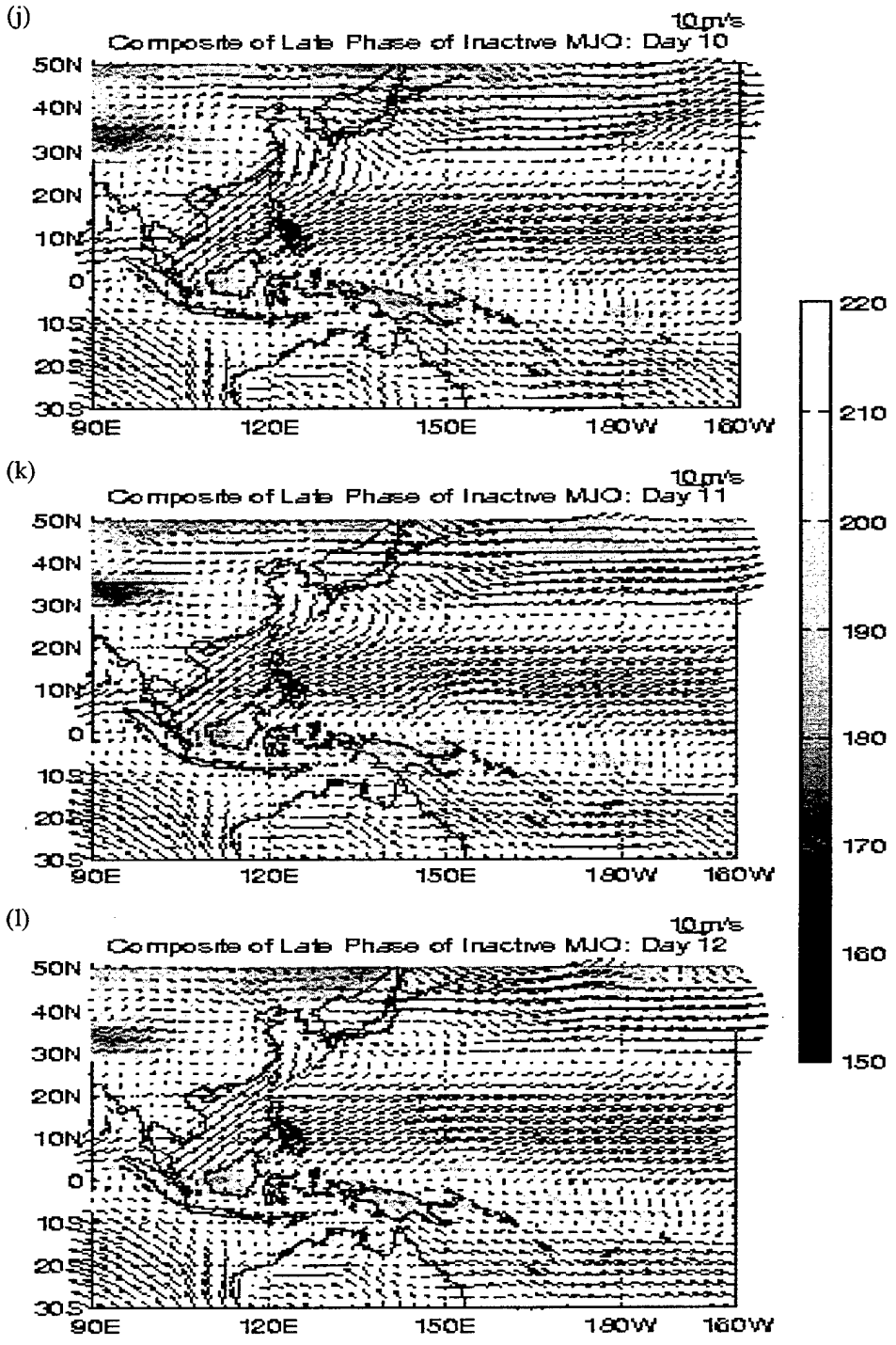

Figure B-3. Continued.

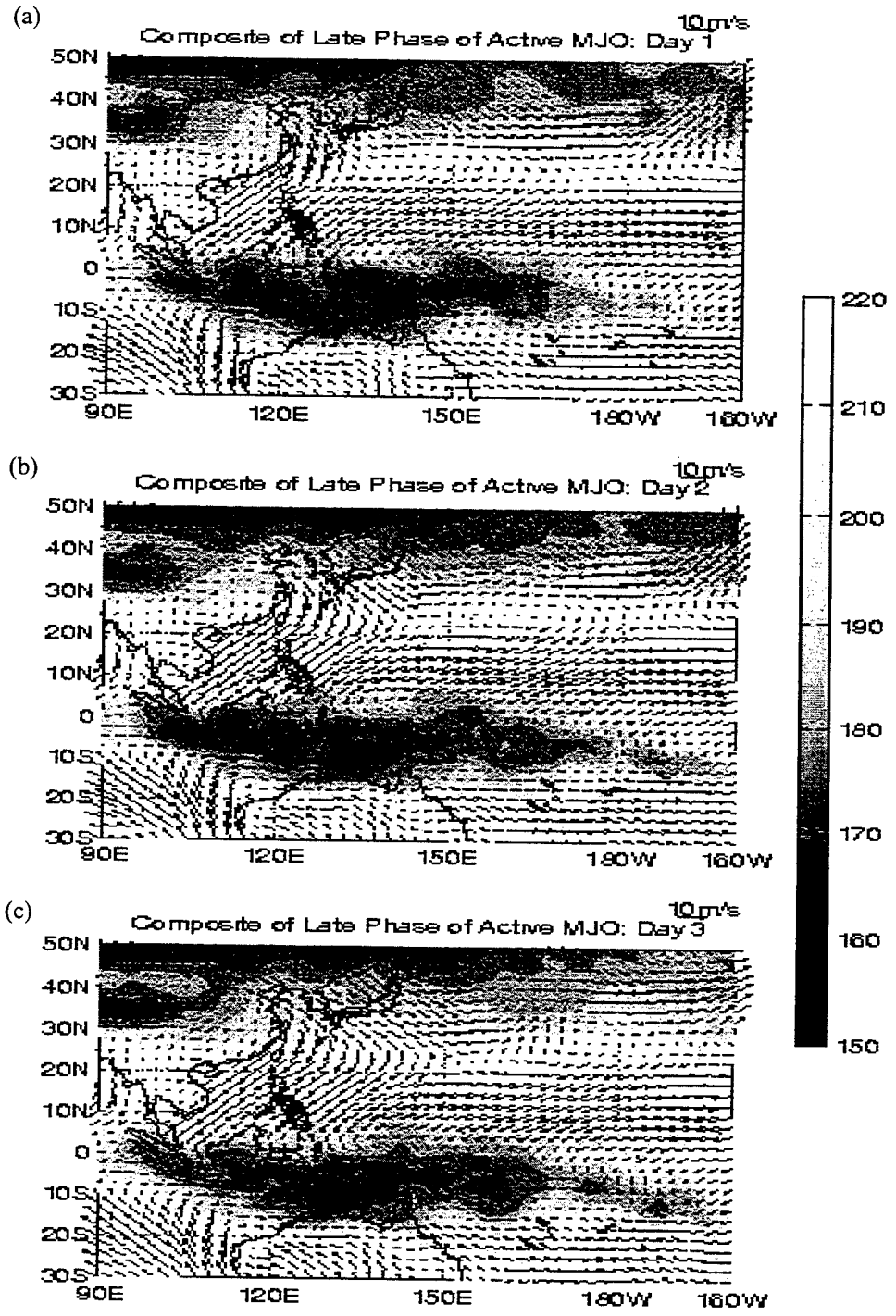

Figure B-4. Composite analysis of 1000 hPa winds and convection for surge events during the late-active phase, Day 1 to Day 12 (a-l).

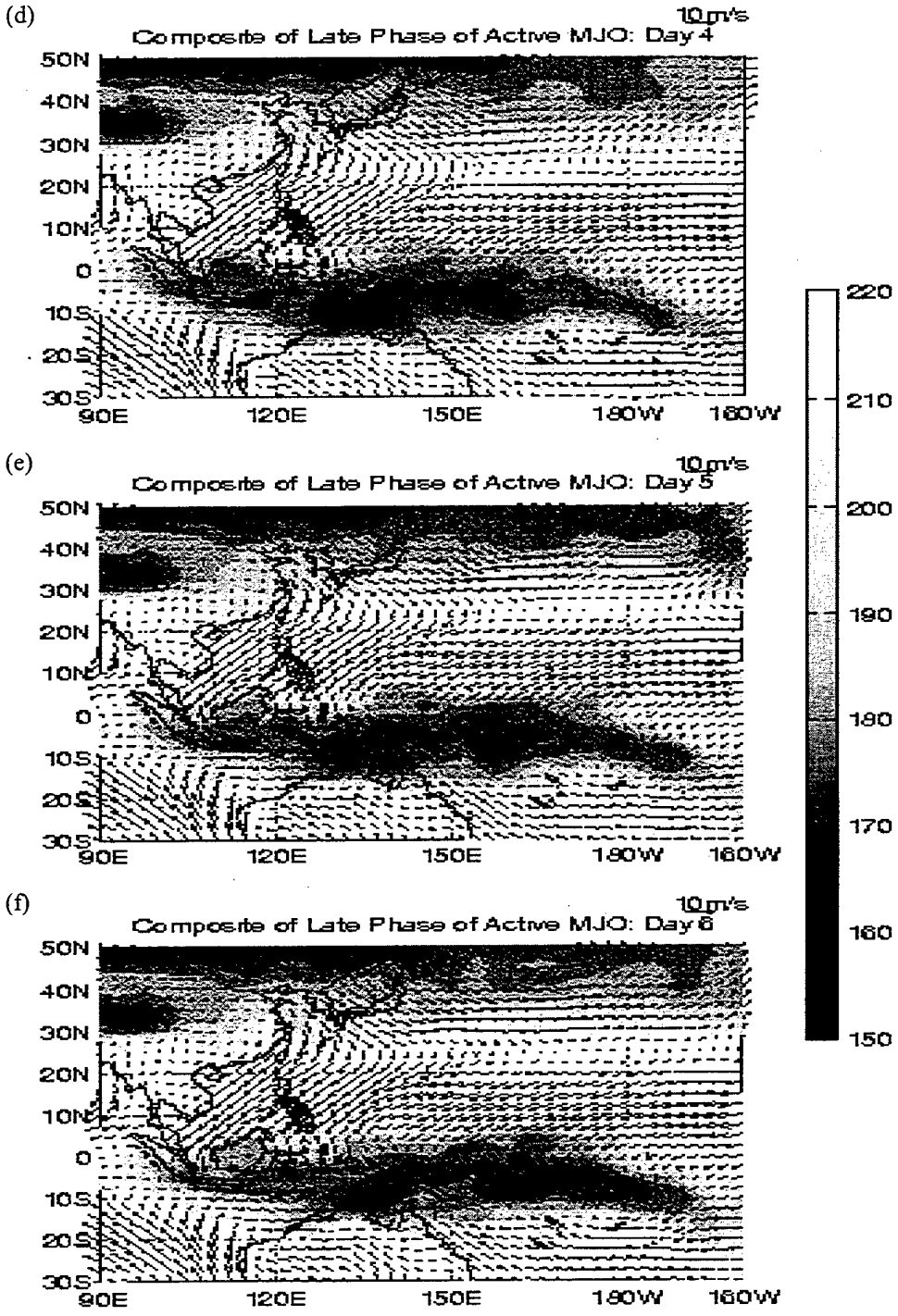

Figure B-4. Continued.

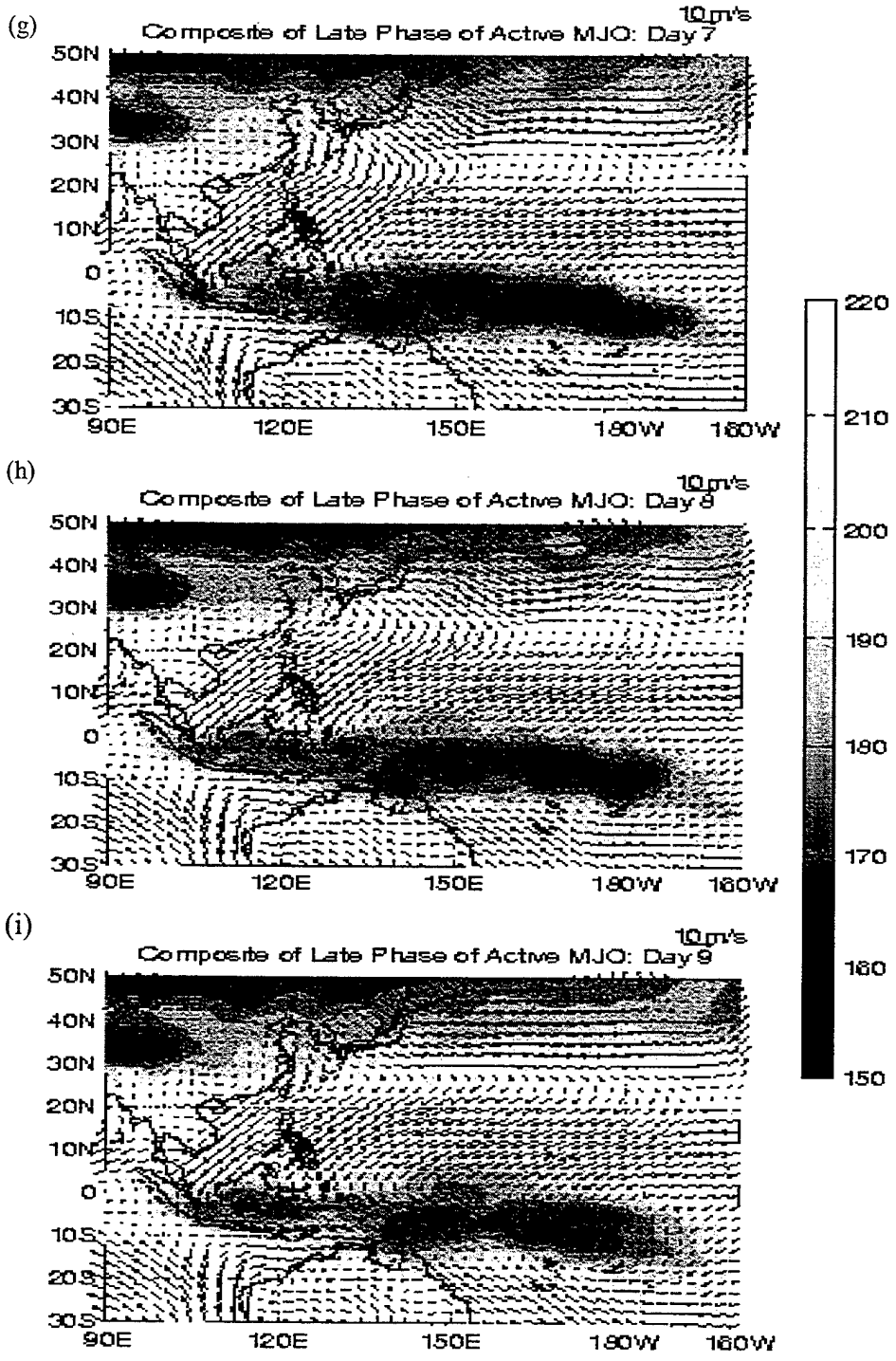

Figure B-4. Continued.

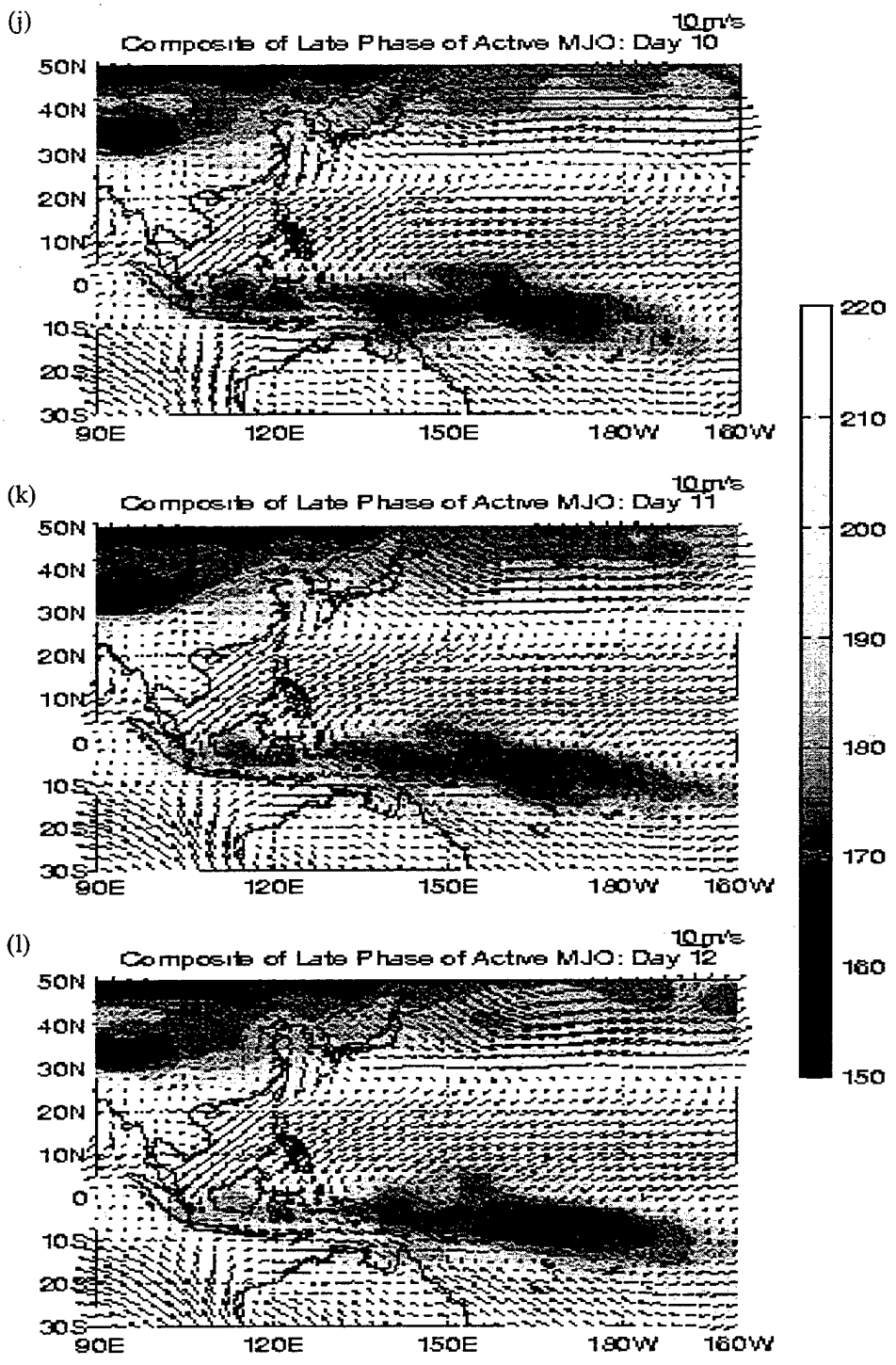

Figure B-4. Continued.

THIS PAGE INTENTIONALLY LEFT BLANK

LIST OF REFERENCES

Compo, G. P., G. N. Kiladis, and P. J. Webster, 1999: The Horizontal and Vertical Structure of East Asian Winter Monsoon Pressure. *Q. J. R. Meteor. Soc.*, **125**, 29-54.

Ferreira, R. N., W. H. Schubert, and J. J. Hack, 1996: Dynamical Aspects of Twin Tropical Cyclones Associated with the Madden-Julian Oscillation. *J. Atmos. Sci.*, **53**, 929-945.

Gill, A. E., 1980: Some Simple Solutions For Heat-induced Tropical Circulations. *Q. J. R. Meteor. Soc.*, **106**, 447-462.

Johnson, R. H., and R. A. Houze, Jr., 1987: Precipitating Cloud Systems of the Asian Monsoon. *Monsoon Meteorology*, C. P. Chang and T. N. Krishnamurti, Eds., Oxford University Press, 298-353.

Lau, K. M., and L. Peng, 1987: Origin of Low-frequency (intraseasonal) Oscillations in the Tropical Atmosphere. Part I: Basic theory., *J. Atmos. Sci.*, **44**, 950-972.

Liebmann, B., H. H. Hendon and J. D. Glick, 1994: The Relationship Between Tropical Cyclones of the Western Pacific and Indian Oceans and the Madden-Julian Oscillation. *J. Meteor. Soc. Japan*, **72**, 401-412.

Love, G., 1985: Cross Equatorial Influence of Winter Hemisphere Subtropical Cold Surges. *Mon. Wea. Rev.*, 113, 1487-1498.

Madden, R. A., and P. R. Julian, 1971: Detection of a 40-50 Day Oscillation in the Zonal Wind in the Tropical Pacific. *J. Atmos. Sci.*, **28**, 702-708.

Madden, R. A., and P. R. Julian, 1972: Description of Global-scale Circulation Cells in the Tropics With a 40-50 Day Period. *J. Atmos. Sci.*, **29**, 1109-1123.

Madden, R. A., and P. R. Julian, 1994: Observations of the 40-50 Day Tropical Oscillation-A review. *Mon. Wea. Rev.*, **122**, 814-837.

Matsuno, T., 1966: Quasi-geostrophic Motions in the Equatorial Area. *J. Meteor. Soc. Japan*, **44**, 25-43.

Rui, H., and B. Wang, 1990: Development Characteristics and Dynamic Structure of Tropical Intraseasonal Convection Anomalies. *J. Atmos. Sci.*, **47**, 357-359.

Taylor, S. C, 1998: Interactions of Large-scale Tropical Motion Systems During the 1996-1997 Australian Monsoon. *Master Thesis, Naval Postgraduate School.* 1-46.

Wang, B., and H. Rui, 1990: Synoptic Climatology of Transient Tropical Intraseasonal Convective Anomalies. *Meteor. Atmos. Phys.*, **44**, 43-61.

Weickmann, K. M. and S. J. S. Khalsa, 1990: The Shift of Convection from the Indian Ocean to the Western Pacific Ocean During a 30-60 Day Oscillation. *Mon. Wea. Rev.*, **118**, 964-978.

Wu, M. C., and J. C. L. Chan, 1995: Surface Features of Winter Monsoon Surges Over South China. *Mon. Wea. Rev.*, **123**, 662-680.

Initial Distribution List

1. Defense Technical Information Center.....2
   8725 John J. Kingman Rd., STE 0944
   Ft. Belvoir, Virginia 22060-6218

2. Dudley Knox Library.....2
   Naval Postgraduate School
   411 Dyer Rd.
   Monterey, California 93943-5101

3. Meteorology Department.....1
   Code MR/Wx
   Naval Postgraduate School
   589 Dyer Rd. Rm 254
   Monterey, California 93943-5114

4. Prof. Chi-Pei Chang.....2
   Code MR/CP
   Naval Postgraduate School
   589 Dyer Rd. Rm 254
   Monterey, California 93943-5114

5. Prof. Patrick Harr.....1
   Code MR/PH
   Naval Postgraduate School
   589 Dyer Rd. Rm 254
   Monterey, California 93943-5114

6. Prof. Johnny C. L. Chan.....1
   Department of Physics and Material Science
   City University of Hong Kong
   83 Tat Chee Ave.
   Kowloon, Hong Kong, China

7. LT John Simms.....3
   c/o J. Simms, III
   5548 Nithsdale Dr.
   Salisbury, Maryland 21801